

NIST Technical Note 1499

Performance Metrics for Fire Fighting Thermal Imaging Cameras – Small- and Full-Scale Experiments



Francine Amon
Nelson Bryner
Andrew Lock
Anthony Hamins



**Homeland
Security**

Sponsored in part by
Department of Homeland Security

NIST

National Institute of Standards and Technology
U.S. Department of Commerce

NIST Technical Note 1499

Performance Metrics for Fire Fighting Thermal Imaging Cameras – Small- and Full-Scale Experiments

Francine Amon
Nelson Bryner
Andrew Lock
Anthony Hamins

*Fire Research Division
Building and Fire Research Laboratory
National Institute of Standards and Technology
Gaithersburg, MD 20899-8661*

July 2008



**Homeland
Security**

Department of Homeland Security
Michael Chertoff, Secretary

Federal Emergency Management Agency
R. David Paulison, Administrator

United States Fire Administration
Gregory Cade, Fire Administrator



U.S. Department of Commerce
Carlos M. Gutierrez, Secretary

National Institute of Standards and Technology
James Turner, Acting Director

ABSTRACT

Thermal imaging cameras (TIC) are becoming an important tool for many firefighters and other first responders. However, due to the lack of performance standards for TIC, a wide variety of designs and capabilities are provided to end users with little consistency in reported performance. In order to understand the performance characteristics of TIC during fire fighting applications, it is critical that a set of performance metrics and standard testing protocols be developed to allow the fire service to evaluate TICs. The National Institute of Standards and Technology (NIST) has been conducting research to characterize and understand TIC performance. This work began with an assessment of the thermal imaging needs and activities of first responders. Existing standards were collected and reviewed to ensure that the recommended testing conditions in this work are consistent with standards on other first responder equipment that are exposed to similar operating conditions, as well as standards and test protocols on infrared cameras that are used in other applications, when appropriate. A survey of the literature was also performed to explore existing work in which the fire environment was well characterized and pertinent to TIC testing.

The consolidation of all of this information, e.g., first responder feedback, literature search, and full- and bench-scale testing results, provided a basis for defining testing conditions that challenge TIC in meaningful ways. Performance metrics that describe TIC image contrast, effective temperature range, spatial resolution, image nonuniformity, and thermal sensitivity were selected or developed, based on an analysis of the information gathered. These imaging performance metrics and test methods have been provided to standards development organizations, such as National Fire Protection Association (NFPA) and ASTM International. NFPA's Technical Committee on Electronic Safety Equipment has incorporated these metrics and test protocols in a draft version of NFPA 1801, Standard on Thermal Imagers for the Fire Service, which is currently in the public proposal phase.

ACKNOWLEDGEMENTS

Funds for this project have been provided by the Department of Homeland Security (DHS), the United States Fire Administration (USFA), the Office of Law Enforcement Standards (OLES), Advanced Fire Service Technology Program (NIST) and Advanced Technology Program (NIST). Mr. William Troup (USFA), Mr. Philip Mattson (OLES), and Mr. Nicholas Paulter (OLES) provided valuable input as contract monitors.

For their effort and participation in conducting the modeling and experimental work, the authors would like to thank Marc Nyden, Justin Rowe, Josh Dinaburg, Chang Bo Oh, Yong Shik Han, Sung Chan Kim, Gwon Hyun Ko, Roy McLane, and Jay McElroy.

The authors would also like to thank the participants of the Workshop on Thermal Imaging Research Needs for First Responders for their expertise, insight, and willingness to provide their input.

The authors express their special appreciation to Gerald C. Holst of JCD Publishing for providing technical advice and encouragement throughout this project.

DISCLAIMER

Certain companies and commercial properties are identified in this paper in order to specify adequately the source of information or of equipment used. Such identification does not imply endorsement or recommendation by the National Institute of Standards and Technology, nor does it imply that this source or equipment is the best available for the purpose.

TABLE OF CONTENTS

1. INTRODUCTION	11
1.1. Approach	12
2. BACKGROUND	13
2.1. Imager design	13
2.2. Detector technologies	15
2.3. Operating environment	19
2.4. Performance metrics	19
3. WORKSHOP ON THERMAL IMAGING RESEARCH NEEDS FOR FIRST RESPONDERS	21
4. SURVEY OF RELEVANT STANDARDS AND WORK BY OTHERS	23
4.1. Relevant standards	23
4.2. Work by others	24
4.3. TIC operations	26
5. INFORMATION CONSOLIDATION- TEST CONDITIONS	27
5.1. Series 1 test facility	27
5.2. Series 2 test facility	30
5.3. FTIR measurements	33
5.4. Hose stream experiments	34
5.5. Full-scale experimental results	35
5.5.1. Heat effects	37
5.5.2. Smoke effects	41
5.5.3. FTIR measurement results	43
5.5.4. Hose stream results	44
5.6. Consolidation of test condition information	47
6. PERFORMANCE METRICS AND TEST METHODS	50
6.1. Image Recognition Procedure	50
6.2. Image capturing procedure	52
6.3. Contrast	52
6.4. Effective temperature range (ETR)	54
6.5. Nonuniformity	56
6.6. Spatial resolution	59
6.7. Thermal Sensitivity	61
7. RESULTS AND DISCUSSION	63
7.1. Contrast and ETR	63
7.2. Nonuniformity	66
7.3. Spatial resolution	68
7.4. Thermal sensitivity	71
7.5. Uncertainty Analysis	73
8. Summary	75
9. REFERENCES	76
APPENDIX A	80
APPENDIX B	82
Index	84

LIST OF FIGURES

Figure 2—1.	Predicted transmittance through a 12.7 cm (5 in) measurement path length for a simulated combustion atmosphere [9]. The soot, gases and wall temperatures are 600 °C.	14
Figure 2—2.	Predicted radiation intensity through a 12.7 cm (5 in) path length for a simulated combustion atmosphere consisting of 0.6 ppm soot, 0.5 % CO, 2.5 % CO ₂ , and 97.0 % H ₂ O [9]. The media temperature is held at 600 °C and the wall temperature varies from 0 °C to 600 °C.....	15
Figure 2—3.	These three TIC are simultaneously viewing an identical thermal scene: a long corridor with a heated mannequin on the floor, and reflective and heated targets mounted on the wall at the end. A fire room is located adjacent to the corridor on the right.	16
Figure 2—4..	Generic schematic of major TIC design components.....	18
Figure 2—5.	Hybrid Pyroelectric BST Detector. This is a solid-state ceramic detector that spontaneously polarizes when exposed to thermal energy [4].....	18
Figure 2—6.	Microbolometer. This is an array of individual sensors, each of which generates a small portion of the overall thermal scene. The sensor material is either vanadium oxide or amorphous silicon [11].....	18
Figure 3—1.	Thermal imaging research needs, as indicated by participants of the Workshop on Thermal Imaging Needs for First Responders in December, 2004. The key to the categories on the abscissa is provided in the following text.	21
Figure 5—1.	Plan view of Series 1 full-scale testing structure with inset showing the target and background. The target was placed on the floor in test configuration A and mounted on the wall 1.5 m from the floor in test configurations B, C, and D.	29
Figure 5—2.	TIC are positioned in the hot upper layer viewing a target through heavy toluene smoke, test configuration D (left), and in the lower layer viewing flames and high heat conditions, test configuration A (right).	30
Figure 5—3.	Plan view of Series 2 full-scale fire test configuration with TIC viewing IR targets having at two distances. A heated mannequin in fire fighter turnout gear was also placed in the FOV.....	31
Figure 5—4.	The TIC were mounted on shelves which were repositioned midway through the tests (left). Two bar targets were used, one in the upper layer and one in the lower layer, along with a heated mannequin in fire fighter turnout gear, shown in infrared (right).....	32
Figure 5—5.	Visible image of typical hose stream test set up. Three TIC (behind foil on far left) are viewing a thermal target through a fog spray in the presence of a 2.2 MW heptane fire.	35

Figure 5—6. Comparison of heat effects, BST detector technology. These two TIC differ only in age, both having a 320 x 240 detector array. (where applicable uncertainties are determined statistically as stated in section 7.5 and reported with a coverage factor of k=2).....	38
Figure 5—7. Comparison of heat effects, VOx detector technology.	39
Figure 5—8. Comparison of heat effects for ASi detector technology.	40
Figure 5—9. Comparison of smoke effects for BST detector technology.	41
Figure 5—10. Comparison of smoke effects for VOx detector technology.	42
Figure 5—11. Comparison of smoke effects for ASi detector technology.....	43
Figure 5—12. The relative FTIR signal measured at two times during an experiment burning carpet, padding, and wood. For comparison, measurement of the relative signal of a blackbody source at 200 °C (± 5 °C, as per manufacturers documentation) is also shown.....	44
Figure 5—13. Thermal images of a scene in which a fog spray is directed toward a wall in front of a 2.2 MW heptane fire. A BST-type TIC produced the center image and ASi-type TIC from different manufacturers produced the two other images.....	45
Figure 5—14. <i>CTF</i> of a thermal target viewed by three TIC through fog and straight (jet) sprays with a 2.2 MW fire in the field of view. The error bars represent the standard deviation of the <i>CTF</i> with a coverage factor of 2 (95 % confidence).....	46
Figure 5—15. Identical scene from full scale test series two observed with three different cameras. From top to bottom VOx, ASi, and BST TIC are utilized to view the same scene at the same time consisting of a mock victim on the floor with smoke and flames in the field of view.	48
Figure 6—1. Reflective test target used for image recognition tests. The test target dimensions are 61 cm (24 in.) in each direction. The white markings shown here are highly reflective foil with an $\epsilon \leq 0.1$ and the background is foam core with a black matte finish having an $\epsilon \geq 0.9$	51
Figure 6—2. An example viewing configuration is also shown (right) with the TIC positioned 1m away from the IRP target surface.....	51
Figure 6—3. Schematic diagram of image capturing setup. As the TIC views a thermal target, a high resolution visible camera is focused on the TIC display. A mounting bracket (not shown) is to be provided by the TIC manufacturer to optimally position the visible camera.	52
Figure 6—4. Test target setup used for the contrast and effective temperature range tests. For large area contrast, the bars in the middle of the test target are ignored. The standard deviation of the combined pixel intensities within the dashed areas on the left and right side of the test target are calculated, then divided by the <i>Bitdepth</i> to determine the contrast as a function of T_2 , which changes from 25 °C to T_{max}	55

Figure 6—5. Alternative test setup for contrast and effective temperature range. When space is an issue mirrors may be used to redirect the thermal radiation to the TIC. The results presented in this paper were obtained in this configuration.	55
Figure 6—6. This test target is used for the contrast and effective temperature range tests. For the effective temperature range, the contrast of the central area, which incorporates bars having a constant temperature difference, is measured while the hot blackbody surface temperature (T_2) increases.	56
Figure 6—7. Test setup for measuring the nonuniformity of a TIC. The TIC is placed close to the surface (~5cm) of a uniform large area blackbody surface. The temperature is increased and the images are taken by the visible camera to determine image nonuniformity.	57
Figure 6—8. Variation in nonuniformity of a TIC with increasing temperature. As the test target temperature increased, nonuniformities became more apparent. The TIC shifted to a less thermally sensitive mode between the 100 °C and 200 °C images.	58
Figure 6—9 Slanted edge spatial resolution test target. The slant is 5 ° from vertical, the hot and surrounding temperatures are held constant throughout the test. The target dimensions are at least 15 cm in each direction. All surfaces in the field of view have $\epsilon \geq 0.94 \pm 0.002$	60
Figure 6—10 Sample spatial resolution data. The spatial resolution is obtained by integrating between the MTF (red line) and the nonuniformity (blue line).	61
Figure 6—11. Experimental setup for thermal sensitivity test. The two blackbodies are adjusted until they both have the same luminance on the TIC display. Then one blackbody temperature is slowly decreased until a 2 % difference in luminance is observed between the two blackbodies.	62
Figure 7—1. Plots of large area contrast and bar contrast data used to determine image contrast and effective temperature range of a TIC using an ASi, 120 x 160 detector array. Test results for two tests are shown.	64
Figure 7—2. Plots of large area contrast and bar contrast data used to determine image contrast and effective temperature range of a TIC using an BST, 240 x 320 detector array. Test results for two tests are shown.	65
Figure 7—3. Plots of large area contrast and bar contrast data used to determine image contrast and effective temperature range of a TIC using an VOx, 120 x 160 detector array. Test results for two tests are shown.	65
Figure 7—4. Actual nonuniformities observed from three different TIC at a variety of temperatures. BST, VO _x , and ASi detector technologies are all represented along with a variety of different nonuniformities present in these cameras.	67
Figure 7—5. Image nonuniformity as a function of target temperature while looking at a uniform temperature surface. For the three specific TIC tested, the VO _x TIC produced the least nonuniformity while the ASi and BST cameras had higher nonuniformities at different temperatures.	67

Figure 7—6. Illustration of how of how three different cameras interpret the same ‘knife edge’ thermal target. The three different cameras have different sensor technology, but also have different pixel resolutions (320x240, 160x120, and 160x120 respectively), optics, and internal image processing that affects the spatial resolution of the image on the display. The analysis of these images is presented in Figure 7-6.	69
Figure 7—7. Comparison of the spatial resolution of the BST, VOx, and ASi TIC. The SFR value given for each camera technology represents the area between the MTF curve and Nonuniformity. The spatial resolution measurement for each camera is dependent upon the nonuniformity measurement as well.....	70
Figure 7—8. Illustration of the temperature independence of the spatial resolution measurement. The temperatures are indicated in Celsius. Once the original values (top) are normalized (bottom) the effect of image contrast (temperature difference) can be eliminated. The line for 40 °C on the right does not follow the other trends because there needs to be a minimum contrast in the knife edge image.	71
Figure 7—9. Example thermal sensitivity response for a characteristic TIC. A smaller value for thermal sensitivity indicates that the camera is more sensitive to small differences in temperature. The thermal sensitivity increases with increasing nominal temperature due to a larger contrast necessary for the user to percieve a temperature difference.	72

LIST OF TABLES

Table 4-1. Thermal Classes (Donnelly et al.)	23
Table 4-2. Peak conditions measured during typical compartment fire experiments.....	25
Table 4-3. First Responder TIC Operations.....	26
Table 5-1. Series 1 test configurations.....	28
Table 5-2. Series 2 test configuration.	33
Table 5-3. Thermal environment (where applicable uncertainties are determined as stated in section 7.5 and expressed with a coverage factor of $k=2$).	36
Table 5-4. Proposed TIC Testing Conditions.	49
Table 7-1: Uncertainty in full scale experimental test data.	74
Table 7-2: Uncertainty in bench scale experimental data.	74

1. INTRODUCTION

Infrared (IR) technology for firefighting applications has matured to the point that most first responder organizations either have purchased or are considering the purchase of thermal imaging cameras (TIC¹). TIC can provide first responders with critical information to size up a fire incident, track fire growth, and to locate victims, other first responders, and egress routes. While these devices represent a significant investment, typically on the order of \$10,000 per camera, first responders have little guidance on instrument performance beyond manufacturer literature and recommendations from other users [1]. These issues are further complicated because the demands placed on TIC are application dependent. The end users may have very different ideas about which imaging properties are most important: sharp image contrast may be sufficient for some fire fighting applications, such as finding the source of a fire, but high thermal sensitivity may be required to locate a person or structural component when flames and water are in the imager's field of view (FOV). Currently, there are no standardized performance guidelines available to aid end users in making purchasing decisions.

Over the past several years, the Fire Research Division at the National Institute of Standards and Technology (NIST) has been conducting research on TIC imaging performance metrics and test methods with the overall objective of providing science-based information to national standards developing organizations (SDO). The National Fire Protection Association (NFPA) is currently developing a standard on first responder thermal imaging cameras, Proposed NFPA 1801 Standard on Thermal Imagers for the Fire Service [2], and ASTM International is revising a test method on infrared detector sensitivity, ASTM E1543-00 Standard Test Method for Noise Equivalent Temperature Difference of Thermal Imaging Systems [3]. Both of these organizations are taking this work into consideration as they move through their standards developing processes.

The SDOs mentioned above operate through committees, which draft a document based on input from users, manufacturers, technical experts, and the public. The committees make decisions regarding the content of the standard on a consensus basis. Before the final form of the standard document is published, draft versions of the document are offered to the public for proposed changes in scope and for revisions to text. As an unbiased, non-commercial entity with experience in fire research and testing of first responder personal protective equipment, the Building and Fire Research Laboratory (BFRL) at NIST is well positioned to assist in the formation of a standard for TIC. At the discretion of the committee, all or part of the recommendations provided to the SDO, including the recommendations resulting from this project, may or may not be included in the final standard documents.

¹ The acronym TIC shall be used throughout this text in reference to both the singular and plural forms, i.e., Thermal Imaging Camera(s), as befits the context of the sentence in which it is used.

1.1. Approach

This work began with an assessment of the thermal imaging needs and activities of first responders. To gather this information, a workshop on Thermal Imaging Research Needs for First Responders was held at NIST in December, 2004 [4]. Ties were established between industry, the first responder community, and NIST that have, over time, helped shape the Proposed NFPA 1801 draft standard and have also accelerated the somewhat protracted standard development process. The results of the workshop will be discussed in Section 3.

Existing standards were collected and reviewed to ensure that the recommended testing conditions in this work are consistent with standards on other first responder equipment that is exposed to similar operating conditions, as well as standards and test protocols on infrared cameras that are used in other applications, when appropriate [3, 5, 6]. A survey of the literature was also performed to explore existing work in which the fire environment was well characterized and pertinent to TIC testing [7]. This work is explained further in Section 4.

Several series of full-scale tests were conducted at NIST's Large Fire Laboratory, in which attention was focused on temperature extremes and the presence of obscuring media such as smoke. These tests, outlined in section 5.5, helped bracket the thermal conditions in which TIC are used and also provided design guidance for bench-scale experiments. Bench-scale test facilities were constructed with an emphasis on developing test methods that can be replicated in testing laboratories that would be engaged in certifying TIC products under the provisions of a national standard. Detailed discussion of the full- and bench-scale tests conducted at NIST to support TIC research are presented in section 6.

The consolidation of all of this information, e.g., first responder feedback, literature search, and full- and bench-scale testing, provided a basis for defining testing conditions that challenge TIC in meaningful ways. Given a set of expected tasks that would potentially be performed by first responders using TIC in each of these testing conditions, which have been categorized into "thermal classes", it is possible to relate performance metrics directly to the environment in which TIC are used and the tasks typically performed by first responders in each thermal class. This is the subject of Section 5.

Performance metrics that describe TIC image performance are discussed in Section 6. These metrics include: contrast, which measures how well the TIC can represent differences in temperature; effective temperature range, which measures the maximum temperature at which the TIC is able to produce an image; spatial resolution, which measures how well the camera can discern small details; nonuniformity, which measures the quantity of noise present in the thermal image produced by the TIC; and thermal sensitivity, which measures the smallest temperature difference that the TIC is able to differentiate. Recommended bench scale experimental setups and test methods used to make these measurements are also presented.

The TIC display screen is the normal user interface and as such must be included as part of the system in imaging performance standards. The user's perception of the image displayed is also important because his/her ability to perform a task, such as finding a hazard, depends on how well he/she can interpret the image displayed on the TIC screen.

2. BACKGROUND

Before delving deeply into the performance metrics and testing procedures presented in this report, it is instructive to begin with some background on thermal imaging. The following subsections are intended to explain how TIC operate for fire service applications. It should be noted that thermal imagers and infrared technology in general are used for many purposes, including industrial processing, military, scientific, and building inspection applications. While there are many commonalities between the applications, there are also many differences.

2.1. Imager design

The nature of the conditions under which TIC are used has in large part influenced the development of imaging technology for fire service applications. For example, a fire fighter may encounter high temperatures, open flames, pools and sprays of water, and thick smoke; therefore it is important that TIC are capable of seeing in these obstructive conditions with a minimum amount of interference from the surrounding environment. Fire service thermal imagers are generally designed to detect radiant thermal energy in the $8\ \mu\text{m} - 14\ \mu\text{m}$ spectral range. This energy is radiated from solid surfaces and from certain gases that radiate.

A characteristic of the radiating surfaces and gases called emissivity affects how the thermal radiation intensity relates to the actual temperature in a way that can make the surface or gas appear to have a temperature that is different from reality [8]. A surface or gas having an emissivity of 1 is said to be a “blackbody”, meaning that it absorbs and re-emits all energy incident upon it, and thus is representative of its actual temperature. A surface or gas having an emissivity of 0 reflects all energy, making the surface or gas appear colder than it actually is. In general, surfaces that are flat black in color and somewhat rough in texture tend to have high emissivities and surfaces that are shiny and smooth tend to have low emissivities. Most TIC are designed to use a constant emissivity value of 0.95 in their internal algorithms used to convert the radiant energy signal to a temperature value. The further away an object’s emissivity is from 0.95, the less accurate that object’s surface temperature will appear to be. The term “apparent temperature” is used to account for temperature deviations caused by differences in emissivity.

Transmittance is a normalized measure of the clarity of a view path, or how much radiant energy is ‘transmitted’ through something, with 0 being completely opaque and 1 being perfectly clear (like looking through clean glass in the visible spectrum). The visible spectrum is between the wavelengths of $0.4\ \mu\text{m}$ and $0.7\ \mu\text{m}$, the infrared spectrum is anything above $0.7\ \mu\text{m}$ in wavelength. Figure 2—1 presents the transmittance of various gasses and soot which are likely to be present in a fire situation. Note that even though CO, CO₂, and water vapor are not visible to us in the visible spectrum, in parts of the infrared spectrum they block out significant quantities of the infrared radiation. A high transmittance band approximately in the $8\ \mu\text{m} - 14\ \mu\text{m}$ spectral range is evident, for this reason the fire fighting TIC are designed to operate in this region of the infrared spectrum.

Radiant intensity (the quantity of radiation emitted by an object) as a function of wavelength is shown in Figure 2—2. Thermal radiation coming from hot surfaces and flames may interfere with TIC imaging performance by creating too much signal. The peak in radiant intensity is well below the spectral range of interest, although it may still interfere with the imager’s ability to see

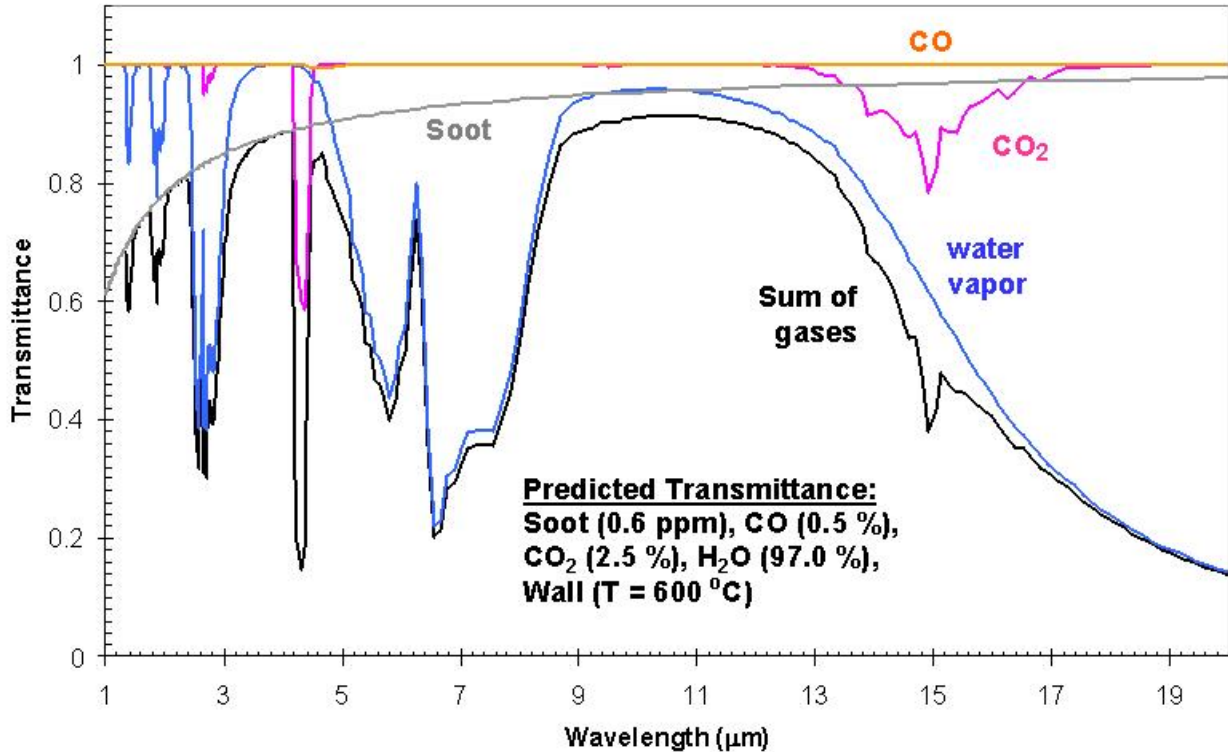


Figure 2—1. Predicted transmittance through a 12.7 cm (5 in) measurement path length for a simulated combustion atmosphere [9]. The soot, gases and wall temperatures are 600 °C.

the target in some test conditions. In some cases the TIC may also be able to recognize radiation emitted from the camera its self, this narcissus is largely avoided by optics design which collimates the infrared radiation, keeping it in a straight line so that only energy from the scene is interpreted by the camera.

The software program RADCAL [9] was used to perform these transmittance and radiant intensity simulations. The soot concentration of 0.6 ppm is a typical value derived from full-scale testing results (Section 5); however, the water vapor value of 97.0 % is based on the maximum water concentration attainable in superheated conditions (above 100 °C at 101.325 kPa). The actual water vapor concentration is expected to be much less than this. Therefore smoke is likely to be the principal absorber in the cell, and thus an important experimental parameter.

Fire fighters may rely in part on a TIC to navigate their way through a burning structure; therefore most imagers employ a wide field of view (FOV) in the range of 40° to 60°. There are few cases in which a fire fighter would need to focus on an object less than 1 m away, which encourages the use of relatively robust and lower cost fixed focal length optics that focus from 1 m to infinity. While temperature measurements provide useful information in a fire situation, the accuracy of the measurement is not as critical as it might be in other thermal imaging applications.

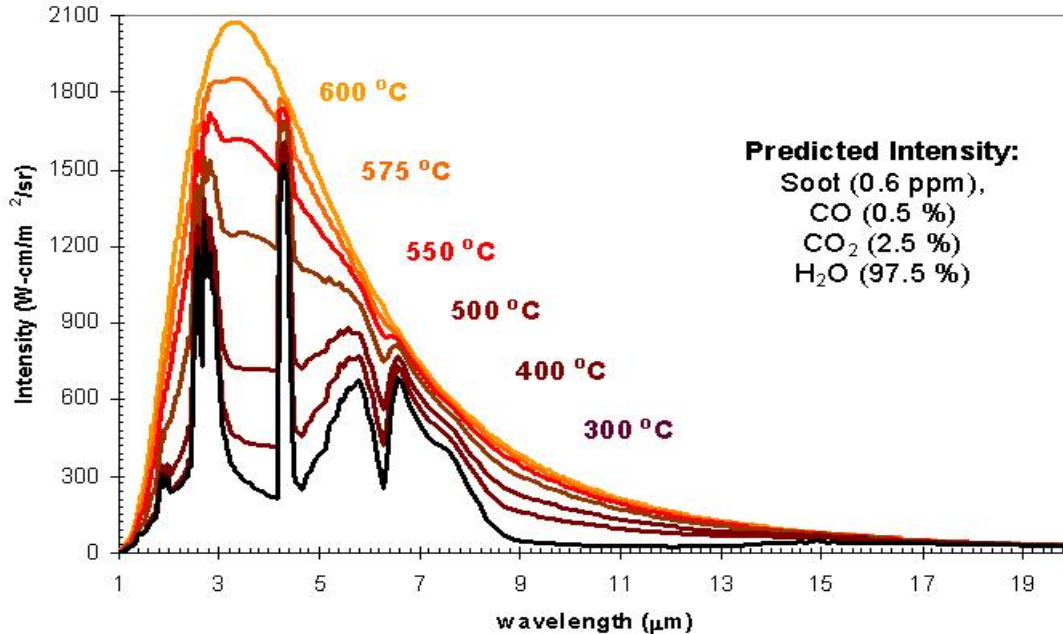


Figure 2—2. Predicted radiation intensity through a 12.7 cm (5 in) path length for a simulated combustion atmosphere consisting of 0.6 ppm soot, 0.5 % CO, 2.5 % CO₂, and 97.0 % H₂O [9]. The media temperature is held at 600 °C and the wall temperature varies from 0 °C to 600 °C.

The urgency of a fire event also dictates the need to keep the operation of the imager as simple as possible. Most TIC feature fully automated gain, focus, and iris settings, generally offering few manual controls other than a large on/off button that can easily be accessed by a fire fighter wearing heavy gloves. In some cases the imager may have one or two added functions, such as a zoom button or a toggle between IR and visible viewing.

2.2. Detector technologies

There are currently three well-established detector/sensor technologies available for purchase: barium-strontium-titanate (BST), vanadium oxide (VOx), and amorphous silicon (ASi). Manufacturers may utilize a single detector technology or may choose to offer a selection of TIC models possessing different technologies. Most detectors used for first responder applications are uncooled focal plane arrays (FPA), utilizing an array of sensors located at the focal plane of the optics, each specific detector technology is capable of generating different levels of information in the displayed image. Both the VOx and ASi cameras utilized uncooled FPAs while they BST cameras have a small thermoelectric cooler to stabilize the detector temperature. VOx and ASi cameras are called microbolometers, which means that the detector pixels are essentially very small heat flux gauges, changing their electrical resistance based on how much heat is absorbed by the pixel. The strengths and weaknesses of each detector technology are evident in Figure 2—3, where TIC representing the three different detector types are viewing an identical thermal scene simultaneously. The differences seen in this figure are the result of not only different detector technologies, but also different optical and electronic systems, which can contribute significantly to overall image quality. These three TIC also are of different sizes, weights, and cost.



VOx



ASi



BST

Figure 2—3. These three TIC are simultaneously viewing an identical thermal scene: a long corridor with a heated mannequin on the floor, and reflective and heated targets mounted on the wall at the end. A fire room is located adjacent to the corridor on the right.

The signal from the FPA is relayed to the imager's signal processor via a charge-coupled device (CCD). The optics package provides an interface between the signal processor and the recorded image and makes an important contribution to the overall performance of the instrument. This fact should be considered when viewing Figure 2—3. There are as many ways of designing optic and electronics packages as there are imager form factors and target market prices. The major design components of a generic TIC are shown below in Figure 2—4.

The thermal energy that radiates onto the TIC lens is focused on the detector. The signals generated by the detector are then manipulated into a video signal that is sent to the display. Some TIC also have a video output that can be used to record the signal via a hardwired connection or wireless transmitter/receiver . The signal that goes to the video output is not usually exactly the same as the signal that goes to the TIC display. The overall usefulness of the TIC is therefore very much dependent on the ability of the observer to interpret the image displayed on the screen well enough to perform a task or operation successfully.

The two typical FPA sensor sizes are 240 rows x 320 columns and 120 rows x 160 columns. The BST detectors, shown in Figure 2—5, are solid-state ceramic devices with an embedded array of sensors (or nodes) that convert changes in electrical polarization to voltage differences. A thermoelectric cooler provides thermal stability. These are AC-coupled detectors that measure relative levels of infrared radiation, thus the detector output requires a correction based on reference points provided by a chopper. A chopper is a bladed wheel that rotates directly in front of the detector such that it sees the chopper blades alternately with the thermal scene. The chopper blades are assumed to have a constant temperature² and the detector nodes are continuously reset to a uniform value corresponding to that temperature every time a chopper blade passes in front of the detector array. The oscillation between the thermal scene and the chopper blades provide the AC component to the detector signal.

The VOx and ASi detectors, see Figure 2—6, are both microbolometer devices that measure changes in the electrical resistance of the sensor material due to heat from infrared radiation. Microbolometers don't require cooling but are relatively sensitive to detector temperature. The output from these DC-coupled detectors is a function of the absolute level of incident infrared radiation. A shutter is used to periodically reset the detector's absolute radiation input level and prevent drift among the detector pixels [10]. Initially VOx was used as the sensor material, however, ASi is now also emerging as a viable sensor material.

Other detector technologies that have not become commercially available yet are under development as well. The performance metrics and test methods proposed with this work are intended to treat TIC as a "black box" from the lens to the displayed image, and therefore are expected to accommodate new technology as it becomes practicable.

² There is very little variation in the uniformity of the chopper blade temperature since the chopper is completely enclosed within the camera and only views the 'hot' scene for a small fraction of each revolution (<10%)

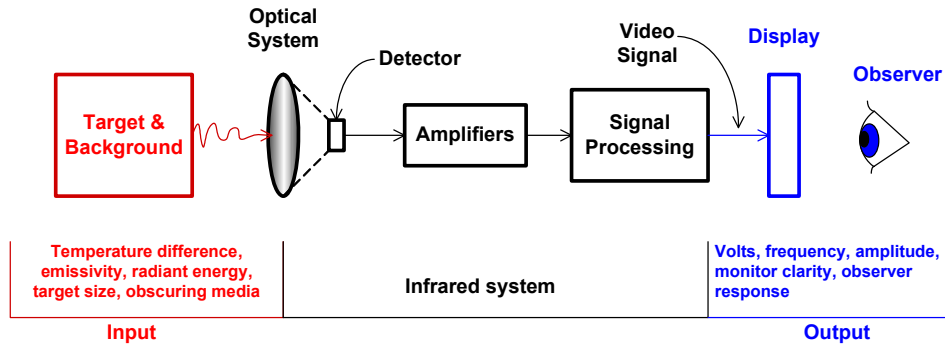


Figure 2—4.. Generic schematic of major TIC design components.

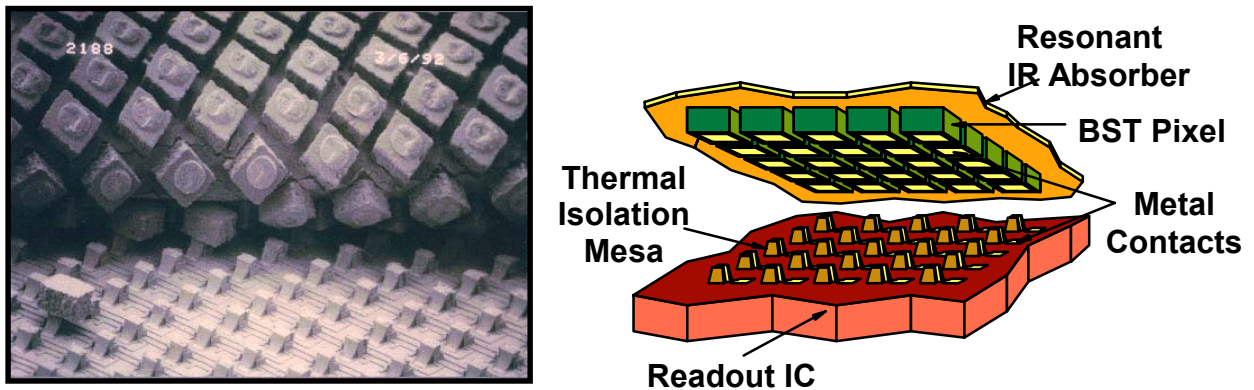


Figure 2—5. Hybrid Pyroelectric BST Detector. This is a solid-state ceramic detector that spontaneously polarizes when exposed to thermal energy [4].

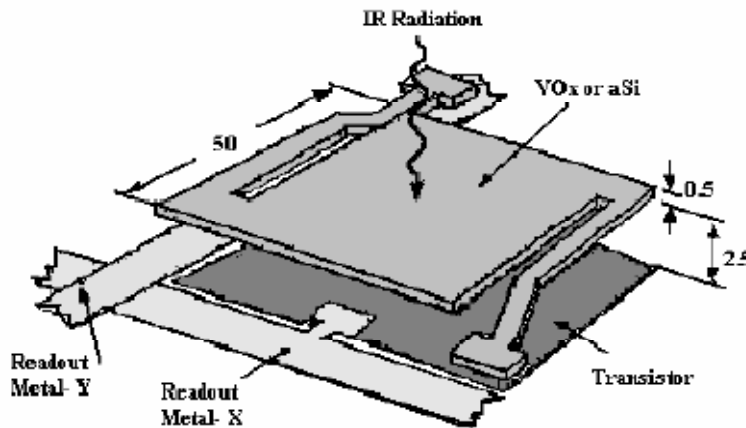


Figure 2—6. Microbolometer. This is an array of individual sensors, each of which generates a small portion of the overall thermal scene. The sensor material is either vanadium oxide or amorphous silicon [11].

2.3. Operating environment

An important step in the process of developing a meaningful performance standard for TIC is to establish test conditions that adequately represent the range of environments in which these cameras are used. First responders may use TIC for field operations ranging from searching for a hidden fire source, to directing a hose stream, to detecting the location of hazardous materials. New uses for TIC are being discovered as they become more widely used in the first responder community. At one boundary of the range of conditions in which the imaging performance of TIC is challenged, open flames and water coated surfaces may be seen in the same FOV. At the other boundary, the ability to see very slight differences in temperature and/or emissivity may be required to discern the level of contents of a chemical drum at near ambient temperature or in cases when a cold basement or warehouse is being searched. While it is relatively simple to capture the essence of the latter test condition in a repeatable laboratory setting, the former scenario, along with other conditions related to fire fighting, can be much more challenging and therefore are given particular attention in this work.

Decades of fire testing have shown that the gas temperature in a naturally ventilated burning room stratifies, due to buoyancy, into a upper layer that contains hot combustion by products and a cooler lower layer composed mainly of ambient air [12, 13]. The time-varying severity of the conditions in the room of fire origin and adjacent or nearby rooms will change depending on the type and amount of materials burning, the thermal properties of the room surfaces, the ventilation conditions, the size of the room, and a number of other factors. As most fire fighters will attest or describe, no two fires are exactly the same. For this reason, incorporating the chaotic and dynamic nature of fire conditions into readily controlled, reproducible, and repeatable tests that will be performed by numerous parties is a difficult task.

There are two basic ways in which operating conditions affect TIC: first, the camera itself must be rugged enough to function in elevated temperatures and humidity, and other adverse conditions; and second, the camera must be capable of producing images that provide useful information to the user. Performance metrics and standard testing protocols address the ability of the TIC to operate in a harsh environment. In 1999 a U. S. Navy report describes a series of tests conducted to determine which of eight commercially available TIC were sturdy enough to function in the harsh environment of a fire onboard a ship [14]. The Navy utilized 27 criteria ranging from battery life to corrosion resistance by which to judge the performance of the imagers. Image quality tests address the ability of the TIC to capture an infrared scene with sufficient sensitivity and detail to enable the user to perform a particular activity, such as searching for a fire victim. The work done to date at NIST on this project is primarily directed toward the evaluation of the imaging performance of TIC, although some related work is also concerned with certain aspects of the physical robustness of TIC.

2.4. Performance metrics

There are many generally accepted performance metrics designed to evaluate TIC used in scientific, security, and industrial applications [15]. A brief list of relevant standards is included in Appendix A of this document. A comprehensive discussion of these metrics and their implementation is provided by Holst [16]. This is a natural place to begin the development of performance metrics for fire service applications, however there are important differences

between scientific and fire fighting thermal imagers that affect the way image quality can be measured. As discussed in Section 2.1, TIC used by fire fighters tend to have fully automated controls, relatively large FOVs, and long minimum focusing distances. These characteristics make some of the established performance metrics difficult or impossible to apply. The NIST evaluation facilities were developed to determine which of the existing performance metrics are feasible to use for this application, to explore possible modifications that may improve their function, and to propose new imaging performance metrics when needed.

Another important consideration is that the end users of these imagers would be better served by performance metrics that are presented in a meaningful context. For example, evaluations involving individual pixels would probably be lost on a fire fighter. Performance metrics that are tied to understandable physical properties of the image and/or test conditions impart additional significance to fire fighters and other first responders, and thus will facilitate their acceptance into practical use.

The objective of this work is not to establish a rating system for all TIC used in first responder applications, rather, it is to provide imaging performance measurements that describe the usefulness of TIC in meaningful operating conditions. This approach leaves the operators free to decide which TIC perform adequately while also considering other criteria such as size, weight, anticipated uses, and cost.

3. WORKSHOP ON THERMAL IMAGING RESEARCH NEEDS FOR FIRST RESPONDERS

The Workshop on Thermal Imaging Research Needs for First Responders [4] was held at NIST in December of 2004 in order to better understand the needs of users, manufacturers, government agencies, and other proponents of TIC technology and to identify barriers that impede advances in the application of thermal imaging technology to emergency response. This workshop provided a forum to discuss the strategies, technologies, procedures, best practices, research, and development that can significantly improve thermal imaging technology for the first responder community. After hearing presentations, the workshop divided into three breakout sessions to discuss and prioritize issues relating to the following four questions.

1. What technological advances are needed?
2. What are the research needs for first responders?
3. What performance metrics are needed and how do they differ from current methods?
4. What standards are needed?

The issues that were found to be most important to the attendees of the workshop, divided into industry and first responder results are shown in Figure 3—1. The workshop proceedings are available at <http://fire.nist.gov/bfrlpubs/fire05/PDF/f05036.pdf>.

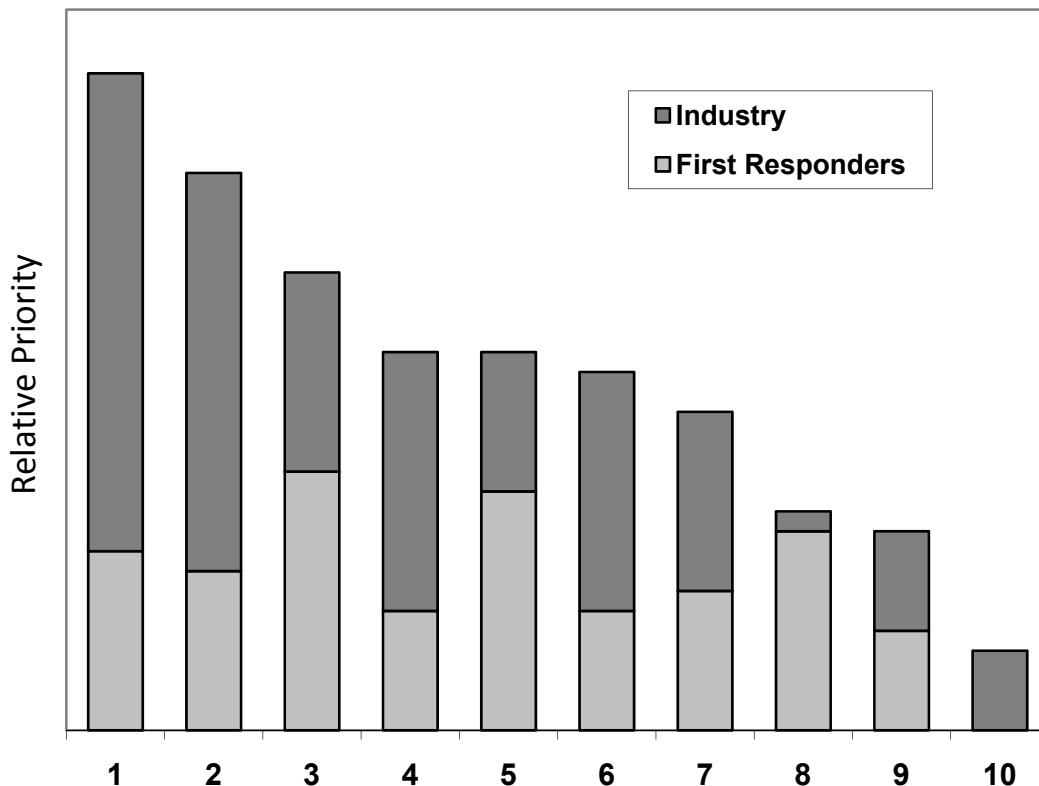


Figure 3—1. Thermal imaging research needs, as indicated by participants of the Workshop on Thermal Imaging Needs for First Responders in December, 2004. The key to the categories on the abscissa is provided in the following text.

Key for item numbers in abscissa of Figure 3-1:

1. Image quality (research, metrics, standards, contrast, sensitivity)
2. Durability (metric, mean time between failures, standard test methods for ruggedness)
3. Training and certification for users
4. Establish minimum/typical test environments
5. Human factor/ergonomic and human dynamics research
6. Image display (technology, viewability, metrics)
7. Battery and charger (life/maintenance, icons, and self-test improvements)
8. Reduction in imager cost (“water bottle” sized package priced at \$2K)
9. Standard target (for field test/calibration and emissivity target for turnout gear)
10. Imager self-test procedure and warning system

One important result of the workshop was the formation of a follow-on group of TIC manufacturers and fire service personnel that began meeting to devise an approach for standardizing the TIC user interface. This group grew to include representatives from all the U.S. manufacturers of TIC and TIC detectors. Eventually the image quality work described herein was included with the user interface results of the follow-on group.

In addition to hearing directly from stakeholders about their TIC research needs, information about fire environments and other operating conditions was also collected from the literature, from existing standards for other personal protective equipment, from internal test reports, and from full-scale and bench-scale testing. In order to gain firsthand experience on the use of TIC in burning buildings, some NIST personnel underwent training through a professional TIC training course³ for first responders. Direct communication between first responders and NIST personnel regarding the use of TIC and the environment in which they are used has continued throughout this research effort.

³ See SAFE-IR, <http://www.safe-ir.com/>

4. SURVEY OF RELEVANT STANDARDS AND WORK BY OTHERS

In this section, existing standards that relate to the development of a TIC performance standard are discussed. Additionally, existing research is presented that reports information on the thermal environment in which TIC may be used.

4.1. Relevant standards

There are several standards developing organizations that produce standards on electronic and other personal protective equipment used by first responders, and standard test methods do exist for TIC used in non-emergency service applications, but at the time of this writing there is no completed standard specifically written for TIC used by the fire service.

The following is a brief discussion of some details of existing standards that may have bearing on TIC operating conditions for design robustness and image quality tests. A list of these standards is provided in Table B-1 of Appendix B. American National Standards Institute (ANSI) standard ANSI/ISA-12.1201 covers intrinsic safety testing for nonincendive devices [17]. Several ASTM International standards are functional tests for exposure to salt spray [18], transmittance of lens [19], flame resistance [20], and liquid penetration [21]. There are also several ASTM test methods for infrared camera image quality [3, 5, 6, 22-24]; however, these test methods do not include extreme operating environments in their tests. Pertinent publications from the International Standards Organization (ISO) include enclosure integrity [25], electromagnetic compatibility [26], functional safety [27], and resolution measurements for still cameras [28]. The Military Standard, MIL-STD 810F, tests resistance to mechanical acceleration [29]. Underwriters Laboratory (UL) produces a large number of standard test methods for many aspects of design for electrical and electronic devices, such as proper grounding and wiring for switches and terminal blocks. The Video Electronics Standards Association (VESA) writes standard test methods for measuring display performance [30]. In addition to the above standards, which are not specifically written for fire service equipment, NFPA produces standards on communications systems [31], protective clothing for structural firefighting [32], protective clothing for wildland firefighting [33], self-contained breathing apparatus [34], and personal alert safety systems [35], which are intended for equipment that might be exposed to thermal environments similar to those experienced by TIC. Note that there are only two NFPA standards, on self-contained breathing apparatus [34, 36] and on personal alert safety systems [35], which are written specifically for electronic devices used in burning structures. Fire fighters sometimes use electronic gas detectors, but these devices have no formal standards for operation or functionality, although some comply with the ANSI/ISA standard on nonincendive devices [17]. Currently, some TIC manufacturers voluntarily adhere to some of the standards discussed here, but are not required to do so.

Table 4-1. Thermal Classes (Donnelly et al.)

Thermal Class	Maximum Time (min)	Maximum Temperature (°C)	Maximum Heat Flux (kW/m ²)
I	25	100	1
II	15	160	2
III	5	260	10
IV	<1	>260	>10

4.2. Work by others

Recent work by Donnelly et al. [7] recommends the concept of thermal classifications to systematize design robustness tests on first responder electronic equipment. The recommendations are based on experiments or studies performed by several research groups. The thermal classes are reproduced in Table 4-1.

The thermal classification system is useful for representing the increased risk to fire fighters related to the thermal environment. The most prevalent use of TIC would be in the first three thermal classes. Systematic use of a TIC in response to the fourth class of fires is unlikely as not enough time would be available under such hazardous conditions, however, brief exposure may occur as a fire fighter retreats from impending severe conditions. In addition, the current generation of TIC detectors tend to become saturated under such conditions, negatively impacting their effectiveness. It is expected that trends in visibility conditions scale with thermal class. For example, it is expected that less smoke is associated with a smaller Class I fire situation than a larger Class II or Class III fire.

It is useful to consider the results from compartment fire experiments to better understand the range of visibility and imaging conditions which a fire fighter may encounter. To evaluate the performance of TIC, the smoke concentration and possibly some gas species must be considered. Unfortunately, the understanding of smoke generation from a fire is incomplete. In a compartment fire burning realistic materials, the smoke generation rate (smoke yield per unit of fuel mass) is difficult to predict to within a factor of six or more, even for relatively simple fuels [37]. The smoke produced will increase with the fuel mass burning rate and the fire heat release rate, so, generally, the smoke concentration can be expected to increase with the thermal class categories listed in Table 4-1 as a fire grows and spreads and a hot upper layer develops.

A typical situation in which a TIC is used may involve a residential or commercial fire, where furnishings, structural materials, electrical appliances, and other materials burn in a flaming or smoldering mode. Many common commodities are composed of either cellulosic or thermoplastic materials. As these commodities burn, smoke and combustion byproducts such as carbon dioxide (CO_2) and water (H_2O) will be produced in significant quantities. Although much fuel mass is converted to CO_2 and H_2O , a significant percentage can also go to the production of smoke, varying from about 1 % to 20 % by mass, depending on the fuel type [38]. Smoke, or soot, is a product of incomplete combustion and is not a gas, but a complex solid particulate whose form and mass concentration depend on the type of fuel and the ventilation conditions within the compartment. Once formed, it is transported with other combustion products, first within a compartment and then beyond the room of origin. In actual fires, trace combustion species that are optically active (e.g., HCN, C_2H_4 , C_2H_6) may also be formed [39, 40]. These species are relevant to TIC performance because they may be optically active in the 8 μm to 14 μm portion of the infrared spectrum which is employed by TIC. In practice, these species may (or may not) negatively impact a TIC in realistic applications, as the combination of concentration and band intensities may (or may not) be significant.

Several full-scale compartment fire experiments in the scientific literature provide information on conditions in enclosure fires, such as those that may be encountered during fire fighting

operations. This information is also relevant when considering the performance of TIC. Table 4-2 summarizes some of these results, listing the fire heat release rate (\dot{Q}), the peak upper layer gas temperature, and the peak concentration of smoke in the room of fire origin. In the experiments listed in the table, the fire was ignited and a hot upper layer developed as noted by increasing values of temperature and smoke density. If the fires were controlled or prescribed, quasi-steady state conditions may have occurred in the upper layer, provided that the fires burned for a sufficiently long duration. Empirical correlations have been derived that relate the hot gas layer temperature and species to the heat release rate. As a fire spreads and grows through an enclosure or building, the hot upper layer in a severe fire can reach temperatures and smoke concentrations as high as 1000 °C and 20 g/m³, respectively. In a fire that is not prescribed (non-steady), the heat release rate depends on naturally occurring fire spread and growth. In that case, the time rate of change of the room conditions will depend on the fire heat release rate, the fuel type, the ventilation, the room size, and a number of other parameters.

Table 4-2. Peak conditions measured during typical compartment fire experiments

Reference	Thermal Class	Heat Release Rate \dot{Q} (kW)	Fuel Type	Peak Temperature (°C)	Peak Smoke Density (g/m ³)
Ref. [41]	IV	1,000 (Peak)	furnishings	1100	1 ⁴
Ref. [42]	III	200 (Peak)	furnishings	nr ³	20
Ref. [43]	IV	3,000	heptane/toluene ¹	540	2
	IV		heptane	500	0.3
Ref. [44]	III	1,000	toluene	200	0.4
Ref. [45]	IV	100	natural gas /acetylene ²	660	nr
Ref. [13]	IV	600	natural gas/wood ⁵	950	nr

1. liquid mixture of 60 % Heptane and 40 % Toluene (by mass).
2. gaseous mixture of 76 % natural gas and 24 % acetylene (by mass).
3. nr: not reported.
4. an optical density (D/l) of 5 m⁻¹ was reported. The value of D/l is related to the smoke density (C_s) and the specific extinction coefficient of smoke (ξ) by C_s = (D/l)/ξ, where ξ is typically on the order of 5 m²/g [42].
5. natural gas burner below wood-lined ceiling.

4.3. TIC operations

Before operating conditions are discussed, it is instructive to list the ways that TIC are currently being used in the field. This information is provided in the table below. From this, one can estimate the thermal and spectral environments that impact the design robustness and imaging performance of the cameras. Table 4-3 is not a comprehensive list; it was compiled from input from a variety of users and is expanding as the first responder community increasingly accepts TIC technology.

Clearly, not all first responders use TIC for every activity listed. Each first responder organization has its own set of thermal imaging needs and would potentially benefit from knowing how well a TIC performs in the activities that are most important to it. Due to trade-offs in the design of a TIC, it is unlikely that a single TIC will perform “better” than all of its competitors in every one of these activities. For example, TIC “A” might be optimized such that it can discern intermediate temperatures (such as a human) relatively well when flames are in the FOV, but it may not provide adequate thermal sensitivity at ambient temperatures to determine chemical levels in containers. On the other hand, TIC “B” may not produce sharply defined images in any of the above listed situations but can produce adequate images to perform the tasks needed. The needs of the first responders are best served when they are confident that the TIC will not fail in adverse conditions, and the image produced by the TIC is of a sufficient quality for their particular suite of activities.

Table 4-3. First Responder TIC Operations

Activity	Description
Size up	Assess hazard, find fire/heat sources, escape points, and vents
Communication	Lead or direct searches, interface with incident command, account for team members
Search	Locate victims, other first responders, fugitives, missing persons in dark and/or smoky environments
Tactical	Direct hose stream, check upper layer temperature, check for changing conditions, detect obstacles, passageways, damaged structural members, judge distances, use in rapid intervention teams
Overhaul	Ensure fire is out, look for hidden smoldering and hot spots
Forensics	Identify source of fire, determine fire spread, record video during fire for later use as evidence
Wildland Fires	Ground and air based search for hot spots and personnel
Hazmat	Determine material levels inside containers, track material movement and spill spread limits
Other	Preventative building maintenance, emergency medical applications, motor vehicle accident investigations

5. INFORMATION CONSOLIDATION- TEST CONDITIONS

As discussed in the previous section, when using a TIC inside a burning building, a fire fighter may encounter high temperatures, open flames, water sprays, dust, and thick smoke. To augment the literature search and to gain firsthand knowledge of TIC imaging performance in structure fires, two series of full-scale tests were conducted wherein the range of operating conditions expected in real structure fires was explored. The objectives of these tests were to characterize the image quality of the TIC and the way it relates to full-scale thermal environments, and to establish boundaries for gas, smoke, and surface temperatures and concentrations to be used in bench-scale tests. Also, these tests contributed to the adoption of a classification system for thermal conditions, which will be discussed in more detail in Section 7. In these tests, a collection of first responder TIC, scientific TIC, and visible cameras were trained on infrared targets, which were placed either in or adjacent to the room of fire origin. Temperature, gas, and smoke measurements were made both within the room of fire origin and in the adjacent spaces. The TIC and the targets were located at various times within the hot, smoke laden upper layer and within the cooler lower layer. Each of the experimental setups will be described in the following two subsections; the results for both test series will be discussed together as a whole in subsection 5.5. An important set of measurements of the constituents of smoke was part of one of the full-scale test series, which warrants special discussion. These measurements, and the results, are presented in subsection 5.3.

5.1. Series 1 test facility

This initial series of full-scale fire tests was designed to provide quantitative information on the thermal environment resulting from different types of structure fires. Qualitative information regarding TIC imaging performance in these conditions was also collected. This information was used to design bench-scale testing facilities and to determine which of the conditions likely to be present in structure fires will most significantly interfere with TIC imaging performance.

Tests were conducted with a variety of hydrocarbon fuels with widely varying smoke characteristics and heat release rates. The fuels included methanol, a commercial blend of heptane isomers, propylene, and toluene. In Table 5-1, the four test configurations are listed, along with the fuels and heat release rates (HRR). The layout of the structure is shown in Figure 5—1, along with the four target/burner/TIC configurations. For these tests, methanol fires were placed between the TIC and the target, and within the camera's FOV but not directly in line with the target. Heptane, propylene, and toluene fires were used to examine the effects of different smoke concentrations and upper layer temperatures on image quality. Dust and water vapor were generated and suspended in the air in conjunction with the various fuels. In some of these tests, flames were also present in the FOV. The three TIC used in each test were representative of each detector technology: ASi, VOx, and BST. A visible camera was also placed near the TIC to record target visibility.

Table 5-1. Series 1 test configurations

Configuration	Number of Tests	HRR (kW)	TIC Position	Target Position	Sight Distance	Fuel/Obscurant
A	8	200 to 300	lower layer	lower layer	3 m	methanol, heptane, toluene, dust, water vapor
B	2	175	upper layer	upper layer	5 m	toluene
C	9	0 to 200	upper layer	upper layer	5 m	methanol, heptane, toluene, dust, water vapor
D	13	12 to 300	upper layer	upper layer	5 m	methanol, heptane, propylene, toluene, dust, water vapor

A full-scale structure was constructed in NIST’s Large Fire Laboratory having standard 5 cm x 10 cm (2” x 4”) studded walls and gypsum board wall coverings, except that the walls in the vicinity of the fire source were covered with sheets of Marinite, a calcium-silicate based fire resistant material. The ceiling and floor were also covered with gypsum board or Marinite. The fire source was confined to various locations in a 3.7 m x 3.7 m (12 ft x 12 ft) room having a ceiling height of 2.4 m (8 ft). The target, shown in the inset to Figure 5—1, is comprised of 1.6 cm (5/8 in) copper tubing through which cooling water flows, and a thin sheet of stainless steel as a background. Thermocouples were placed on the inlet and outlet regions of the bars and on corresponding locations of the background. This simple target had a single bar frequency and was intended to provide an estimate of the TIC response to the operating conditions by measurement of the contrast between the target bars and the background. All target surfaces were coated with a paint having an emissivity of 0.94. Note that, for this test series, each test contained a single fire source and target. Temperatures in the room and corridor were measured using Type K, 24 gauge thermocouples arranged vertically at 0.3 m intervals in a “tree” formation. Smoke concentrations were measured gravimetrically for some of the tests by drawing a known volume of smoke laden gas through a particle filter.

The smoke and combustion gases were ventilated through a 6 m x 6 m hood and scrubbed in the Large Fire Laboratory’s exhaust system. In general, the repeatability of fire tests decreases as the scale of the tests increases; however, conditions inside the Large Fire Laboratory are controlled such that the full-scale fire tests are as consistent and repeatable as possible. Photos of the test setup and structure are shown for two test configurations in Figure 5—2.

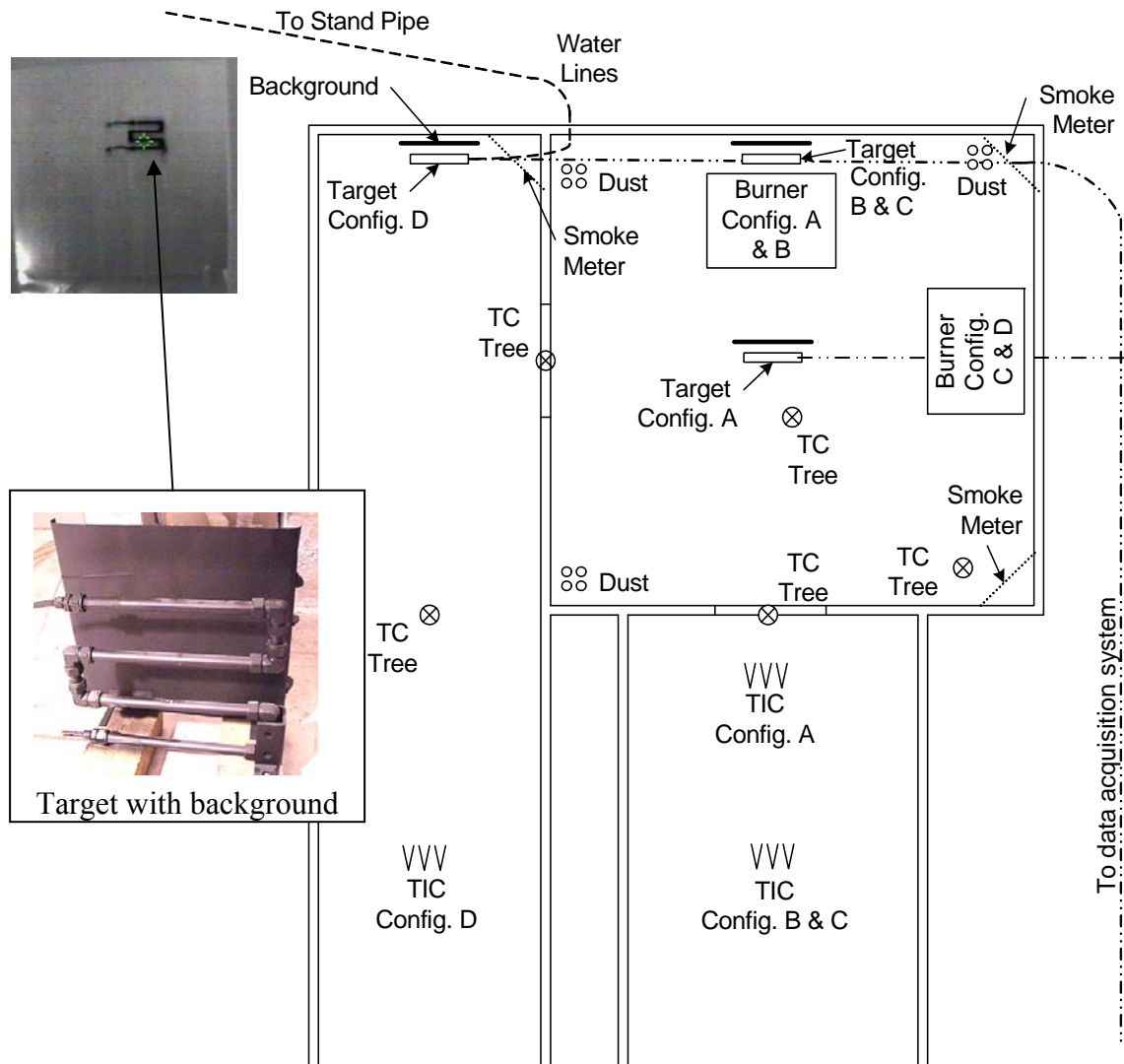


Figure 5—1. Plan view of Series 1 full-scale testing structure with inset showing the target and background. The target was placed on the floor in test configuration A and mounted on the wall 1.5 m from the floor in test configurations B, C, and D.



Figure 5—2. TIC are positioned in the hot upper layer viewing a target through heavy toluene smoke, test configuration D (left), and in the lower layer viewing flames and high heat conditions, test configuration A (right).

This first test series began to characterize the high temperature or fire conditions to be studied in greater detail in a second series of full-scale testing. The results of this first series will be discussed together with the results of the second test series in Section 5.5.

5.2. Series 2 test facility

For this second test series, more emphasis was placed on TIC imaging performance. The primary goal of these tests was to determine the extent to which the heat and smoke that is generated in structure fires affects TIC performance. The quality of the TIC images was measured in terms of the Contrast Transfer Function (*CTF*). This performance metric is used in different ways for several test methods proposed in this work. Used in the context of these full-scale tests, the *CTF* measures the contrast differences between the hot and cold bars of the targets as a function of their width or frequency. This measurement will be discussed further in Section 5.5.

This test series examined four different effects of fire on TIC image quality independently: effects of heat, effect of smoke, effects of real fuels versus idealized hydrocarbons, and the effects of gas versus smoke. Methanol fires having heat release rates ranging from 50 kW to 350 kW were used to isolate the effects of heat on image quality, as this fuel produces no smoke. Methanol, propylene and toluene produce increasing volumes of smoke, respectively, and were used to isolate the effects of smoke concentration on image quality. Real furnishings such as carpet and cushions were tested to examine the differences between actual furnished structure fires and hydrocarbon fires. A Fourier Transform Infrared Spectrometer (FTIR) was used to characterize the gases and smoke in the corridor.

For the second series of full-scale fire tests, a similar structure was built, having a long corridor with an adjacent fire room, except that in this case the TIC did not view the fire directly. The layout of this structure is shown in Figure 5—3. The TIC were placed on shelves that could be repositioned during the tests to view the targets from the upper layer, simulating a person standing, and from the lower layer, simulating a person on hands and knees. The shelves could also be relocated during the tests to either an alcove 6 m from the targets or the end of the corridor at 12 m from the targets. The targets were large bar targets that filled the end of the corridor, one in the upper layer and one in the lower layer. Water at approximately 20 °C flowed through the bars. The background for the bars was provided by hollow panels through which flowed hot water at approximately 50°C. All target and background surfaces were coated with paint having an emissivity of 0.94. An attempt was made to keep the target and background temperatures as constant as possible, however, this was very difficult to achieve during some of the more intense fire tests. Thermocouples were placed at numerous locations on the bars and the background. In addition to the bar targets, a heated mannequin fitted with fire fighter turnout gear was placed on the floor at the end of the corridor.

The structure was fitted with thermocouple trees and smoke measurement instruments. Smoke concentration measurements were made gravimetrically or, in a few cases, with a smoke meter that could slide along tracks down the length of the corridor. In addition to these measurements, O₂, CO and CO₂ volume fractions inside the fire room and corridor were measured using a Servomex 540A and Seimens Ultramat 6 gas analyzers, respectively. The heat release rate was measured by analyzing the composition, temperature and flow rate of the exhaust gases [46].

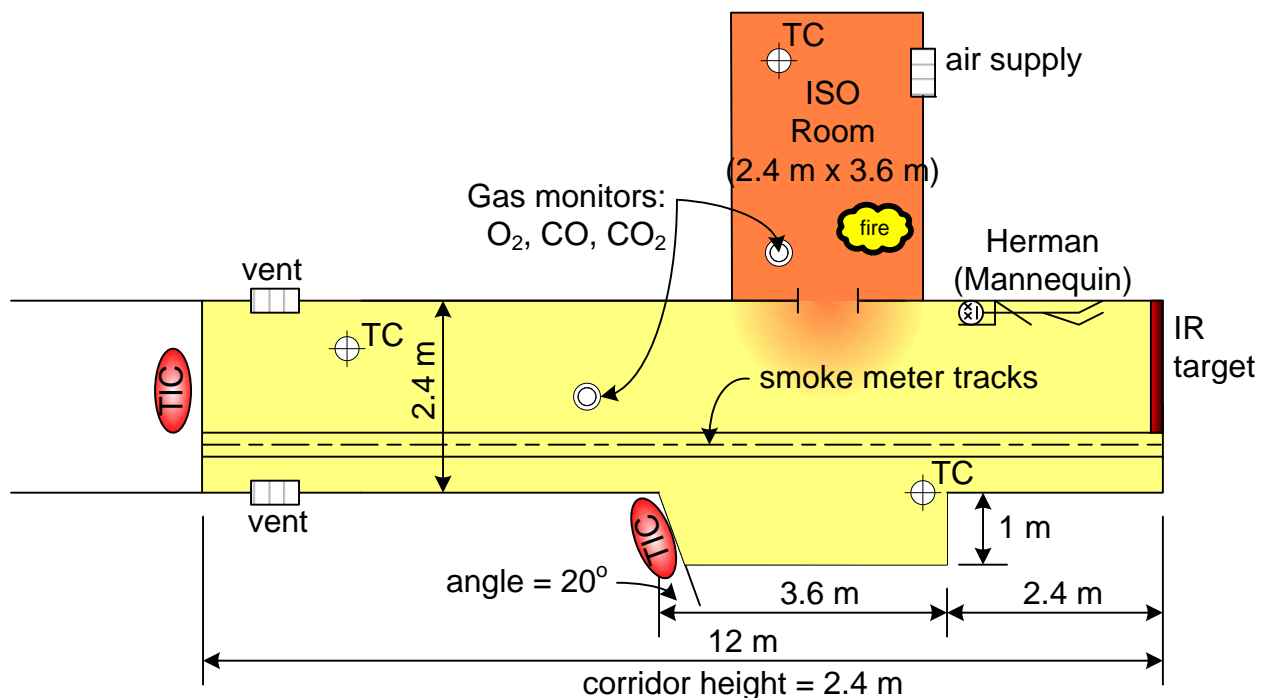


Figure 5—3. Plan view of Series 2 full-scale fire test configuration with TIC viewing IR targets having at two distances. A heated mannequin in fire fighter turnout gear was also placed in the FOV.

The collection of TIC used in this test series was comprised of 8 fire fighting TIC, of which 2 had BST detectors, 2 had ASi detectors, and 4 had VOx detectors. In addition to the fire fighting TIC, 2 scientific infrared cameras and 2 visible cameras were tested. The cameras were rotated through a sequence of four positions during each test, such that each TIC viewed the targets through the lower layer and through the upper layer at each of the two sight distances for at least 5 minutes in each position. For the unsteady tests this system made it difficult to maintain repeatability because the fire intensity grew and declined as the TIC were moved from position to position. In Figure 5—4, a photo of the TIC shelves at the end of the corridor are shown on the left and the two bar targets and mannequin are shown in infrared on the right.

The infrared targets can be seen in the background on the right of Figure 5—4. The width of the hot/cold bars in the infrared targets is 10 cm, 7.5 cm, and 5.0 cm, which were viewed at sight distances of 6 m and 12 m. The image on the right in Figure 5—4 shows these bars: the three left-most bars in this image have a frequency of 0.03 cyc/mrad at 6 m (0.06 cyc/mrad at 12 m), the next three bars to the right have a frequency of 0.04 cyc/mrad at 6 m (0.08 cyc/mrad at 12 m), and the four right-most bars have a frequency of 0.06 cyc/mrad at 6 m (0.12 cyc/mrad at 12 m). The redundant frequency of 0.06 cyc/mrad enabled an examination of sight distance effects.

The fire heat release rate and the peak CO₂ volume fraction, peak temperatures, and smoke concentrations that were measured in the line of sight between the TIC and the infrared targets are reported in Table 5-2. In some cases these measurements were made in the fire room, and in some cases they were made in the corridor, where the first responder would be operating, see the notes in Table 5-2.



Figure 5—4. The TIC were mounted on shelves which were repositioned midway through the tests (left). Two bar targets were used, one in the upper layer and one in the lower layer, along with a heated mannequin in fire fighter turnout gear, shown in infrared (right).

Table 5-2. Series 2 test configuration.

Number of Tests	HRR (kW)	TIC Position	Target Position	Site Distance (m)	Fuel
2	50	upper and lower layers	upper and lower layers	6, 12	methanol
2	350	upper and lower layers	upper and lower layers	6, 12	methanol
1	8	upper and lower layers	upper and lower layers	6, 12	propylene
3	32	upper and lower layers	upper and lower layers	6, 12	propylene
3	200	upper and lower layers	upper and lower layers	6,12	toluene
1	200 max	upper and lower layers	upper and lower layers	6, 12	single wood crib
1	300 max	upper and lower layers	upper and lower layers	6, 12	double wood crib
3	600 max	upper and lower layers	upper and lower layers	6, 12	cushions
3	2300 max	upper and lower layers	upper and lower layers	6, 12	Carpet/padding/wood

5.3. FTIR measurements

The intervening media between a target and an imager may impact the view of a TIC through emission, absorption, or scattering. The current generation of commercial TIC detect in the long wave-infrared region of the spectrum, from wavenumbers of about 700 cm^{-1} to 1250 cm^{-1} (wavelengths $14\text{ }\mu\text{m}$ to $8.0\text{ }\mu\text{m}$, respectively). As mentioned in Section 2.1, this region is selected for use because there is minimal overlap with the spectra of the most common combustion species. The spectral response of TIC may fluctuate between different technology types, and thus imager performance may be differentially affected by the presence of a hot layer of combustion products including smoke. In a typical compartment fire, smoke may easily obscure the presence of a human in the visible spectrum ($0.4\text{ }\mu\text{m}$ to $0.7\text{ }\mu\text{m}$). The impact of an intervening smoke aerosol on an imager's view depends on its temperature and its concentration as compared to the temperature and emissivity of a target. Smoke may absorb and scatter thermal radiation, but will not emit significantly.

Chemical compounds that give rise to a dipole moment absorb and emit infrared radiation at unique and characteristic frequencies. In the experiments reported here, a portable Fourier Transform Infrared Spectrometer (FTIR) was used to characterize the line of sight radiative emission in the infrared, from 650 cm^{-1} to 5000 cm^{-1} ($15.4\text{ }\mu\text{m}$ – $2.0\text{ }\mu\text{m}$), covering the entire spectral range of a typical TIC. The FTIR was positioned outside the corridor and was aligned to detect the same bar target that the TIC were positioned to view, looking through the hot upper layer of the full 12 m corridor length. The measurements were made at 0.5 cm^{-1} resolution,

which resulted in a sampling rate of about 1 scan/s. The measurements were stored as averages of sixty scans, or 1 min of data. The FOV was collimated, having a diameter on the order of 5cm at the 12 m distance. The results of this measurement are presented in section 5.5.3.

5.4. Hose stream experiments

Full-scale tests of the effectiveness of different types of hose streams were conducted. The objectives of these experiments were to understand the spray characteristic and suppression effectiveness of smooth bore (jet) and wide angle (fog) hose stream sprays, and to use this information to enhance the fire prediction capability of the Fire Dynamics Simulator (FDS) developed and maintained at NIST [47]. While these experiments were not intended to further the goals of the thermal imaging project, they offered an opportunity for collection of qualitative information about TIC imaging performance in the presence of water sprays and wetted surfaces.

The testing facility consisted of a 7.0 m x 7.0 m x 3.3 m compartment with a 4.6 m x 2.1 m opening. A heptane spray burner was located in one rear corner and an array of water collection apparatus was located in the other rear corner. The heat release rate of the fires was 2.2 MW. The water nozzles were oriented to spray diagonally across the enclosure into the water collection area. The water pressure and flow rate were varied throughout the test series. Gas temperatures and velocities, heat flux, and the mass of applied water were measured. Three thermal imagers were set up outside the enclosure to view, through the water sprays, a thermal target mounted on the back wall midway between the fire and the water collection apparatus. This arrangement is shown in Figure 5—5, with the TIC mounted on a rack covered in aluminum foil on the far left side of the image. The simple thermal target was comprised of a heated copper plate behind copper tubing through which flowed cold water. The temperature of the target background varied from 55 °C to 120 °C during the course of a typical 10 min test, while the cold tubing varied from 15 °C to 34 °C.

As mentioned above, these hose stream tests were intended to provide qualitative information about the effect of water sprays and wetted surfaces on image quality. The effect of flames in the field of view was also a significant factor in image quality. The results of these experiments are discussed in subsection 5.5.4.

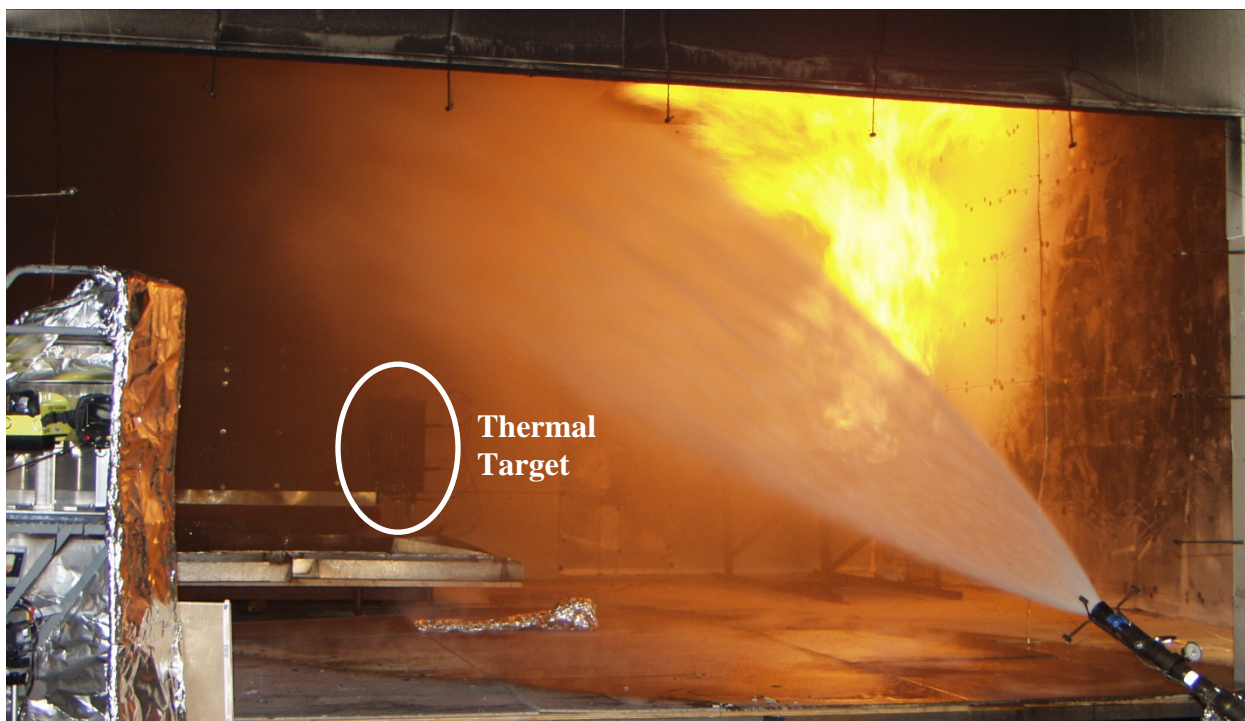


Figure 5—5. Visible image of typical hose stream test set up. Three TIC (behind foil on far left) are viewing a thermal target through a fog spray in the presence of a 2.2 MW heptane fire.

5.5. Full-scale experimental results

In broad terms, both full-scale test series (Series 1 and Series 2) were intended to provide information about the thermal environment in which TIC are expected to function. Both test series also investigated TIC imaging performance as a function of various environmental parameters, with the first test series acting as a scoping exercise for the second, more substantial test series. This information was used to determine which of the conditions likely to be present in structure fires will most significantly interfere with TIC imaging performance and to design bench-scale testing facilities.

Since the thermal environments that occurred during both full-scale test series are similar in nature, they will be presented together in the following text. Smoke and post combustion gas concentrations and temperatures, and surface temperatures are of particular interest as they tend to have the most significant impact on TIC imaging performance. Recall from Figure 2—1 that CO₂ and water vapor can potentially interfere with the transmittance of radiated energy, particularly around the outer edges of the TIC sensing region (8 μ m and 14 μ m). At the time these full-scale tests were conducted, the large fire laboratory did not have the ability to collect water vapor concentration data. In Table 5-3 the thermal environment data are presented for both full-scale test series. Note that CO concentrations were measured but not reported, as CO has a minimal influence on TIC imaging performance.

Table 5-3. Thermal environment (where applicable uncertainties are determined as stated in section 7.5 and expressed with a coverage factor of k=2).

Heat Release Rate \dot{Q} (kW)	Fuel Type	Peak CO ₂ Concentration (vol %)	Peak Temperature (°C)	Peak Smoke Density (g/m ³)
200	Methanol	nr	191 ¹ (± 3 %)	0.04 ¹ (± 10 %)
200	Heptane	nr	203 ¹	0.10 ¹
175	Heptane	nr	180 ¹	0.11 ¹
175	Toluene	nr	140 ¹	0.76 ¹
175	Heptane	nr	190 ¹	nr
12 to 21	Propylene	nr	83 ¹	0.14 ¹
33	Propylene	0.5 ² (± 10 %)	62 ³	0.15 ³
200	Toluene	2.9 ²	141 ³	0.46 ³
175	Toluene	nr	123 ³	0.45 ³
350	Methanol	5.9 ²	220 ³	nr
200	Methanol	nr	184 ³	0.1 ³
100	Methanol	nr	128 ³	0.1 ³
50	Methanol	0.6 ²	56 ³	nr
300 (Peak)	Double wood crib	6.5 ²	150 ³	nr
200 (Peak)	Single wood crib	2.0 ²	110 ³	0.01 ³
600 (Peak)	Cushions	5.7 ²	142 ³	0.75 ³
nr	Wood crib over carpet and padding	9.3 ²	200 ³	0.58 ³

1. Average peak temperature and smoke density values measured in room of fire origin.
2. Average peak CO₂ concentration measured in corridor adjacent to room of fire origin.
3. Average peak temperature and smoke density values measured in corridor adjacent to room of fire origin.

The qualitative TIC imaging performance results obtained for the first full-scale test series indicate that the presence of dust and water vapor do not significantly impair the imaging performance of TIC, even in high concentrations. Water mist, sprays, and wetted target surfaces were not tested at this time. Hot smoke and flames in the FOV, however, do have a negative impact on TIC imaging performance. It was found that the TIC detector technologies tested, an ASi, a VOx, and a BST, did not perform consistently across the different test conditions. Although the detector technology alone is not a sufficient indicator of TIC imaging performance, it appeared that low heat conditions were more amenable to microbolometers (VOx and ASi) than BST detectors. Conversely, conditions in which a wider range of gas and surface temperatures are present appear to be more suitable for BST detector technology, as seen in Figure 2—3. It should be emphasized that the TIC optical system, electronic processing, and display quality make large contributions to overall image quality. Advances in microbolometer technology in recent years have improved TIC performance greatly and other new detector

technologies are being developed that may prove to perform much better than anything currently available in the fire fighter market.

The above observations were used to design the test matrix for the second full-scale test series. For these imaging performance results the figure of merit is the Contrast Transfer Function (*CTF*), which is measured for the worst case test condition: upper layer position for both the TIC and the target. The video signal is averaged for 5 minutes at each of the two sight distances. The error bars in the following figures are derived from the standard deviation from the mean image pixel intensity, with a coverage factor of 2. The images were collected from digital videotape and have an 8-bit signal depth. The *CTF* is calculated using this equation:

$$CTF = \frac{I_{max} - I_{min}}{Bitdepth} \quad (1)$$

where I_{max} and I_{min} are the maximum and minimum image pixel intensities, respectively, and *Bitdepth* is the maximum possible image pixel intensity determined by the output signal. In this case $Bitdepth = 2^8 = 256$. The *CTF* can vary from 0 to 1, with a value of 0 indicating that there is no contrast in the image and a value of 1 indicating that the maximum possible contrast is present. It is expected that the *CTF* will decrease with increasing bar frequency as the TIC reach their limits of spatial frequency and the bar frequency goes into the signal noise (nonuniformity). Ordinarily, the *CTF* curve is normalized to a “zero” frequency, making it strictly a spatial resolution metric. This was not done for these tests because the absolute value of the contrast was also of interest.

Recall that there were five unique bar frequencies in the test configuration, with a redundant frequency at 0.06 cyc/mrad resulting from the bar dimensions combining with the sight distances in an equivalent way. This redundancy allows observation of the effects of sight distance, in other words, the difference between viewing a set of 5 cm thick bars from 6 m and viewing a set of 10 cm thick bars from 12 m is attributed to the TIC sight distance.

5.5.1. Heat effects

The two major areas of investigation for TIC image quality are heat effects and smoke effects. Results are reported for a total of six TIC, with two TIC representing each of the three detector technologies. In the following three figures, comparisons are made of TIC employing BST, VOx, and ASi detectors in two heat conditions. The fuel for these two test conditions was methanol, which produces a minimal amount of smoke, burning at a constant HRR of 50 kW and 350 kW. Recall from Table 5-3 that the maximum gas temperature in the TIC line of sight was 56 °C for the 50 kW fires, and 220 °C for the 350 kW fires.

The heat test results for the BST-type TIC are shown in Figure 5—6. These two TIC are the same model, purchased approximately 4 years apart. Significant differences in test results can be attributed to maintenance needs of the older TIC and to upgraded electronics in the newer TIC. The older TIC (TIC A) was sent to the manufacturer several months after this test series for maintenance. The detector array size for both TIC is 320 x 240 sensing elements. TIC B shows very little difference in *CTF* due to sight distance, and in fact no *CTF* degradation is apparent in the 50 kW case until the highest bar frequency is measured, whereas the *CTF* for TIC A drops considerably at 0.06 cyc/mrad, indicating a large sight distance effect, and continues dropping to

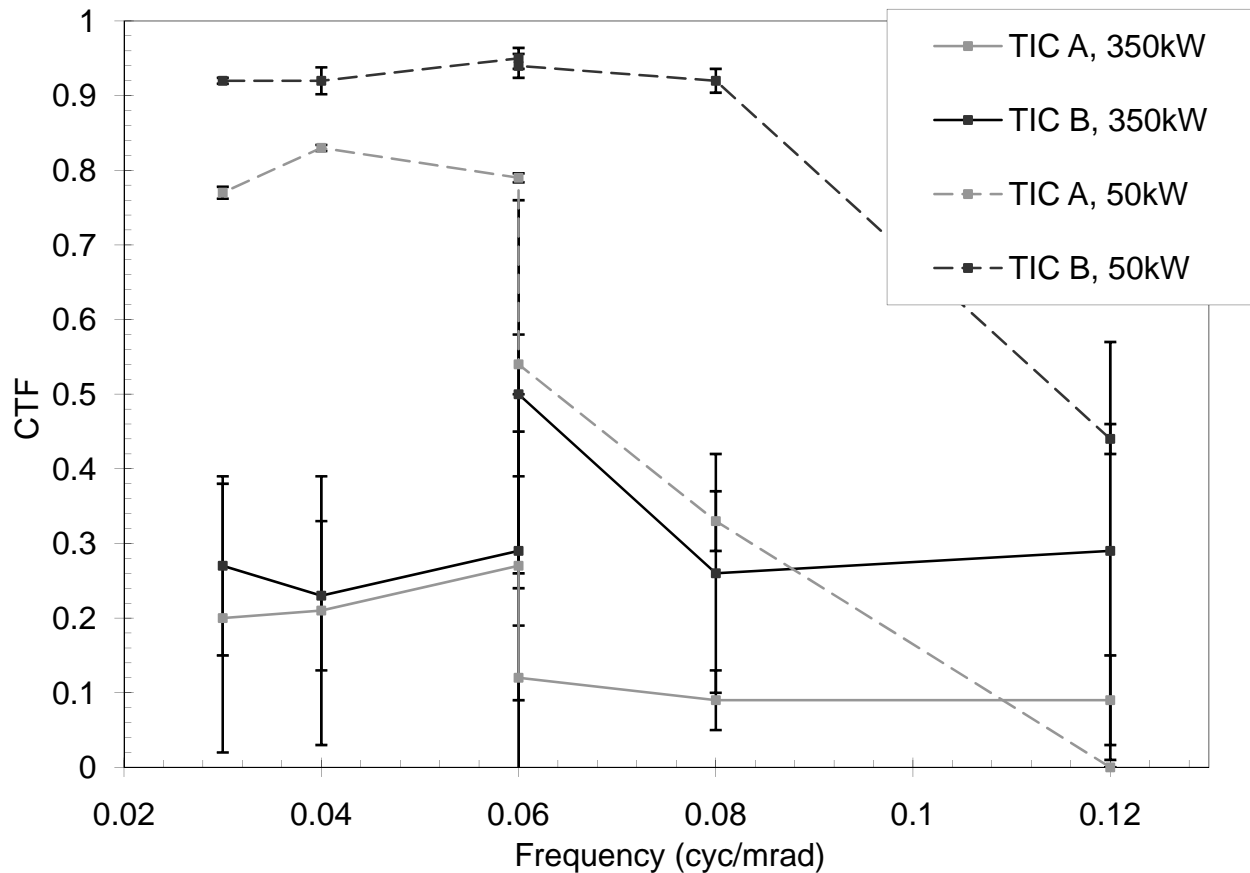


Figure 5—6. Comparison of heat effects, BST detector technology. These two TIC differ only in age, both having a 320 x 240 detector array. (where applicable uncertainties are determined statistically as stated in section 7.5 and reported with a coverage factor of k=2)

virtually zero at 0.12 cyc/mrad. The results for TIC B for the 350 kW case is somewhat puzzling. Here the *CTF* jumps *higher* at 0.06 cyc/mrad, meaning that the bars were more distinct to the TIC from a longer distance than they were at the shorter distance. This is the only time in this test series that this result occurred. In spite of this unusual result, TIC B still performed better than TIC A throughout the bar frequency range, although there was a lot of deviation in the signal, as seen in the length of the error bars. Neither TIC responds to increasing bar frequency at the 12 m sight distance for the 350 kW case.

The heat test results for the VOx-type TIC are shown in Figure 5—7. Both TIC used in these tests utilize a 160 x 120 pixel detector array that is produced by different detector manufacturers. The TIC themselves are also produced by different manufacturers, employing different optics and electronics systems. TIC C and D both show the characteristic decline in *CTF* with increasing bar frequency for the 50 kW case, although only TIC D is sensitive to sight distance effects. The absolute value of the *CTF* for TIC D at a bar frequency of 0.03 cyc/mrad in the 50 kW case compares well with that of TIC B above, however the *CTF* of TIC B remains much higher throughout the rest of the frequency range. This indicates that TIC B can distinguish finer image detail (has a larger spatial resolution). In the 350 kW case, the *CTF* of TIC D is

significantly higher than that of TIC C at the shorter sight distance, but both TIC perform virtually the same at the longer sight distance, with no response to increasing bar frequency. Again, TIC D shows a sensitivity to sight distance that is missing in TIC C.

The heat test results for the ASi-type TIC are shown in Figure 5—8. Both TIC used in these tests utilize a 160 x 120 pixel detector array that is produced by the same detector manufacturer but are not the same detector model. The TIC themselves are produced by different manufacturers, employing different optics and electronics systems. In Figure 5-8 the general shape of the curves for ASi-type TIC is similar to those in Figure 5—7 for VOx-type TIC, although the overall *CTF* values are slightly lower. In general, the microbolometers tested, both VOx and ASi, performed at a lower level in these tests than the BST-type TIC. This difference can be attributed in part to the smaller detector arrays and to the responsivity of the sensing materials. In the 50 kW case, TIC E performed better at the lower bar frequencies but about the same as TIC F beginning at 0.06 cyc/mrad. In the 350 kW case, TIC F does not show a sight distance effect, however, given the length of the error bars, the imaging performance of both TIC is considered to be statistically the same. Although the *CTF* values for the two TIC used in these tests are lower than the other TIC, ASi is attractive to TIC manufacturers because it is less expensive and can be housed in a smaller form factor. One of these TIC is a helmet-mounted device, which allows fire fighters to keep both hands free.

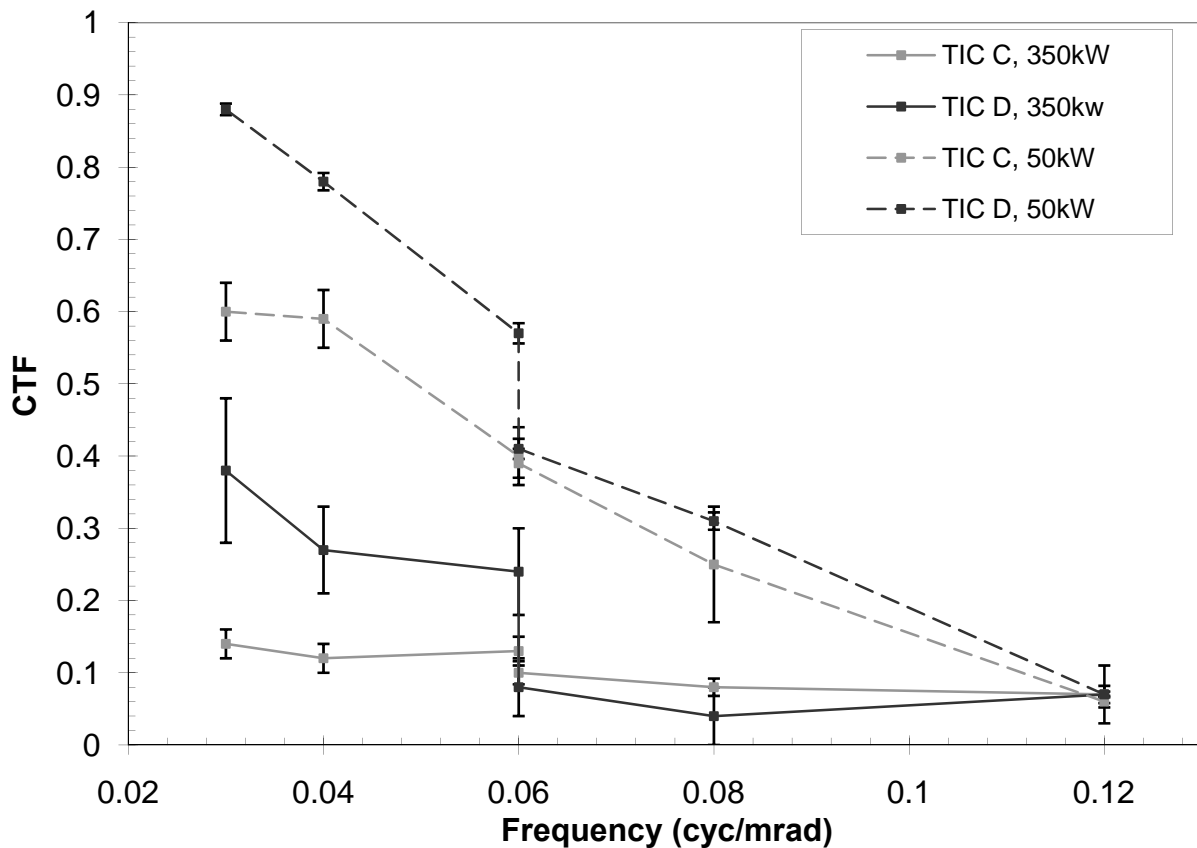


Figure 5—7. Comparison of heat effects, VOx detector technology.

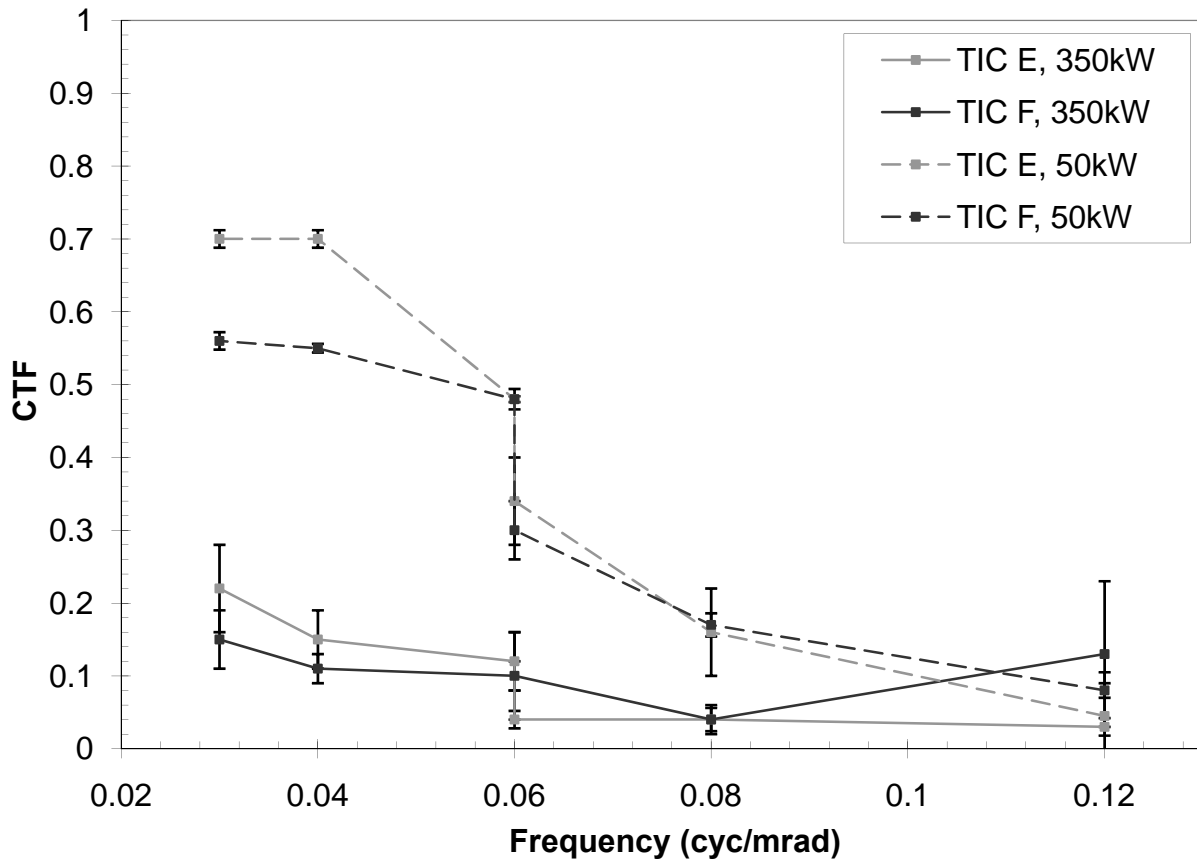


Figure 5—8. Comparison of heat effects for ASi detector technology.

In summary, these results show that some TIC are sensitive to sight distance effects when viewing a target through hot gases, while others are not. TIC with 320 x 240 detector arrays have higher CTFs at higher bar frequencies than TIC with 160 x 120 detector arrays indicating a larger spatial resolution of the camera. At the time of this writing, there are no ASi-type TIC that have detector arrays larger than 160 x 120 available on the fire fighting market. There are, however, VOx-type TIC available with 320 x 240 detector arrays, but none were available to the researchers at the time these tests were conducted. This type of testing, under more controlled conditions and in a bench-scale testing facility may be useful to indicate the need for TIC maintenance. Imaging performance is an important criterion to aid TIC users in their purchasing decisions, but it is not the only thing to consider. TIC size and weight, cost, handheld vs hands free, and other practical considerations also play important roles in determining the TIC that best matches the needs of a particular fire department.

5.5.2. Smoke effects

For these comparisons, the 50 kW test, which produces very little smoke, is again used as the base case. The light smoke condition is produced by 32 kW propylene fires, in which case the smoke concentration was measured at $0.143 \pm 0.02 \text{ g/m}^3$. The heavy smoke condition is produced by 200 kW toluene fires, where the smoke concentration was measured at $0.671 \pm 0.09 \text{ g/m}^3$. The same six TIC, positioned in the same locations as in the previous tests were used. The HRRs for the 50 kW methanol and 32 kW propylene fires make them better comparisons than the 200 kW toluene fires, which would also incorporate heat effects. The toluene fires, producing both high heat and smoke environments, are included as a worst-case condition.

The smoke test results for the BST-type are shown in Figure 5—9. Sight distance effects play an important role in image quality for both these TIC, rather than only TIC A, as was the case when heat only was being examined in Figure 5—5. For TIC B, the shorter sight distance combined with the light smoke condition appears to have no effect on the *CTF*. The heavy smoke condition, however, significantly reduces the *CTF* at the shorter sight distance for both TIC. As expected, increased smoke concentrations cause a decrease in the ability of these TIC to distinguish detail in a thermal scene. The heavy smoke condition for TIC B, and both smoke conditions for TIC A indicate that neither TIC is responding to increasing bar frequencies at the longer sight distance.

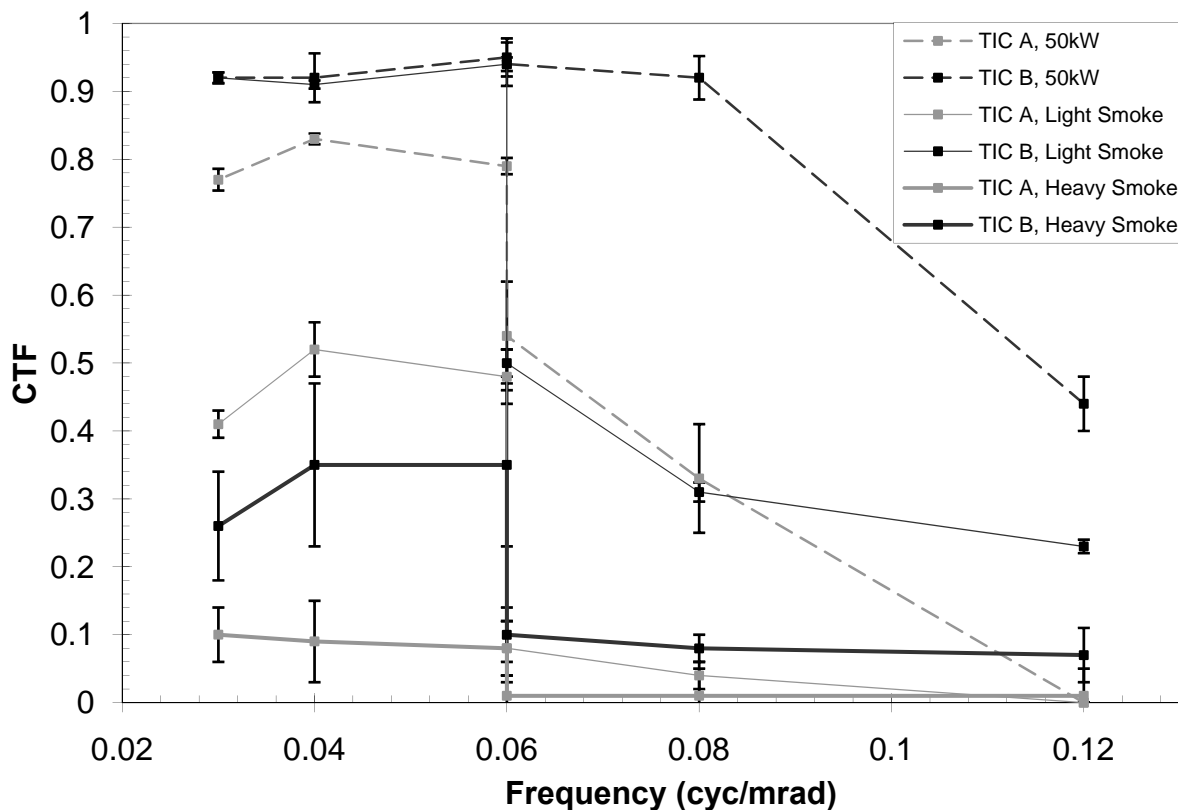


Figure 5—9. Comparison of smoke effects for BST detector technology.

The smoke test results for the VOx-type TIC are shown in Figure 5—10. Sight distance again appears to play an important role in TIC imaging performance, especially in the light smoke condition for both TIC tested. In the heavy smoke condition, neither TIC performed well regardless of sight distance. As with the BST-type TIC shown in Figure 5-9 above, the VOx-type TIC response to increasing bar frequencies disappears or is negligible in heavy smoke, particularly at the longer sight distance, producing about the same as or slightly lower *CTF* values than the BST-type TIC in these conditions.

The smoke test results for ASi-type TIC are shown in Figure 5—11. As with the comparison of heat effects between ASi and VOx-type TIC, the smoke effects are similar in the general shape of the *CTF* curves except that the *CTF* values are somewhat lower for ASi-type TIC, especially in the lower bar frequency range. Again, similar to the VOx-type TIC, it can be seen that these two ASi-type TIC are not useful tools in heavy smoke and heat conditions. When comparing the light smoke results with those of the VOx-type TIC, the ASi-type TIC show very similar performance.

In summary, these results show that all of the TIC tested were sensitive to sight distance effects when viewing a target through smoke. The microbolometers were unable to discern the target bars in high heat and smoke conditions even at low bar frequencies, while only one of the BST-type TIC was able to see the target bars at low frequencies. In light smoke conditions, the performance of the four microbolometers was similar, but only exceeded the performance of one of the BST-type TIC at bar frequencies above 0.06 cyc/mrad.

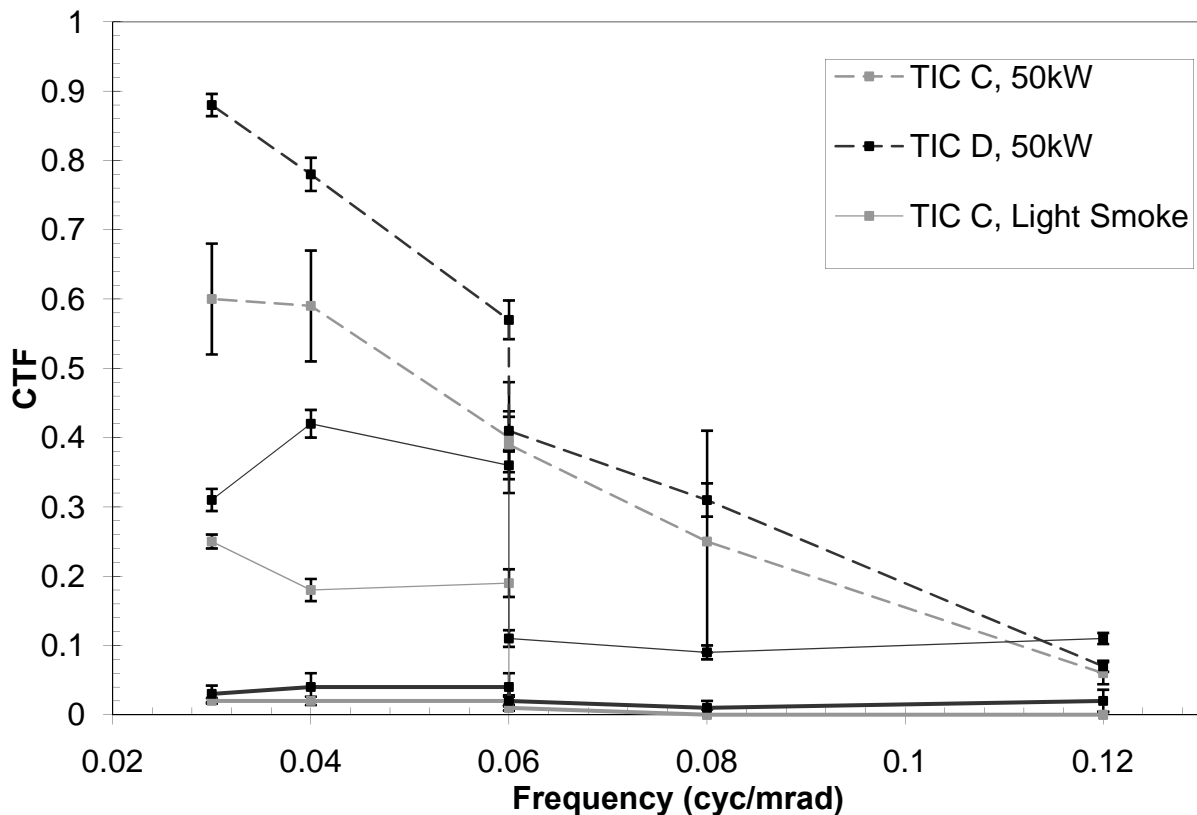


Figure 5—10. Comparison of smoke effects for VOx detector technology.

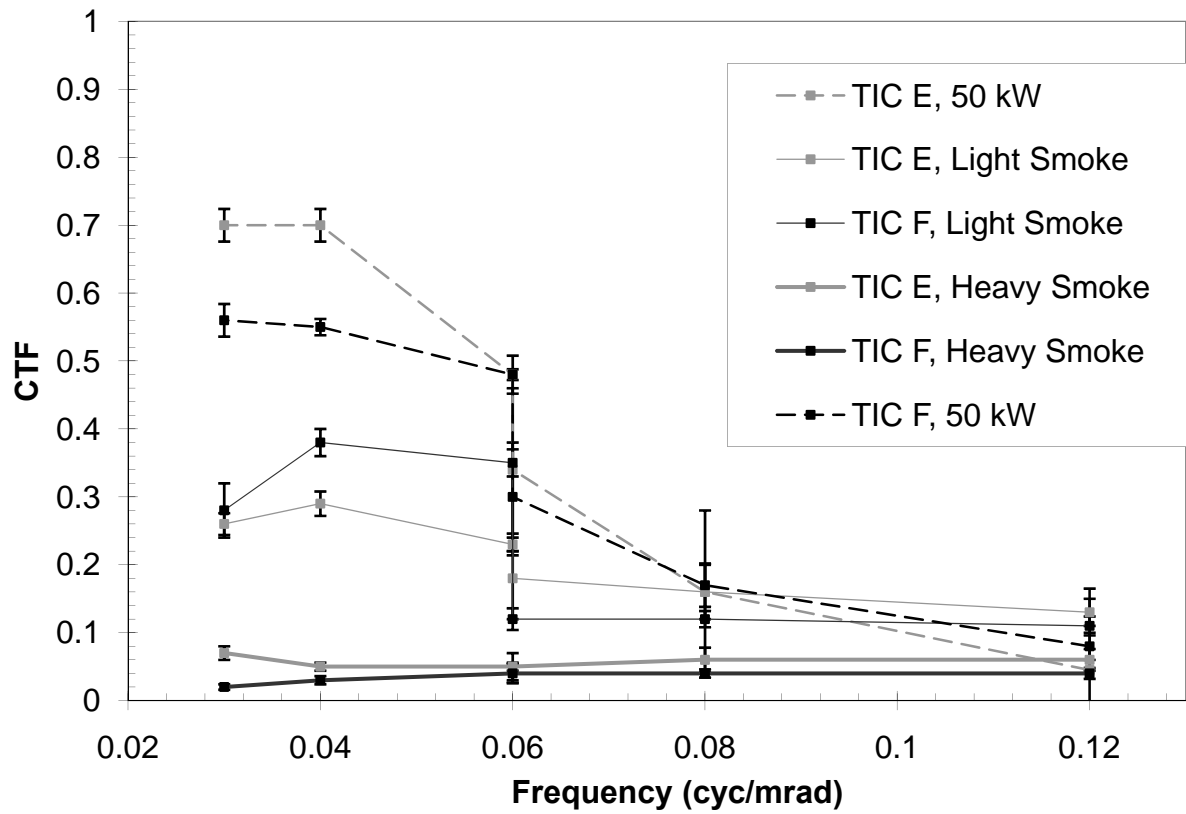


Figure 5—11. Comparison of smoke effects for ASi detector technology.

5.5.3. FTIR measurement results

Figure 5—12 shows the measured relative radiant intensity as a function of wavenumber during an experiment in which the burning fuel source was a wood crib over carpet and padding (see the last entry in Table 5-3). FTIR results are shown at 0min and 4 min after ignition in the experiments. The relative FTIR signal increased significantly with time. Table 5-3 shows that the upper layer temperature in the experiment obtained a peak value of about 200 °C, which occurred about 4min into the experiment. The upper layer temperature at 4 min suggests that the experiment was a Class III thermal condition at that time (see Table 4-2). At early times in this experiment, and for some of the other experiments, Class I and Class II conditions were tested. The FTIR measurement of a blackbody source at 200 °C (Type B uncertainty of ± 5 °C, based on accuracy of temperature measurements) is also shown in Figure 5—12, which is consistent with the experimental spectrum. This suggests that the smoke was optically thick in the hot upper layer of the corridor. Band absorption by water vapor is seen for wavenumbers between about 1300 cm^{-1} and 2000 cm^{-1} ($7.7\text{ }\mu\text{m}$ and $5.0\text{ }\mu\text{m}$). The figure shows recognizable emission signatures for individual species during the experiment, but not in the spectral region in which TIC are sensitive, recall from discussion of Figure 2-1, which reinforces the reason TIC are designed to operate in this portion of the infrared spectrum. The results for the other fuels types yielded similar results, as little band radiation was observed in the portion of the spectrum where the TIC are sensitive.

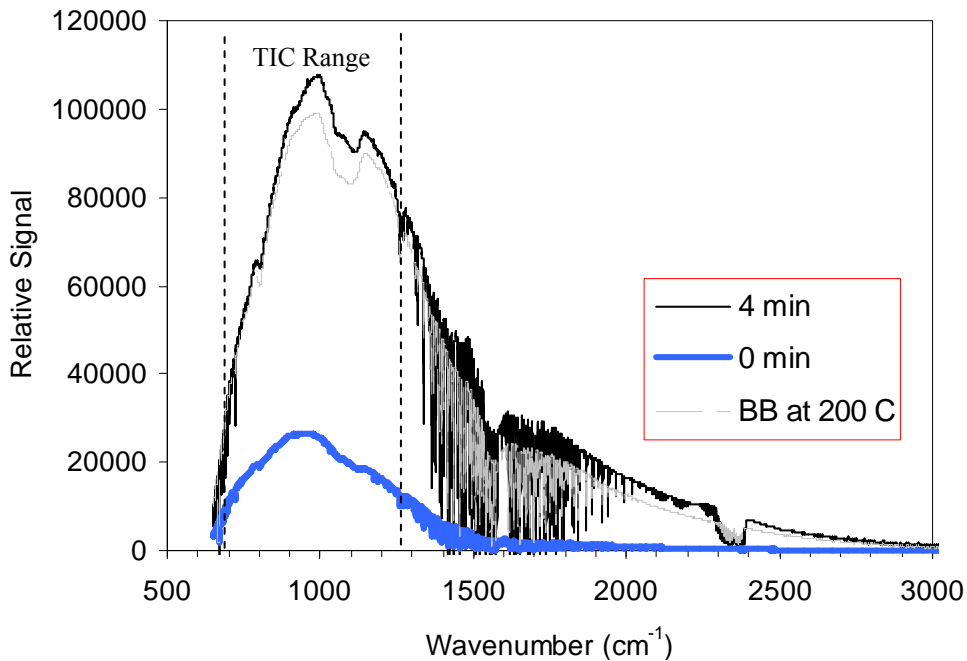


Figure 5—12. The relative FTIR signal measured at two times during an experiment burning carpet, padding, and wood. For comparison, measurement of the relative signal of a blackbody source at 200 °C (± 5 °C, as per manufacturer’s documentation) is also shown.

5.5.4. Hose stream results

The three TIC chosen for this work were selected because they were available at the time the hose stream tests were conducted. Therefore, due to a temporary lack of availability of one type of TIC detector, the usual mix of BST, VOx and ASi detector technology was not used. In Figure 5—13 below, the center image was produced by a BST-type TIC and the top and bottom images were produced by two different manufacturers’ ASi-type TIC.

Note in Figure 5—13 that there is a distinct difference in the amount of detail between the center image and the others, and that, while the top and bottom images are relatively similar, there are also noticeable differences as well. For example, the water spray is barely visible in the right image. Other observations were: prior to ignition of the fire, all three TIC showed gray scenes with only the target and the pilot light for the fire being distinctly visible. The cold target bars were visible only in the BST-type TIC images prior to fire ignition. After the fire was ignited but prior to the application of water, the two ASi-type TIC behaved somewhat similarly. The cold target bars were barely visible in one case and quite visible in the other case, and then the entire target turned dark while the rest of the image was saturated (bright white) as the compartment surface temperatures rose and saturated the TIC detectors. The BST-type TIC continued to show the target bars and a gray scene elsewhere in the image. During the application of water sprays, as shown in Figure 5—13, the target is not readily apparent, however, it does appear to some degree in the *CTF* calculations for all three TIC.



Figure 5—13. Thermal images of a scene in which a fog spray is directed toward a wall in front of a 2.2 MW heptane fire. A BST-type TIC produced the center image and ASi-type TIC from different manufacturers produced the two other images.

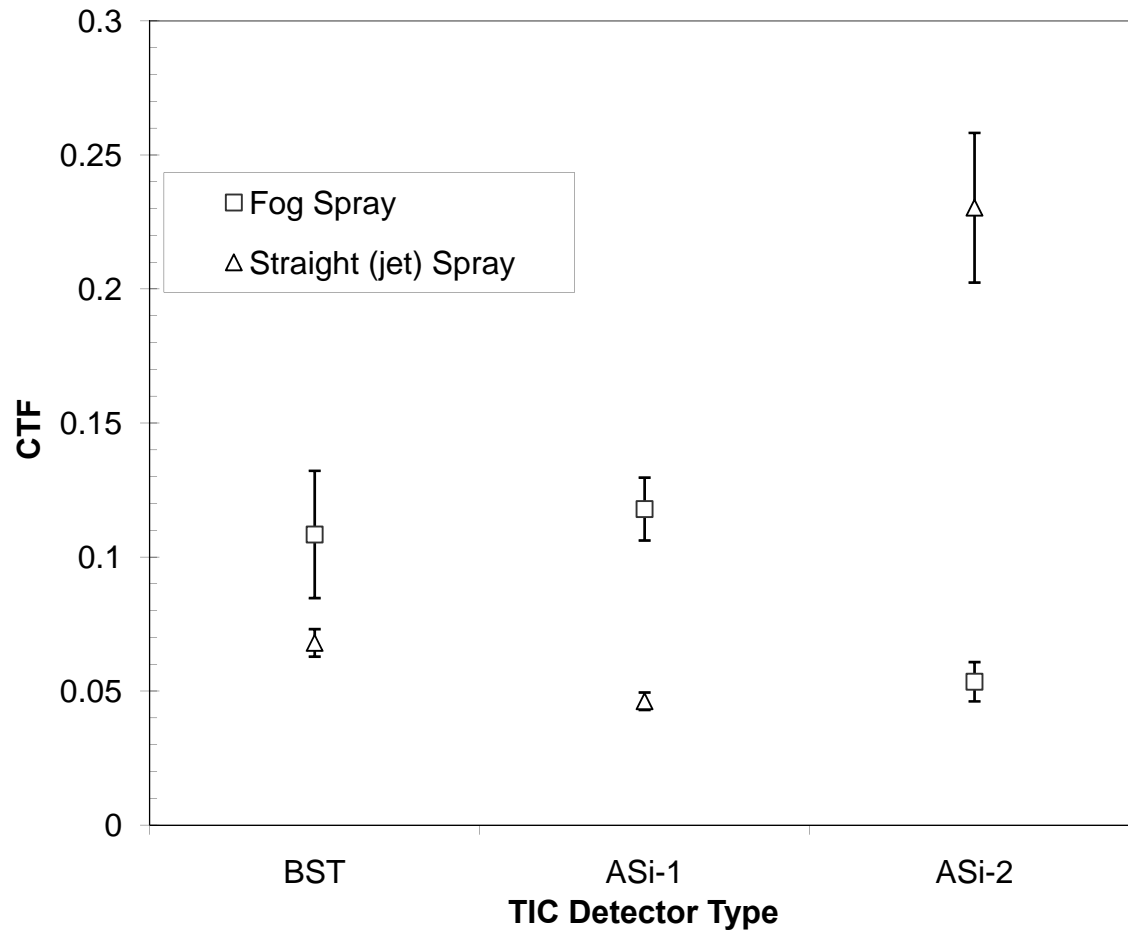


Figure 5—14. *CTF* of a thermal target viewed by three TIC through fog and straight (jet) sprays with a 2.2 MW fire in the field of view. The error bars represent the standard deviation of the *CTF* with a coverage factor of 2 (95 % confidence).

The *CTF* was calculated during the water spray application; images that were captured from digital videotape at a rate of 30 frames/sec for a period of 40 s were averaged to determine the *CTF*. The *CTF* data are presented in Figure 5—14. The error bars represent the standard deviation of the *CTF* measurements with a coverage factor of 2 (95 % confidence).

Although the bars of the thermal target observed in images on the BST-type TIC display and in the videotaped images appeared to be more visible than those of the other two TIC, the data displayed in Figure 5—14 shows that one of the ASi-type TIC provided significantly better target contrast in the jet spray case. It is possible that the jet was not positioned directly between the TIC and the target when the data was collected, in which case the obscuring effect would be minimal. It should be noted that *CTF* values below about 0.2 indicate contrasts that are only marginally useful to TIC users since they are likely to be in the noise floor of the camera caused by image nonuniformity. Human perception of contrast, noise, spatial resolution, and other image characteristic are not being studied as a part of this work.

5.6. Consolidation of test condition information

Based on the survey of previous work and the full scale investigations discussed above TIC activities have been categorized in Table 5-4. Table 5-4 is based on the thermal classes noted before in Table 4-1 but has been modified to more accurately reflect the specific situations necessary to be evaluated for TIC performance. The test results reported in Table 4-2 provides guidance as to the nature of the thermal environment that might be encountered while the TIC operators are engaged in fire fighting activities such as those listed in Table 4-3. Existing standard requirements for design robustness tests are embedded in the development of the four thermal classes, e.g., a TIC used in a Class III environment should be able to function properly under the same conditions in which fire fighter turnout gear is tested (e.g. withstand temperatures up to 260 °C for 5 min per NFPA 1971 [32], see Appendix B).

With respect to image quality, there are two general areas of interest. First, the ability of a TIC to discern detail in a thermal scene has important implications regarding the suitability of that TIC to perform certain activities. For example, being able to see a victim on the floor as illustrated in Figure 5—4 or being able to see through a hose stream as illustrated in Figure 5—5 and Figure 5—13. Second, the thermal sensitivity of the TIC is important, because the range of surface temperatures that may co-exist in the FOV may be very wide or very narrow. To illustrate the way these two performance metrics interact, recall the earlier example of a TIC used to observe a human with flames in the FOV illustrated below in Figure 5—15. If the spatial resolution (ability to discern detail) is poor, the TIC user may not be able to see any difference between a human and building clutter, regardless of the thermal sensitivity of the TIC. If the thermal sensitivity is poor, the TIC user may not be able to differentiate items having small temperature differences, regardless of the detail in the TIC images. Table 5-4 consolidates the operating environment, expected TIC activities, and imaging performance needs with each thermal class. A natural outgrowth of Table 5-4 is the selection or development of appropriate imaging performance metrics and tests that meet the needs of the fire service community. This is the subject of section 6 on imaging performance metrics and test methods, where the proposed tests in Table 5-4 are explained in detail.



Figure 5—15. Identical scene from full scale test series two observed with three different cameras. From top to bottom VOx, ASi, and BST TIC are utilized to view the same scene at the same time consisting of a mock victim on the floor with smoke and flames in the field of view.

Table 5-4. Proposed TIC Testing Conditions.

<u>Class</u>	Class I <i>(water, fog, or snow possible, minimal heat, smoke and flames)</i>	Class II <i>(elevated temperatures, water, dust, smoke and flames may be present)</i>	Class III <i>(high temperatures and smoke concentrations, flames, dust, and water are likely)</i>
<u>Activity</u>	Hazmat Medical Motor vehicle accident Search	Overhaul Size up Forensics Preventative maintenance Search	Overhaul Forensics Wildland fires Size up TacTIC Communication Search
<u>Proposed Test</u>	Measure smallest ΔT at nominal target temperatures of 1 °C, 30 °C, and 100 °C. <u>Also</u> , measure spatial resolution and nonuniformity of image.	Measure smallest ΔT at nominal target temperature of 160 °C. <u>Also</u> , measure <i>largest</i> overall ΔT at which target with small ΔT is visible. <u>Also</u> , measure spatial resolution and nonuniformity of image.	Measure smallest ΔT at nominal target temperature of 260 °C. <u>Also</u> , measure spatial resolution and nonuniformity of image.
Note: TIC would not likely be used in a Class IV thermal environment. First responders operating in Class IV thermal conditions would be in retreat, rather than viewing the scene through a TIC, although one might reasonably expect to view a Class IV scene from a distance.			

6. PERFORMANCE METRICS AND TEST METHODS

While this work focuses on imaging performance metrics and test methods, it is also necessary to consider the effects of performance requirements for TIC design robustness because image quality may be used as the pass/fail criteria for many of these tests used by standards organizations. For example, an environmental temperature stress test may require the TIC to be exposed to an elevated temperature of 60 °C for 4 hours, then be exposed to a low temperature of –20 °C for 4 hours, and then experience a thermal shock (changing from –20 °C to 60 °C within 5 min.). Immediately after each of these three procedures the thermal image produced by the TIC is evaluated to determine whether the procedure had an adverse effect on image quality. The procedure for examining the effect of a design robustness test on image quality is the Image Recognition Procedure and will be discussed in section 6.1. The images used to evaluate image quality, other than the Image Recognition Procedure, are collected directly from the TIC display. A brief description of the setup used to capture and process these images is provided in section 6.2.

There are five image quality performance metrics, along with their accompanying test methods, which were developed to measure various aspects of image quality as presented to the end user on the TIC display. Going back to Table 4-1, after considerable investigation, several tests were proposed in common with Class I, II, and III environments. They are contrast, image nonuniformity, spatial resolution, and thermal sensitivity. In addition, a new test was developed for Class II environments: the effective temperature range (ETR) test, which measures TIC performance with a wide range of temperatures in the FOV. The ETR is only included for a Class II environment because the Class II environment encompasses the largest temperature range and overlaps both the Class I and Class III environments. These science-based, objective tests are described in detail in sections 6.3 through 6.7. Test results, which highlight the range and variability of TIC imaging performance, are presented and discussed briefly in section 7.

6.1. Image Recognition Procedure

The Image Recognition Procedure (IRP) is a relatively simple method of determining whether a design robustness test has adversely affected the image quality of a TIC. Image recognition may be included as a pass/fail criterion for other physical performance tests: Environmental Temperature Stress, Immersion/Leakage, Vibration, Impact-Acceleration, Corrosion, Heat Resistance, and the “Torture Test”. For the IRP, the test operator uses the TIC under test to view a reflective test target with converging lines in the vertical and horizontal directions is viewed at a distance of 1m, as shown in Figure 6—1 and Figure 6—2, and records the vertical and horizontal values at which the lines appear to blur together. The reflective surface of the target (white areas in Figure 6—1) has an emissivity (ϵ) ≤ 0.1 and the black matte background has $\epsilon \geq 0.9$ in the 8 μm to 14 μm wavelength range. The target reflects radiation from an extended area blackbody or similar heat source. The resulting image recognition values, each of which correspond to a nondimensionalized spatial resolution, must exceed the minimum values established in the performance requirements. The target design for this procedure was adapted from a portion of the ISO 12233 test chart [28].

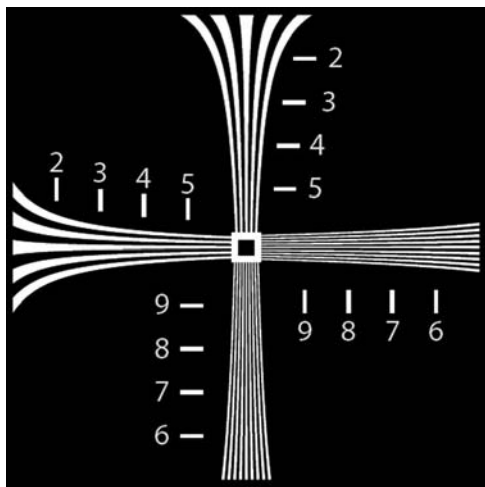


Figure 6—1. Reflective test target used for image recognition tests. The test target dimensions are 61 cm (24 in.) in each direction. The white markings shown here are highly reflective foil with an $\epsilon \leq 0.1$ and the background is foam core with a black matte finish having an $\epsilon \geq 0.9$.

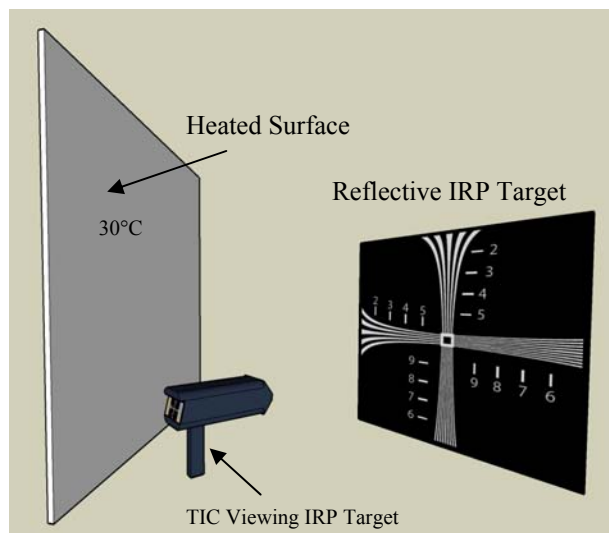


Figure 6—2. An example viewing configuration is also shown (right) with the TIC positioned 1m away from the IRP target surface.

Before any other testing begins on the TIC, the test operator performs the IRP in order to establish that the TIC can provide an image of acceptable quality. If the TIC cannot provide such an image there is no point in further testing. If the image is acceptable, the TIC is tested as required by the standard. After each of the design robustness tests is performed, the IRP is conducted to ensure that the TIC is still capable of providing an acceptable image. In some cases additional pass/fail criteria are stipulated, for example in a Immersion/Leakage test, the TIC may be required to provide an acceptable image and also have no water inside its electronics compartment.

The image recognition test target is situated as illustrated in Figure 6—2. The test is conducted in a thermally stable 25 °C (77 °F) environment, surrounded by a shroud (not shown), and reflects only heat generated by a blackbody or similar extended area source set at 30 °C (86 °F). The TIC under test is positioned 1 m from the test target, such that the test target is visible and in focus on the TIC display. The test operator views the TIC display and determines the location where the vertical and horizontal converging lines become indistinguishable. These vertical and horizontal values must exceed the minimum values established in the performance requirements through the standards development process.

6.2. Image capturing procedure

In keeping with the treatment of TIC as black boxes, it is necessary to evaluate the TIC in a manner consistent with their use by the fire service. Thus, the images that are presented to the user on the display are the same images that are examined to determine whether the TIC meets the imaging performance requirements as developed through the standards development process. In Figure 6—3, a thermal bar target (shown on the right) is viewed by a TIC under test, while the TIC display is viewed by a high resolution, calibrated visible camera (shown on the left).

Through the development of standard testing methodology, the performance of the visible camera and lens to be used by third-party testing organizations will be available to the TIC manufacturers so that they can design and build a mounting bracket to position the visible camera such that it generates an optimized view of the TIC's entire display area.

6.3. Contrast

In the context of fire service applications, contrast measurements determine whether the TIC is capable of producing sufficient contrast for the user to identify objects of interest such as victims and potential fire hazards. With respect to a grayscale image, contrast is a measure of the relative luminance (or pixel intensity) of portions of the image. Contrast in an image can be measured several ways, depending on the type of test target used and the reason for the measurement. The definition of contrast is:

$$C = \frac{2\sigma}{\text{Bitdepth}}, \quad (1)$$

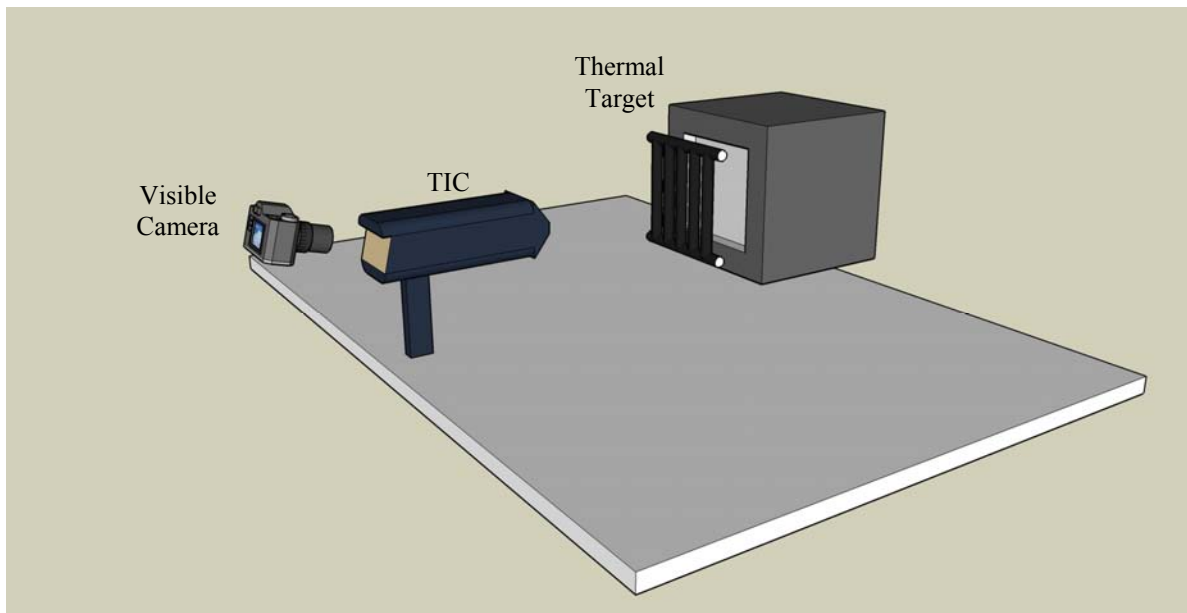


Figure 6—3. Schematic diagram of image capturing setup. As the TIC views a thermal target, a high resolution visible camera is focused on the TIC display. A mounting bracket (not shown) is to be provided by the TIC manufacturer to optimally position the visible camera.

where C is the contrast, σ is the standard deviation of pixel intensities, and *Bitdepth* is the pixel intensity resolution. Most, if not all, currently available TIC displays have an 8-bit pixel intensity resolution, in which case the $Bitdepth = 2^8 = 256$. There are two applications of contrast measurements in this work: large area contrast, to which this section applies; and bar contrast, which is part of the effective temperature range (ETR) measurement discussed in section 6.4. Different parts of the same test target, shown in Figure 6—4, are used for both contrast measurements, which are collected concurrently. The target consists of three blackbodies and a heated bar target. A room temperature blackbody, 25 °C, can be seen in the right of Figure 6—4, a 25 °C blackbody with 30 °C bars is in the center of Figure 6—4, and a hot blackbody, which has its temperature varied in a range from 25 °C to 350 °C (the maximum range of the blackbody) can be seen in the left of Figure 6—4. A detailed discussion of the development of contrast as it applies to fire service TIC can be found in [48].

The standard deviation of the combined pixel intensities within the leftmost and rightmost areas of the test target shown in Figure 6—4 (pixels exposed to T_2 and T_{sur} , which have the same size areas) is calculated, then divided by the *Bitdepth* to determine the large area contrast. The bars in the middle of the test target are ignored for large area contrast measurements. The large area contrast reported for this test is the maximum contrast obtained while T_2 is ramped from ambient to T_{max} at a rate of 10 °C/min. T_2 is the temperature of a surface of area large enough to cause the TIC under test to shift sensitivity mode, if the TIC is designed to shift mode. The minimum size of the T_2 area may vary from TIC to TIC, depending on the specific algorithm used to trigger a mode shift. It is important to confirm that T_2 has a sufficiently large area prior to conducting the contrast/ETR tests.

The ambient surface area (T_{sur}) is held constant at 25 °C ± 1 °C throughout the test. T_{max} is the temperature to define the scene temperature range within which TIC should be expected to provide useful images. The areas within the dashed lines represent the middle 90 % of each temperature-controlled surface area and are specified to avoid edge effect issues. The large area contrast obtained throughout the test period is compared with the range of acceptable pass/fail criteria, determined by the Standards Development Organization, to determine the TIC contrast performance.

To perform the large area contrast test, the TIC is positioned 1 m from the test target. Figure 6—5 illustrates how mirrors may be used to facilitate the measurement if space and/or alignment is a problem. For the data that was collected to support this work, a 17.8 cm square extended area blackbody was used as the radiation source. A 20.3 cm (8 in.) diameter gold-plated off-axis parabolic mirror having a focal length of 1 m and an offset angle of 10° was used to position the T_2 surface within the field of view. All surfaces in the field of view except the mirror were painted with black paint, which has a stated $\epsilon = 0.94 \pm 0.002$ in the 8 μm to 14 μm wavelength range within which the fire service TIC operate.

6.4. Effective temperature range (ETR)

The ETR test is intended to measure the range of temperatures at which the TIC provides a useful image to the fire fighter. Useful means here that the image quality is adequate for the user to take appropriate action. It is not unusual for a fire fighter to use a TIC to search for objects having intermediate surface temperatures, for example a human victim, another fire fighter, or an egress route, when flames are in the field of view. In this situation, the presence of flames or other extreme conditions may cause the TIC to “wash out” or lose contrast in the object of interest. The ETR test measures the temperature range within which objects of intermediate temperature retain enough contrast to be discernable to the user, i.e., the temperature range of a useful image. A detailed discussion of the development of effective temperature range as it applies to fire service TIC can be found in [48].

The same test target is used for the ETR as for the large area contrast test, including the central area of the test target, in which bars of constant intermediate temperature are used to calculate the bar contrast. This test target, now showing the full complement of target areas, is shown in Figure 6—6. The bars in the test target had an outside diameter (OD) of 1.3 cm (0.5 in.) spaced 1.3 cm apart, were constructed from copper tubing, producing a frequency of 0.04 cyc/mrad at a 1 m distance from the TIC. For the bar contrast, T_{bar} is held constant at $30\text{ }^{\circ}\text{C} \pm 1\text{ }^{\circ}\text{C}$ and T_{sur} is the background temperature. A constant temperature heating fluid (silicone oil) was pumped through the tubes to achieve a uniform test target temperature. As previously mentioned, the size of the T_2 surface area must be large enough to cause the TIC under test to shift sensitivity mode, if the TIC is designed to shift mode, and the T_{sur} area has the same size as the T_2 area. The T_{bar} area is large enough to include at least 3 full bar cycles at 0.04 cyc/mrad.

The contrast of the bars in the central area is calculated according to equation 1. The low temperature boundary of the ETR is held constant at $25\text{ }^{\circ}\text{C} \pm 1\text{ }^{\circ}\text{C}$ and the high temperature boundary is T_{max} , defining the ETR as shown below:

$$ETR = T_{\text{max}} - 25^{\circ}\text{C}, \quad (2)$$

The ETR is the temperature range to be established as the minimum acceptable operating temperature range for TIC. The bar contrast pass/fail criteria will be determined by the standards development organization. If during this test the TIC dips below the pass/fail value at any point in the test, then the corresponding T_2 temperature is used in place of T_{max} in equation 2 to calculate the ETR. If the TIC is designed to shift modes, then the T_2 temperature corresponding with each mode shift is recorded as T_2 moves through its range.

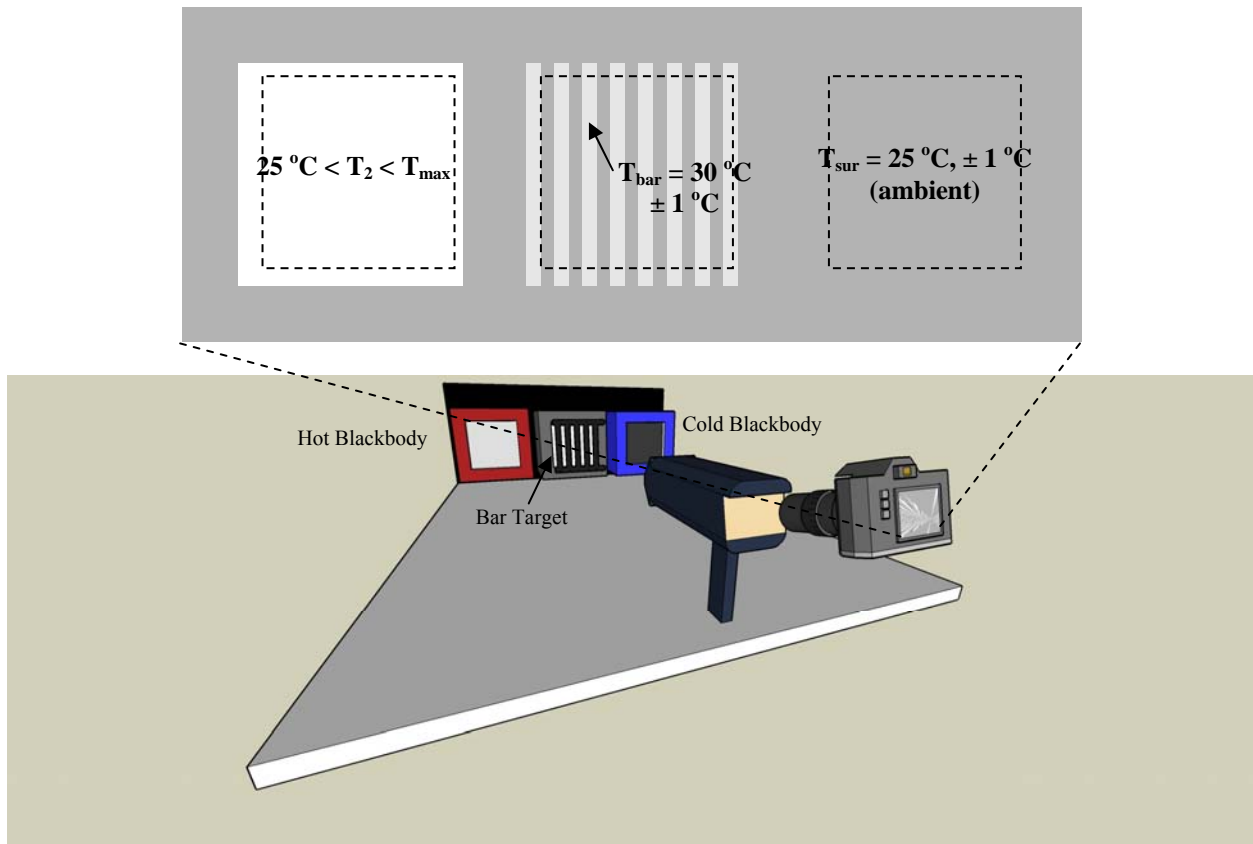


Figure 6—4. Test target setup used for the contrast and effective temperature range tests. For large area contrast, the bars in the middle of the test target are ignored. The standard deviation of the combined pixel intensities within the dashed areas on the left and right side of the test target are calculated, then divided by the *Bitdepth* to determine the contrast as a function of T_2 , which changes from 25 °C to T_{\max} .

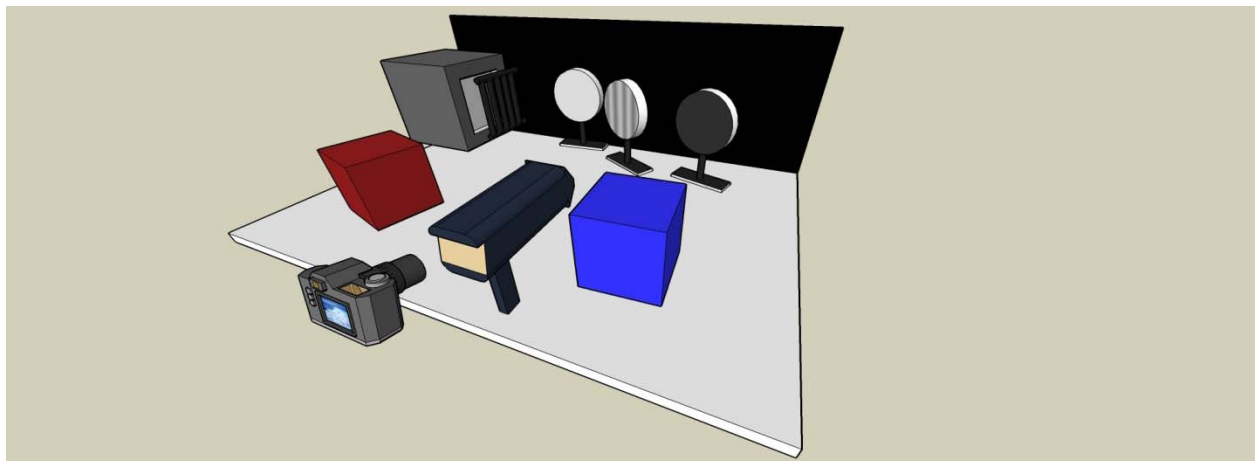


Figure 6—5. Alternative test setup for contrast and effective temperature range. When space is an issue mirrors may be used to redirect the thermal radiation to the TIC. The results presented in this paper were obtained in this configuration.

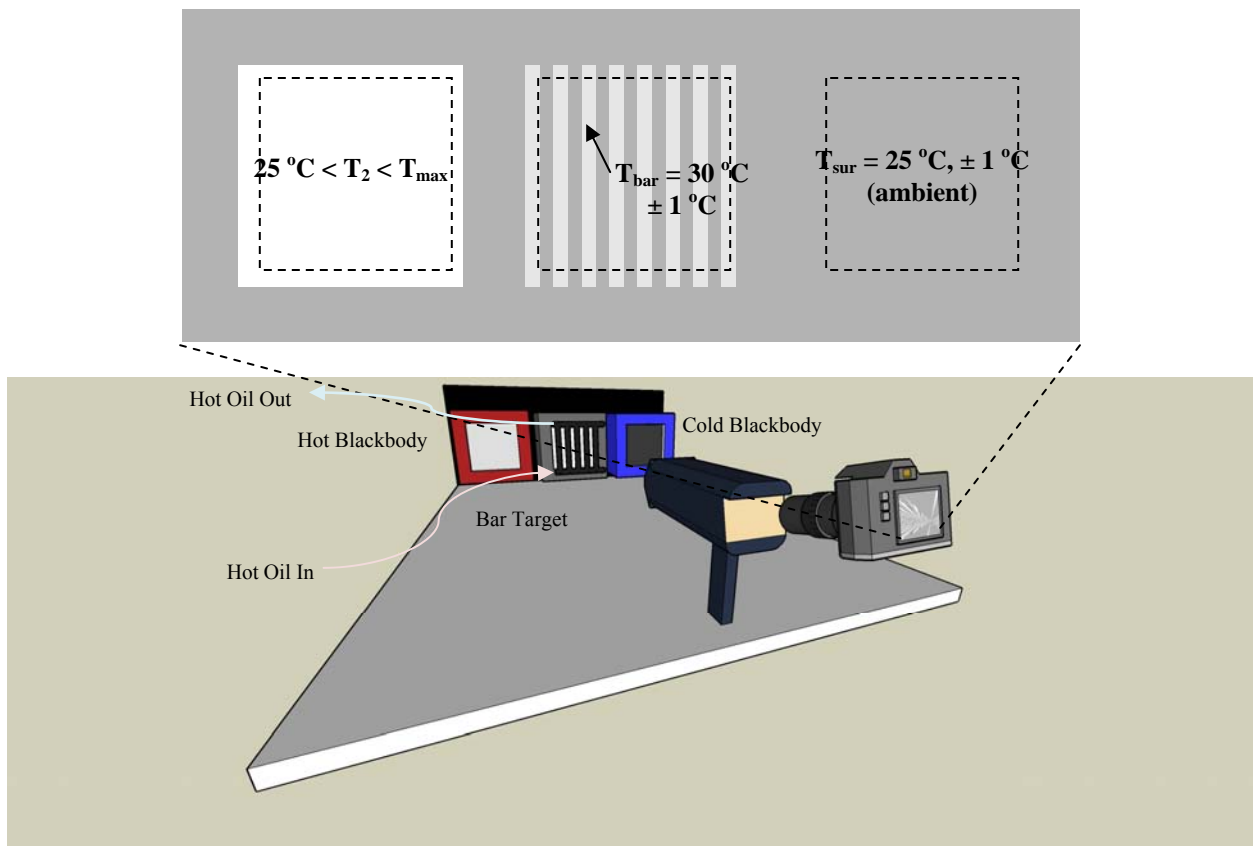


Figure 6—6. This test target is used for the contrast and effective temperature range tests. For the effective temperature range, the contrast of the central area, which incorporates bars having a constant temperature difference, is measured while the hot blackbody surface temperature (T_2) increases.

6.5. Nonuniformity

Nonuniformity is a measure of the variation of the TIC's response to a uniform test target. The uniform thermal test target used here is an extended area blackbody as shown in Figure 6—7. The TIC is placed close to the blackbody surface ($\sim 5\text{cm}$) and the surface is assumed to be Lambertian, uniform irradiance in all directions, so that the TIC is interpreting a uniform temperature field. There are many ways that the TIC response may be nonuniform [49]: there can be gradients in pixel intensity across the image, various patterns such as narcissus may appear, some degree of broadband noise may be present, as well as blemishes and blotches, and combinations of these nonuniformities can occur. In Figure 6—8, images are presented from the same TIC, viewing a uniform target at four temperatures. As can be seen, as the test target temperature increased, nonuniformities in the images became generally more apparent. This TIC shifted to a less thermally sensitive mode between the 100 °C and 200 °C images. A detailed discussion of the development of nonuniformity as it applies to fire service TIC can be found in [50].

Nonuniformity is usually measured by entirely filling the field of view of the TIC under test with the blackbody surface set at a prescribed temperature. The image will not be in focus. The target is imaged and recorded, and the statistical mean, m , and standard deviation, σ , of the image pixel intensities are calculated. The nonuniformity, NU , is then given by the ratio of the standard deviation to the statistical mean, as shown in equation 3, which effectively makes the NU independent of system gain [16].

$$NU = \frac{\sigma}{m}, \quad (3)$$

TIC have automatic nonuniformity corrections that are either continuously present or are triggered by various proprietary algorithms. Many sophisticated methods of correcting nonuniformity exist, however most fire service TIC utilize a linear correction to the offset of each pixel at ambient temperatures. As mentioned in section 2.2, TIC with BST-type detectors continuously correct the image by using a chopper to reset the detector's nodes to uniform values. TIC with microbolometer detectors use a shutter to reset the pixels, which is triggered according to the manufacturer's proprietary algorithm. During the shutter operation, which usually occurs in timed intervals, the displayed image freezes, therefore, for nonuniformity testing of TIC with microbolometers, it is important to time the data collection for this test such that it is free of automatic corrections.

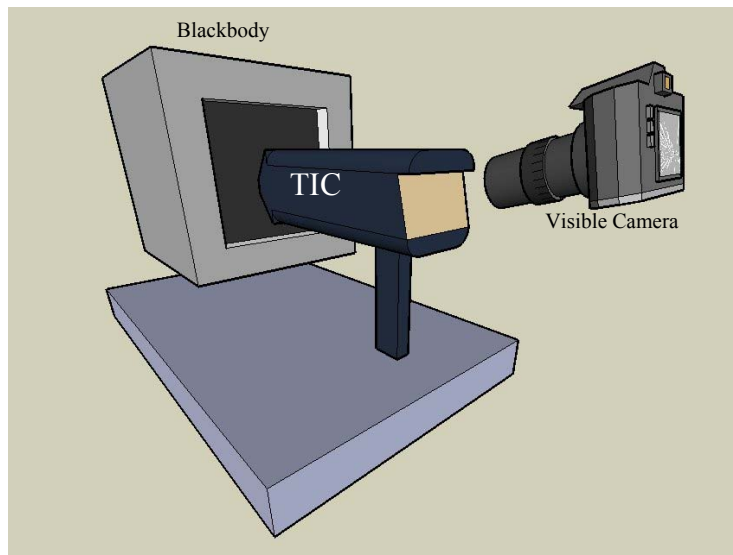


Figure 6—7. Test setup for measuring the nonuniformity of a TIC. The TIC is placed close to the surface (~5cm) of a uniform large area blackbody surface. The temperature is increased and the images are taken by the visible camera to determine image nonuniformity.

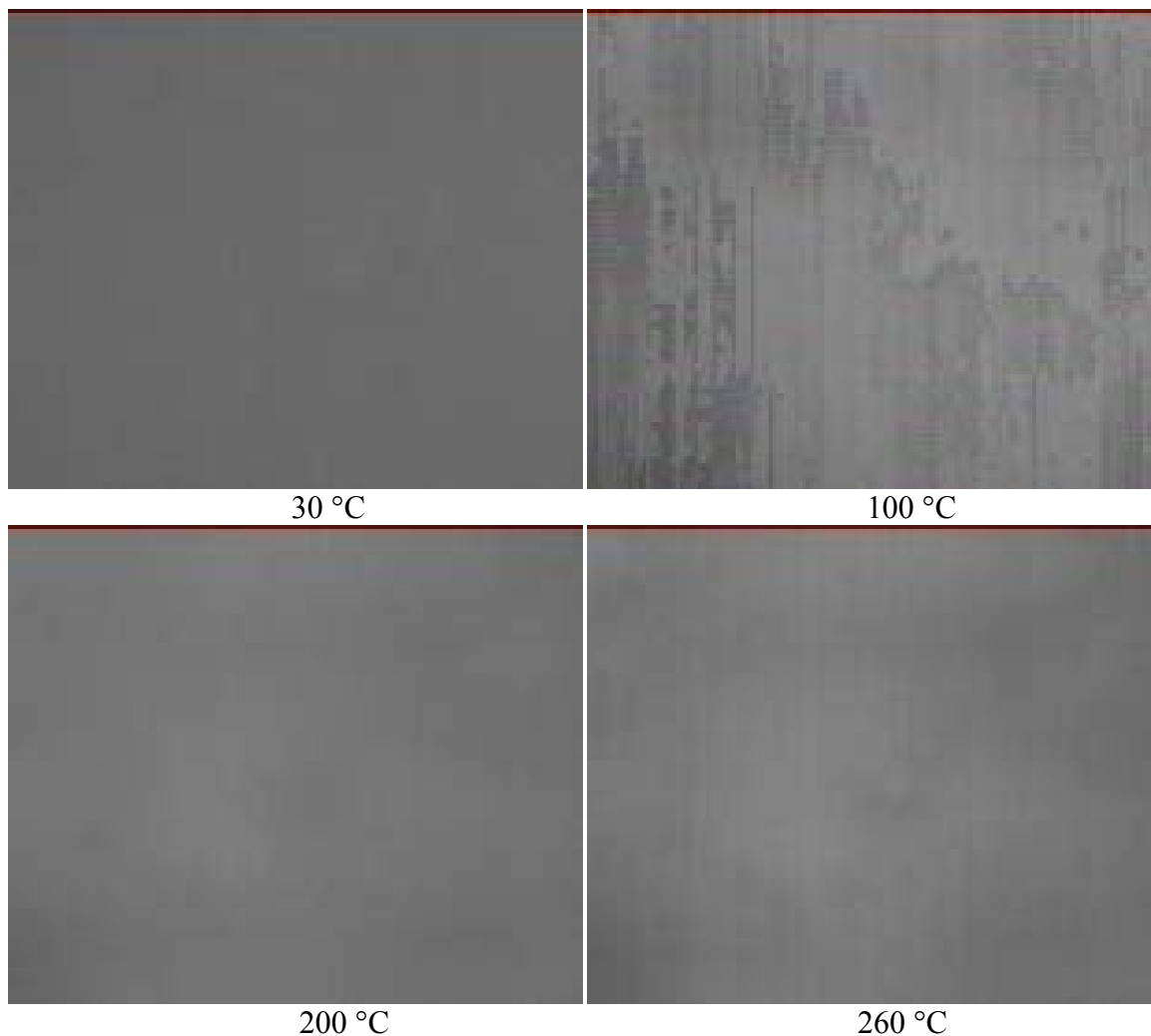


Figure 6—8. Variation in nonuniformity of a TIC with increasing temperature. As the test target temperature increased, nonuniformities became more apparent. The TIC shifted to a less thermally sensitive mode between the 100 °C and 200 °C images.

As seen in Figure 6—8, image nonuniformity is sensitive to the test target temperature, therefore it is measured at several critical temperatures: water freezing temperature, 1°C, human body temperature, 30°C, water boiling temperature, 100°C, and two temperatures at which other fire service equipment such as turnout gear is tested, 200°C and 260°C respectively. Tests have not been performed at 1 °C at this time. Small values of *NU* are desired for this test, therefore the nonuniformity is determined at all these test target temperatures and compared with the maximum pass/fail criteria determined by the standards development organization to characterize the TIC contrast performance. Nonuniformity also plays a role in the determination of the TIC's spatial resolution, as discussed in the following section.

6.6. Spatial resolution

Spatial resolution is a measure of the amount of detail in an image. A fire fighter may observe a hotspot, noticeable by a difference in contrast, but not realize that the source is a warm but harmless household item (e.g., a computer, coffee pot, power strip, lamp, etc...). Without enough detail in the image to identify the item of interest, the fire fighter may lose valuable time inspecting everything that looks relatively warm. A detailed discussion of the development of spatial resolution as it applies to fire service TIC can be found in [51].

There are numerous ways to measure spatial resolution, most of which are discussed in [51]. The slanted edge Modulation Transfer Function (MTF) measurement was chosen for this test because it has high repeatability and is relatively easy to perform. An existing test method for visible cameras, ISO 12233 [28], was used as the basis for this test, with modifications related to the thermal target. The test target is configured as shown in Figure 6—9. The slant is 5° from vertical and the hot, cold, and surrounding temperatures are held constant throughout the test. The 5° angle avoids aliasing by not aligning with the camera pixels and facilitates oversampling of the edge by four times to get a more accurate representation of the gradient and resultant frequency response. The test target dimensions are at least 15 cm in each direction. For the data that was collected to support this work, a 17.8 cm square extended area blackbody was used as the heat source and a thin sheet of aluminum, coated with black paint having $\epsilon = 0.94 \pm 0.002$ and cut at the appropriate angle, was placed directly in front of the blackbody surface.

Spatial resolution is independent of the test target temperatures, so long as the steady (non-gradient) temperatures on either side of the test target produce at least a 20 % pixel intensity difference in the images generated by the TIC. The TIC is positioned 1 m away from the target. The image data are captured, then processed using software based on the ISO 12233 test method [52], resulting in a curve of MTF as a function of frequency, which is normalized to a value of 1 at zero frequency. The process of determining the MTF function includes combining 4 lines of the image together to effectively oversample the edge four times. Then the edge is differentiated to produce a line. A Fourier transform of the line is taken and the data points are taken as the maximum amplitude of each frequency derived from the image. Finally the MTF function is normalized to the zero frequency MTF response. This method provides a purely relativeistic measurement of the frequency response which only has quantitative value once the MTF is normalized to the zero frequency. This has the added benefit of producing a measurement method that is independent of target temperature, as long as a sufficient temperature difference is present for the camera to respond to. A sample MTF curve is given in Figure 6—10. The

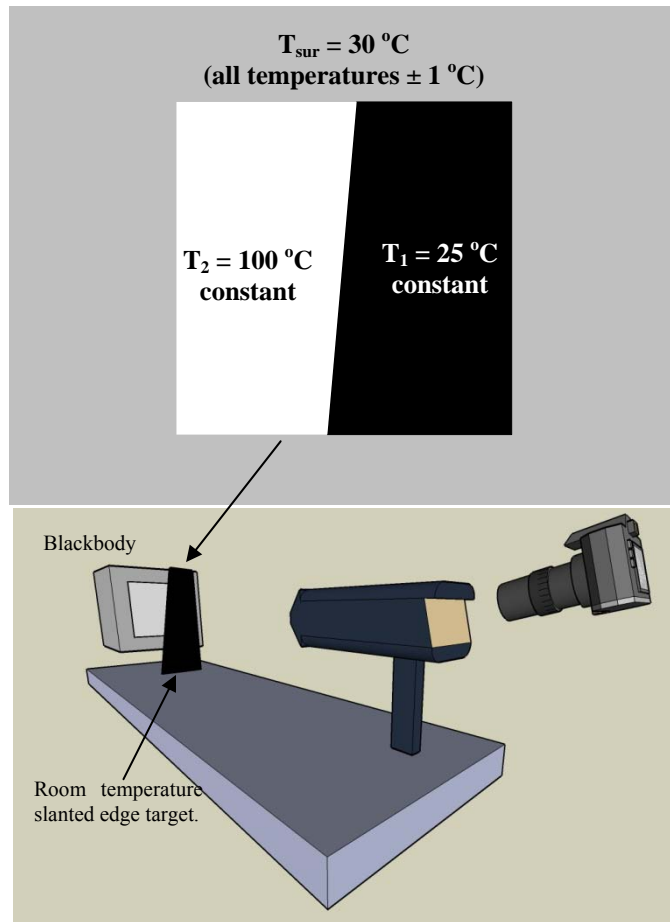


Figure 6—9 Slanted edge spatial resolution test target. The slant is 5° from vertical, the hot and surrounding temperatures are held constant throughout the test. The target dimensions are at least 15 cm in each direction. All surfaces in the field of view have $\epsilon \geq 0.94 \pm 0.002$.

nonuniformity value obtained at 100 °C from the test method described in section 6.5 is considered the “noise floor,” wherein the measured MTF is due to contrast variations caused by the noise in the signal rather than the test target’s contrast. The noise floor can vary significantly among TIC, therefore it is important to compensate by removing it from the spatial resolution calculation.

As the frequency increases, the MTF flattens because the fluctuations in the noise inherent in any image approximate the length scale of the image frequency. The spatial resolution is obtained by integrating the area between the curve and the noise floor shown in Figure 6—10.

The spatial resolution obtained in this test method is compared with the minimum pass/fail criteria determined by the standards development organization to determine the TIC spatial resolution performance.

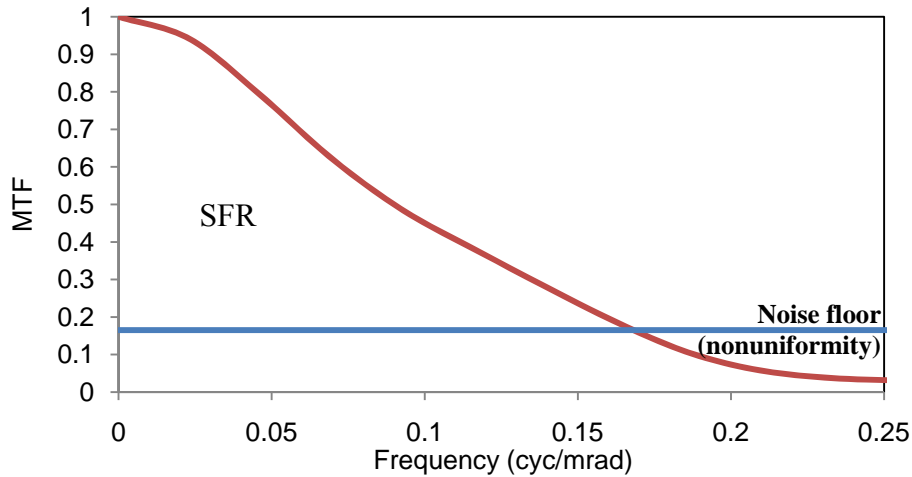


Figure 6—10 Sample spatial resolution data. The spatial resolution is obtained by integrating between the MTF (red line) and the nonuniformity (blue line).

6.7. Thermal Sensitivity

The thermal sensitivity test measures the smallest temperature difference that the TIC is capable of resolving. The sensitivity of most TIC to temperature differences is a function of the nominal scene target temperature, therefore this test is performed at the same critical temperatures identified previously in the discussion of nonuniformity in section 6.5. These temperatures are 1 °C, 30 °C, 100 °C, 160 °C, and 260 °C.

To measure thermal sensitivity, two extended area blackbodies are placed in the TIC field of view such that they each show an equal area in the displayed image as seen in Figure 6—11. The blackbodies do not need to be in focus. One blackbody is set at a prescribed temperature and the other blackbody set point is adjusted until the luminance of both areas in the displayed image is equal. The adjusted blackbody set point is then incrementally increased until the luminance value increases by 2 %; this temperature is recorded as T_1 . The blackbody set point is then incrementally decreased until the luminance value decreases by 2 %; this temperature is recorded as T_0 . The thermal sensitivity (TS) is calculated by equation 4.

$$TS = \frac{T_1 - T_0}{2}, \quad (4)$$

TS measurements are determined at all five of the test target temperatures. Small values of thermal sensitivity are desired for this test. The test results are compared with the maximum pass/fail criteria determined by the standards development organizations to determine the TIC contrast performance.

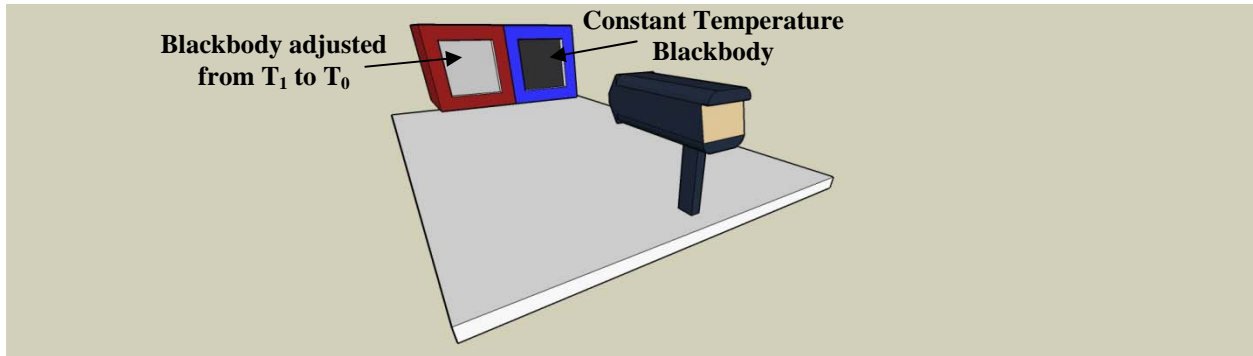


Figure 6—11. Experimental setup for thermal sensitivity test. The two blackbodies are adjusted until they both have the same luminance on the TIC display. Then one blackbody temperature is slowly decreased until a 2 % difference in luminance is observed between the two blackbodies.

7. RESULTS AND DISCUSSION

In this section, examples are given of test data collected during the development of the test methods discussed in section 6. They are intended to illustrate the differences between TIC and to clarify the intention of the tests. The TIC are differentiated by their detector technology because it is an easy and obvious way to compare TIC performance. It should be emphasized that detector technology alone does not determine the relative performance of TIC. The size of the detector array, the electronic processing, the optical system, and the quality of the display play very important roles in TIC performance but are not directly useful to differentiate performance.

7.1. Contrast and ETR

In this discussion the TIC are differentiated by their detector technology because it is an easy and obvious way to compare TIC performance. It should be emphasized that detector technology alone does not determine the relative performance of TIC. The size of the detector array, the electronic processing, the optical system, and the quality of the display play very important roles in TIC performance but are not directly usable to differentiate performance.

The large area contrast and the bar contrast are plotted in

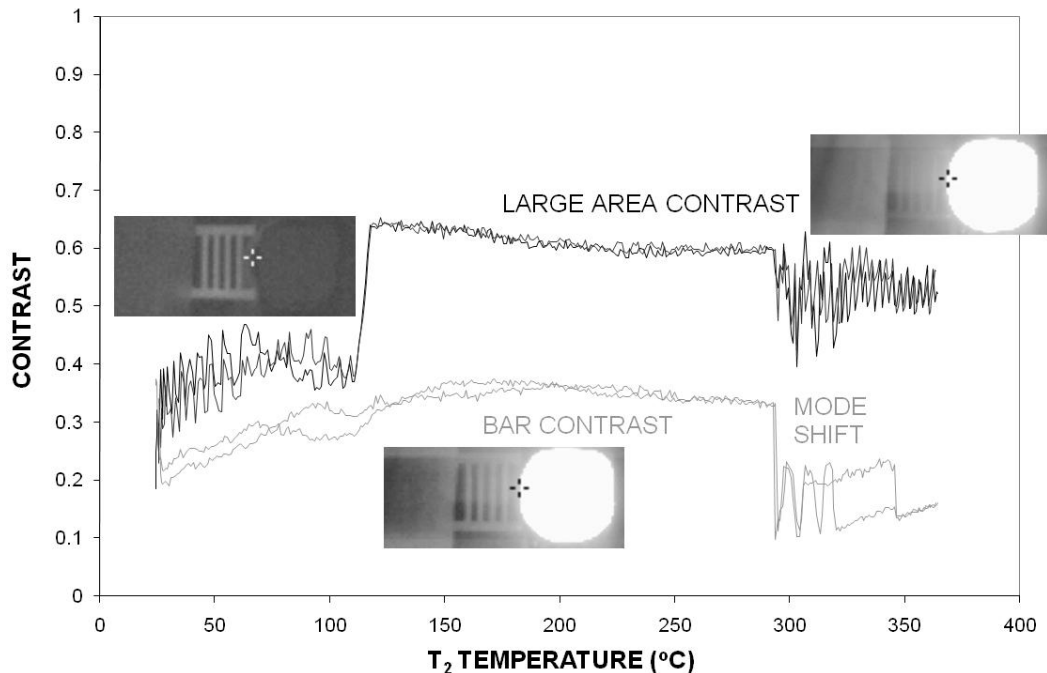


Figure 7—1 to Figure 7—3 as a function of T₂ temperature; there are two tests shown in each graph. T₂ is the temperature of a surface of area large enough to cause the TIC under test to shift

sensitivity mode (if the TIC is designed to shift mode). In

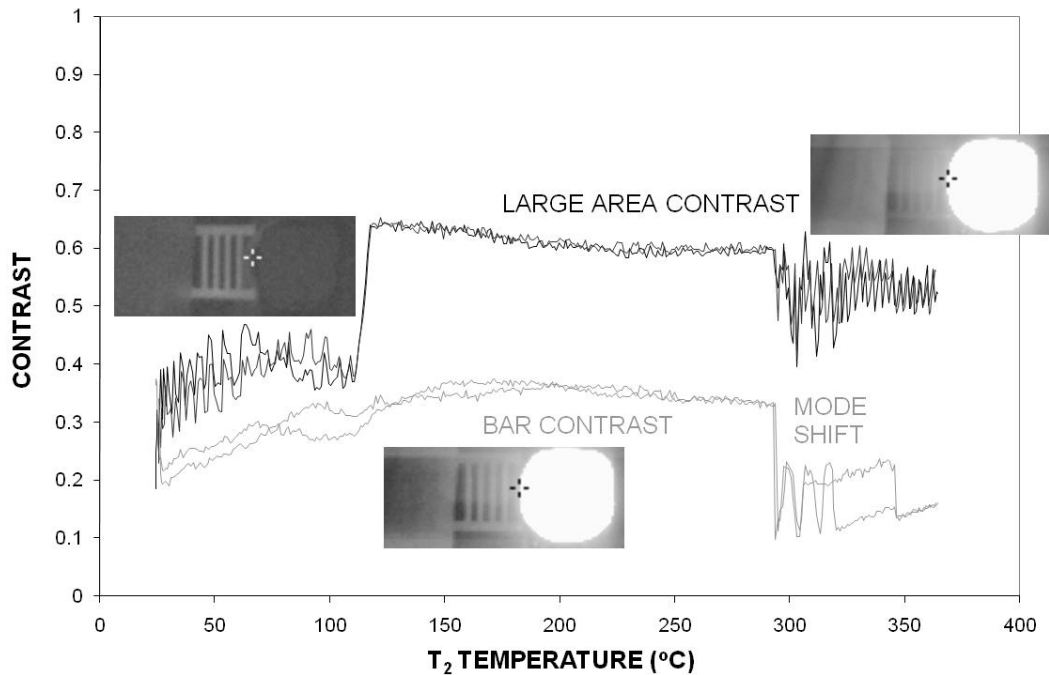


Figure 7—1, the ASi TIC did not provide a stable image until the T_2 temperature reached about 125 °C. Below 125 °C, the large area contrast instability manifested itself as flickering between brighter and darker images. Above 125 °C, the image stabilized until the TIC shifted mode, which occurred at around 290 °C. After the mode shift, the fluctuations in large area contrast were larger than at lower T_2 temperatures. This behavior occurred in both tests and appears to be a characteristic of the specific TIC tested. The bar contrast was unaffected by the fluctuations of the hot pixels but degraded significantly after the TIC shifted mode. After the mode shift both the large area and bar contrasts were more unstable than at lower T_2 temperatures.

In Figure 7—2, the BST TIC presented very different results, with the large area contrast improving dramatically with the initial increase in T_2 temperature. The maximum large area contrast was achieved at $T_2 = 170$ °C, although the contrast for this TIC was generally lower than either of the other TIC. Recall that BST detectors do not shift modes. The bar contrast became quite low after the initial increase in T_2 temperature and stayed low throughout the remainder of the test.

Similar to the BST TIC, in Figure 7—3 it can be seen that the VO_x TIC large area contrast also improved greatly with the initial increase in T_2 temperature. Unlike the ASi TIC, the VO_x TIC large area contrast did not suffer noticeably after the mode shift, remaining consistently higher than the other two TIC throughout the tests. There were a few brief but significant contrast excursions that occurred during several of the TIC's automatic nonuniformity corrections. The bar contrast declined somewhat during the period prior to the mode shift. After the mode shift the bar contrast became quite low and stayed low throughout the remainder of the test.

The bar contrast is used to determine the TIC's ETR. As mentioned previously, the minimum acceptable bar contrast and the minimum ETR will be established by the standards development

organization. For the sake of discussion, assume that the minimum bar contrast has been arbitrarily set at 0.2. In Figure 7—1, the ASi TIC shows an ETR of about 265 °C (290 °C – 25 °C), in Figure 7-2 the BST TIC shows an ETR of about 15 °C (40 °C – 25 °C), and in Figure 7-3 the VOx TIC shows an ETR of about 125 °C (150 °C – 25 °C). Note that the bar contrast value of 0.2 was chosen for this discussion strictly to illustrate the differences in TIC performance and how they might relate to a pass/fail criterion and is not intended to indicate a preference for any specific value. These results indicate the wide range in image performance.

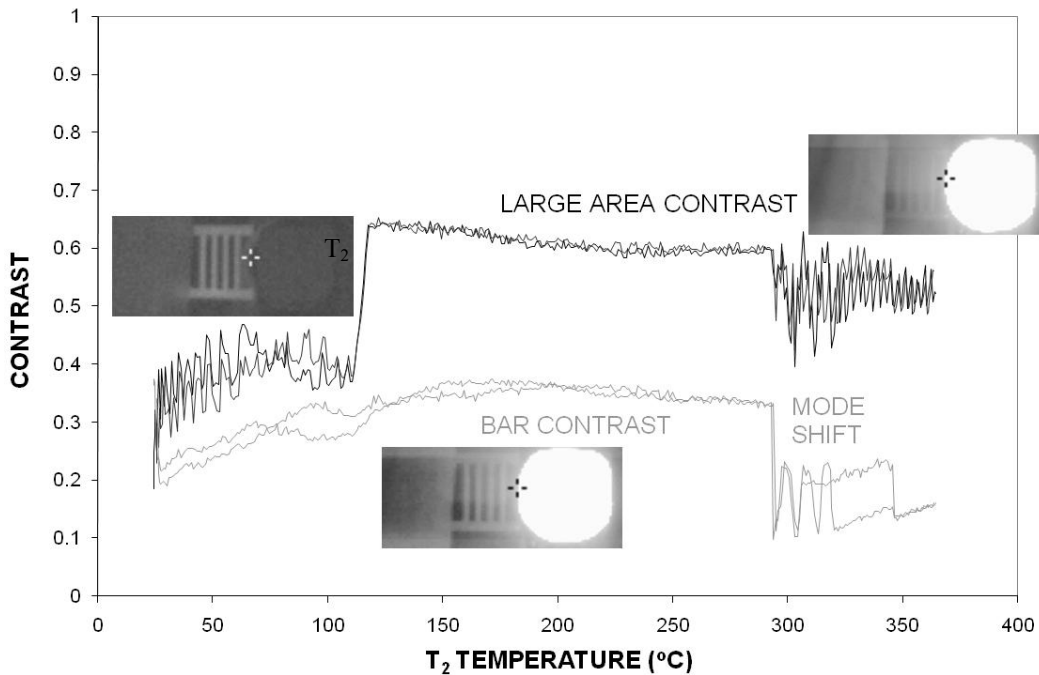


Figure 7—1. Plots of large area contrast and bar contrast data used to determine image contrast and effective temperature range of a TIC using an ASi, 120 x 160 detector array. Test results for two tests are shown.

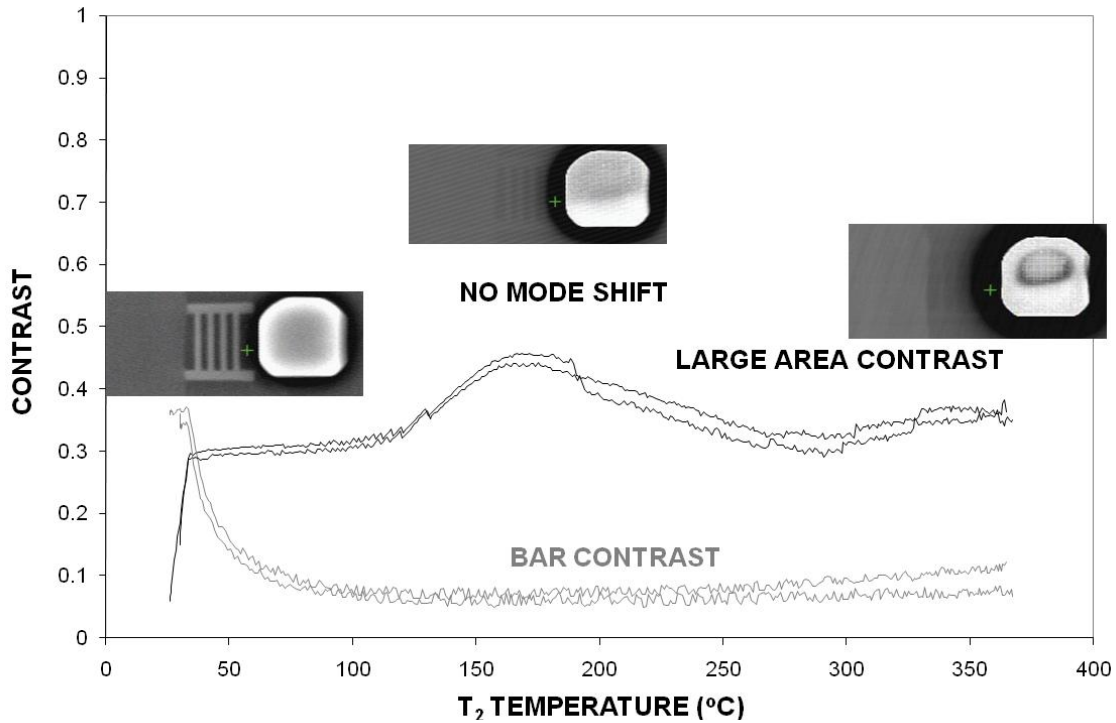


Figure 7—2. Plots of large area contrast and bar contrast data used to determine image contrast and effective temperature range of a TIC using an BST, 240 x 320 detector array. Test results for two tests are shown.

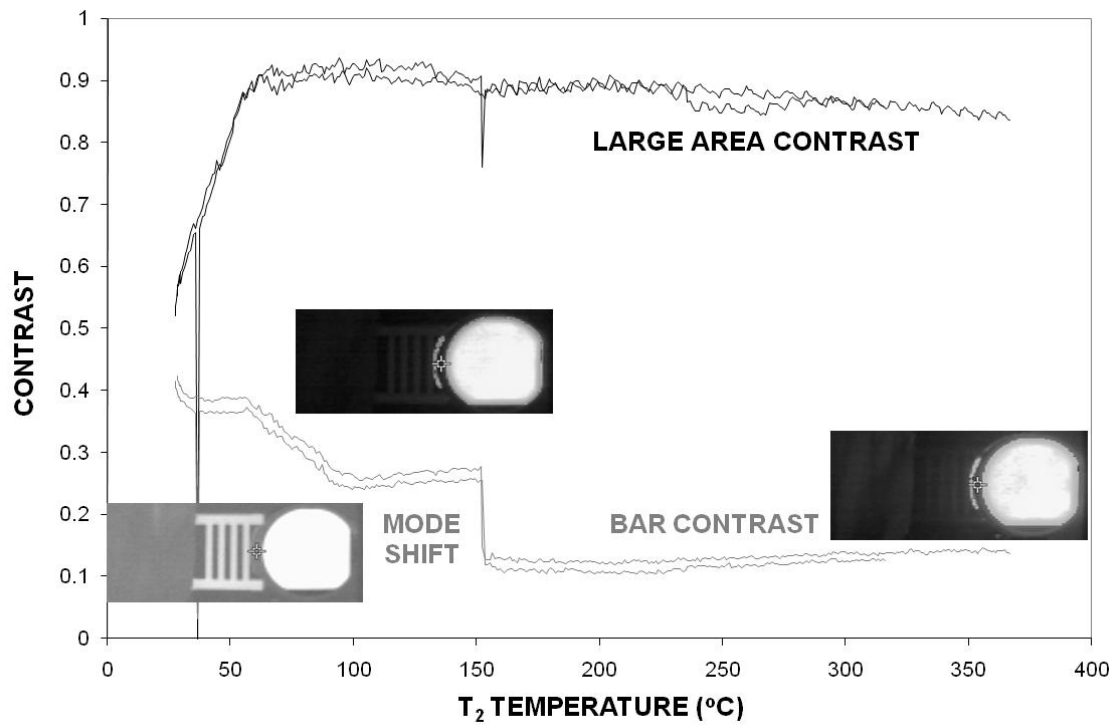


Figure 7—3. Plots of large area contrast and bar contrast data used to determine image contrast and effective temperature range of a TIC using an VOx, 120 x 160 detector array. Test results for two tests are shown.

7.2. Nonuniformity

The nonuniformity of three TIC is displayed for several temperatures in Figure 7—4 and the nonuniformity values are plotted as a function of target temperature in Figure 7—5. It can be seen that nonuniformity generally increases with increasing target temperature, although a discontinuity may occur when the TIC shifts sensitivity mode. Note that the BST TIC showed a monotonically increasing nonuniformity. For the three specific TIC tested, the VO_x TIC produced the least amount of nonuniformity (provided the most uniform images). When the sensitivity of the systems decreased due to the mode shift, there was a corresponding decrease in nonuniformity. This suggests that the nonuniformity scaled with temperature, but on a fundamental level it actually scaled with pixel saturation. The BST TIC was more sensitive to target temperature than the other two TIC.

Several different examples of nonuniformities can be observed in Figure 7—4. The BST camera at 100 °C exhibits a narcissus effect which can be seen as the faint circle in the center of the image. Narcissus is when internal reflections occur in the camera causing it to see its own optics. As the temperature increases for the BST camera more drastic nonuniformities become apparent in the form of diagonal shading of the image. This is partially due to the design of the BST camera and its use of a chopper. The chopper is still at room temperature while the camera is observing a high temperature input. The effect is a continuous switching between high temperature uniform input and low temperature uniform input and presents as the diagonal shading seen at 200 °C and 260 °C.

The ASi images shown in Figure 7—4 present several additional types of nonuniformity. At 100 °C, prior to the mode shift, the camera exhibits some pixel saturation near the bottom of the image. This is a good illustration of the need for a mode shift and how that reduced sensitivity mode affects the image presented by the camera. The pixel saturation is gone at 200 °C because of this mode shift. Another type of nonuniformity that can be seen for the ASi camera is the presence of physical defects in the camera as evidenced by the dark and light circles on the image which can be seen at elevated temperatures.

All of these different nonuniformities can affect camera output differently, and if localized may not significantly impact the gross image. However, all the nonuniformities are treated numerically as broadband noise in the image. Additionally, nonuniformity impacts the spatial resolution of the camera as well. If the amplitude and frequency of noise is at the same spatial frequency of some detail in a scene that is being imaged then that detail will be lost in the noise and not be detected. For this reason the nonuniformity of each camera is used as a ‘noise floor’ in the spatial resolution measurements. The camera is assumed to be unable to discern detail that is in the noise. The implementation of nonuniformity to the spatial resolution calculation is discussed in section 7.3.

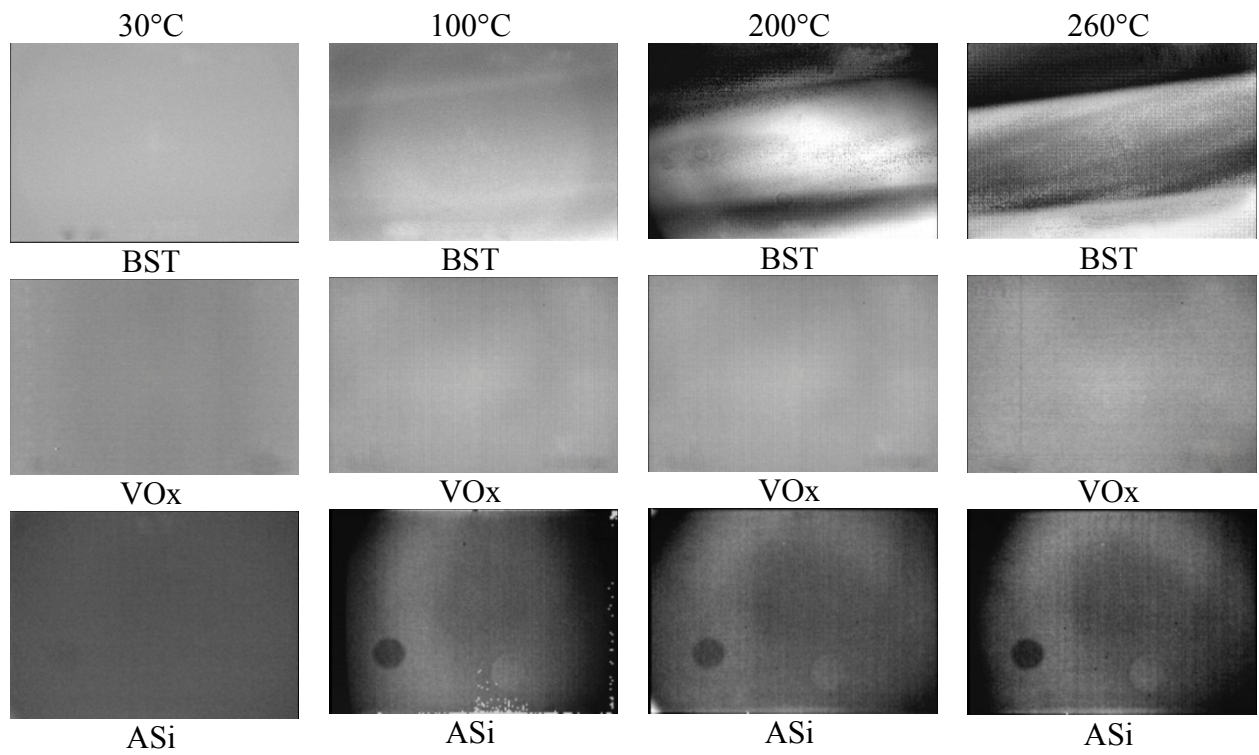


Figure 7—4. Actual nonuniformities observed from three different TIC at a variety of temperatures. BST, VO_x, and ASi detector technologies are all represented along with a variety of different nonuniformities present in these cameras.

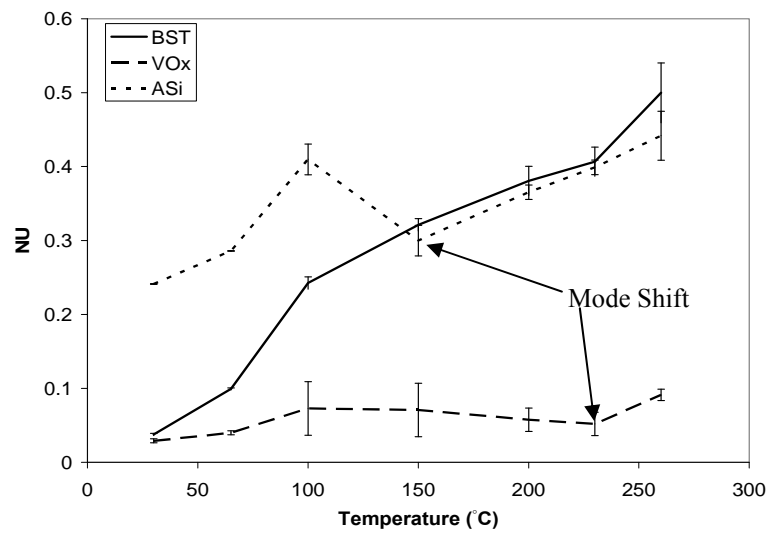


Figure 7—5. Image nonuniformity as a function of target temperature while looking at a uniform temperature surface. For the three specific TIC tested, the VO_x TIC produced the least nonuniformity while the ASi and BST cameras had higher nonuniformities at different temperatures.

7.3. Spatial resolution

The spatial resolution of a TIC is representative of how well that TIC can see detail. Since the methodology is built upon the ISO 12233 standard for determining the spatial resolution of visible spectrum cameras a similar figure of merit is used here, namely the Spatial Frequency Response (SFR). Based on the discussion in Section 6.6, the SFR is a nondimensional number that varies from 0 to 1 and a larger value indicates a better representation of spatial detail in an image. Figure 7—6 illustrates how a perfect knife edge is interpreted by three different cameras. As mentioned earlier, the spatial resolution of each TIC is dependent on the camera's optics, internal image processing, and display screen in addition to the physical pixel resolution of the internal sensor. This can be clearly seen in Figure 7—6. The actual MTF curves (see Section 6.6) calculated from these slanted edge images are presented in Figure 7—7.

The contrast of the image does not affect the spatial resolution measurement of the camera. The ASi camera appears to have a much higher image contrast than the VOx, however when you look at the actual measured SFR value, the VOx camera has a larger SFR value than the ASi camera. This may seem counterintuitive, and if the MTF values are not normalized to the zero frequency there is in fact a significant effect of contrast (or target temperature differential) on the SFR value obtained. Figure 7—8 presents three MTF curves taken from the same camera at different temperatures. Without normalization the SFR appears to improve significantly as the temperature, or contrast, of the scene increases. However, once the values are normalized, as seen in the right of Figure 7—8, they all collapse together and return essentially the same result. This is important to take into account for spatial resolution since contrast is measured separately. There is however a need to have a minimum contrast for the measurement to work. Observing the 40 °C curve in the normalized plot of Figure 7—8, errantly high MTF are reported at higher frequencies while identical, low values are observed for 80 °C and 100 °C.

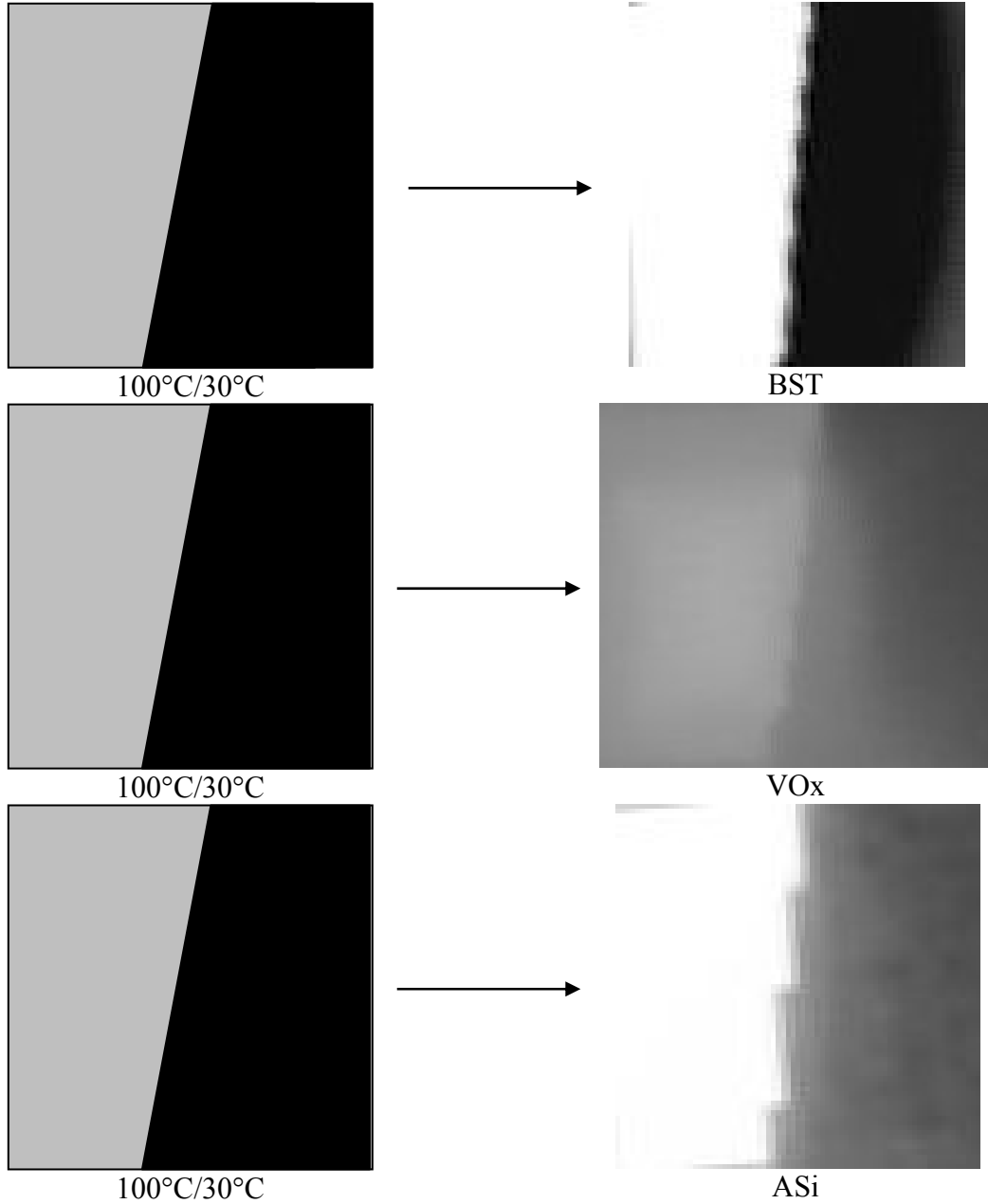


Figure 7—6. Illustration of how of how three different cameras interpret the same ‘knife edge’ thermal target. The three different cameras have different sensor technology, but also have different pixel resolutions (320x240, 160x120, and 160x120 respectively), optics, and internal image processing that affects the spatial resolution of the image on the display. The analysis of these images is presented in Figure 7-6.

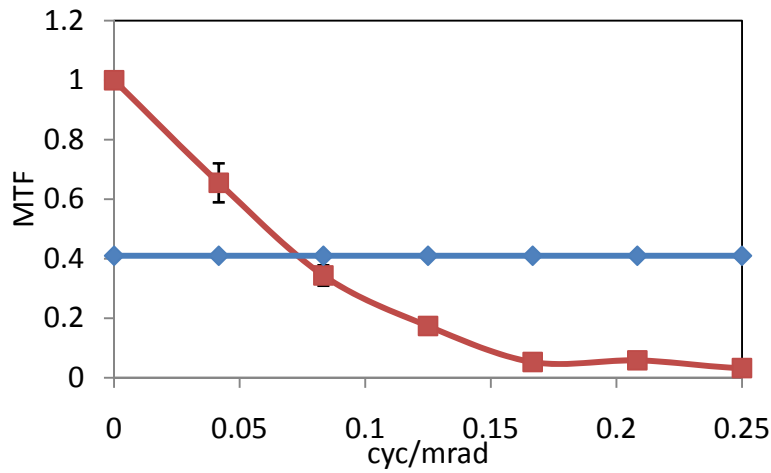
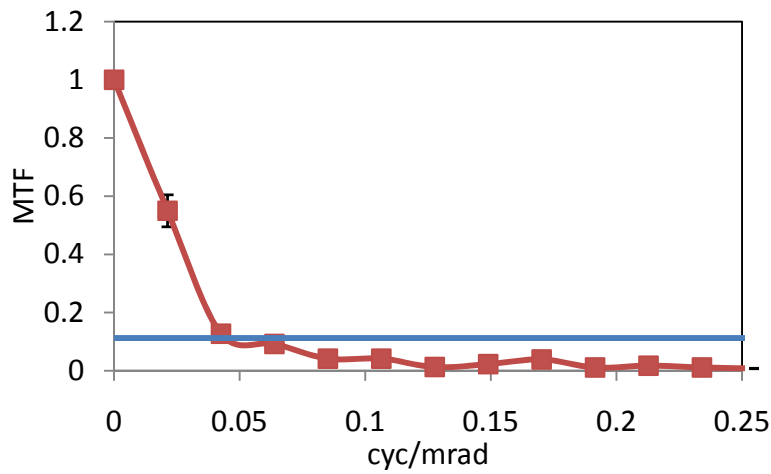
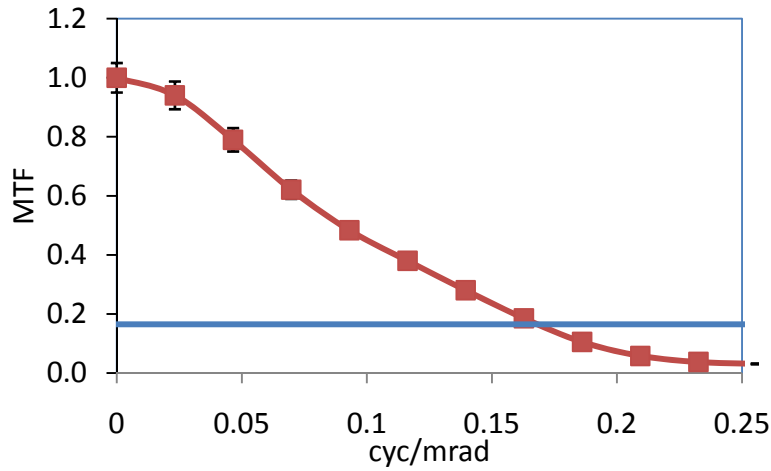


Figure 7—7. Comparison of the spatial resolution of the BST, VOx, and ASi TIC. The SFR value given for each camera technology represents the area between the MTF curve and Nonuniformity. The spatial resolution measurement for each camera is dependent upon the nonuniformity measurement as well.

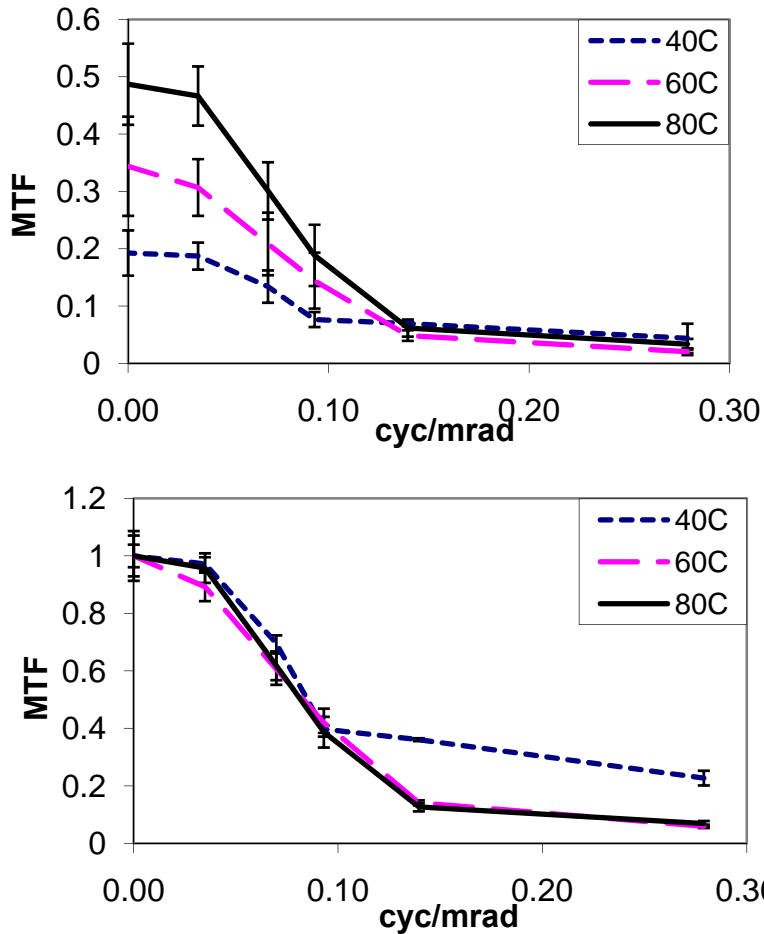


Figure 7—8. Illustration of the temperature independence of the spatial resolution measurement. The temperatures are indicated in Celsius. Once the original values (top) are normalized (bottom) the effect of image contrast (temperature difference) can be eliminated. The line for 40 °C on the right does not follow the other trends because there needs to be a minimum contrast in the knife edge image.

7.4. Thermal sensitivity

As discussed earlier, thermal sensitivity is the ability of the camera to convey small changes in temperature to the users. As discussed in section 6.7 two blackbodies are used and the temperatures are initially set so that the intensities measured on the display, by the visible camera are equal, and then varied until a 2 % difference in measured pixel intensity is measured. The test is repeated at several different temperatures in each of the temperature classes. Only data for a single TIC was available at the time of this writing. More test data will be available in the near future, however, it is not available. Figure 7—9 presents a sample thermal sensitivity curve for a VOx TIC. When a TIC has a smaller the thermal sensitivity value then the better the camera performs as the smaller temperature difference it can percieve. As the nominal temperature, T_1 , increases a larger temperature difference is necessary to produce sufficient contrast for the user to percieve. Additionally, when some cameras ‘mode shift’ at higher temperatures this decreases

the sensitivity of the detector resulting in a necessarily larger temperature difference to be present in order for the camera to respond. No mode shift is observed in Figure 7—9.

The pass/fail criteria for the thermal sensitivity of a TIC will be determined by the standards development organization that is creating the standard.

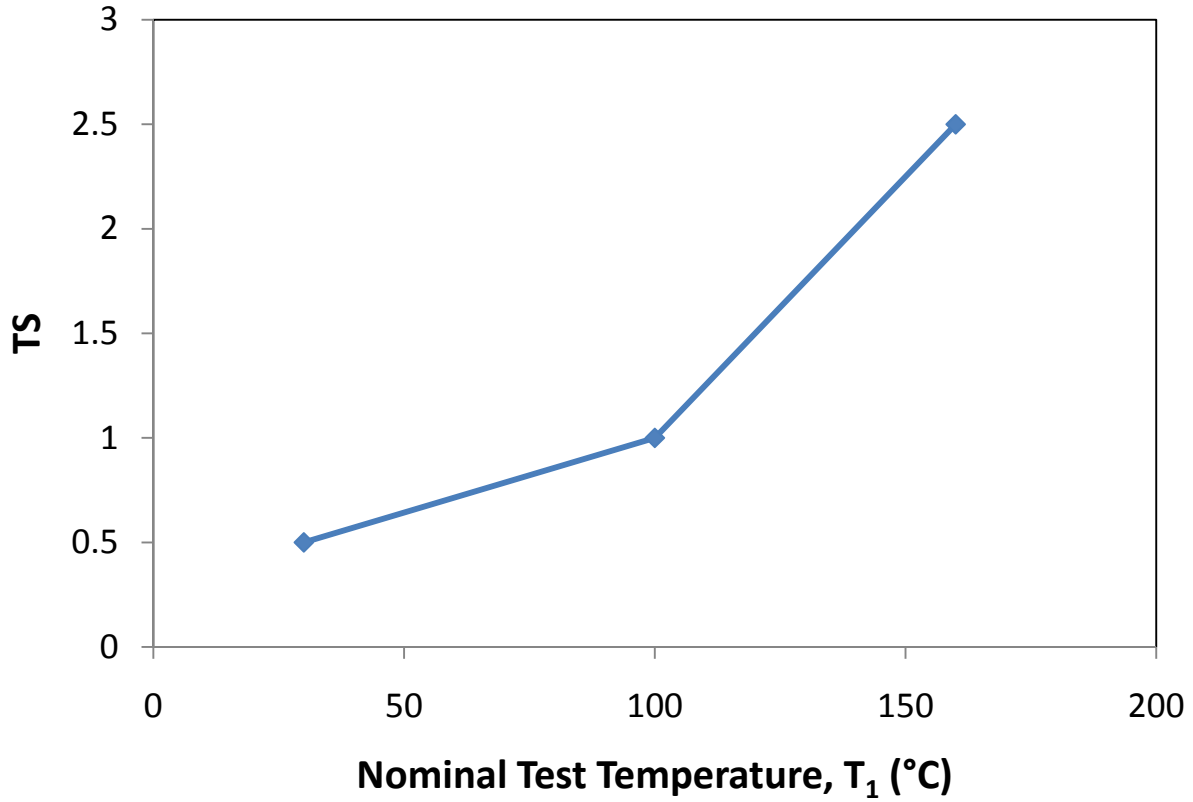


Figure 7—9. Example thermal sensitivity response for a characteristic TIC. A smaller value for thermal sensitivity indicates that the camera is more sensitive to small differences in temperature. The thermal sensitivity increases with increasing nominal temperature due to a larger contrast necessary for the user to perceive a temperature difference.

7.5. Uncertainty Analysis

There are different components of uncertainty in the temperatures, total heat flux, and time to activate data reported here. Uncertainties are grouped into two categories according to the method used to estimate them. Type A uncertainties are evaluated by statistical methods and type B are evaluated by other means [53]. Type B analysis of systematic uncertainties involves estimating the upper (+a) and lower (-a) limits for the quantity in question such that the probability that the value would be in the interval ($\pm a$) is essentially 100 percent. After estimating uncertainties by either Type A or B analysis, the uncertainties are combined in quadrature to yield the combined standard uncertainty. Multiplying the combined standard uncertainty by a coverage factor of two results in the total expanded uncertainty that corresponds to a 95 percent confidence interval (2σ).

Components of uncertainty are tabulated in Table 7-1 and Table 7-2. Some of these components, such as the zero calibration elements, are derived from instrument specifications. Other components, such as path length and image digitization include past experience with positioning these devices and the image digitization equipment used. The uncertainty in the air temperature measurements does not include radiative cooling because of the relatively low temperatures being measured. Smoke density measurements were conducted gravimetrically. Part of the uncertainty was attributed to the accuracy of the mass scale used to weigh the soot filters and part of the uncertainty was due to the flow rate which is measured after the gases have been cooled and is therefore highly depended on the temperature at the entrance to the soot probe. The contrast transfer function (CTF) measurements involved looking down a long corridor. There can be significant variations in the composition and temperature of the gases in this length. The uncertainty also varies with the amount of smoke loading and turbulent flow in the corridor. The uncertainties are reported as a range in Table 7-1 and are represented by error bars in the associated figures.

The bench scale experiments are by their very nature more controlled and thus expected to have smaller uncertainties associated with them. The blackbodies used in these experiments are very well controlled devices and generally have a small uncertainty associated with their temperature set point and an even smaller uncertainty associated with their temperature steadiness. Due to the wide variations in the TIC form factors it is very difficult to position each camera so that the lens is in the same position for each of these tests, this results in a positioning uncertainty mostly manifested by variations in the path length. For the Nonuniformity test the uniformity of the blackbody surface is very important. The blackbody used in these experiments had its uniformity quantitatively measured by the Physics Laboratory at NIST. The resultant uncertainty in the blackbody surface is much smaller than that being measured by the test and is represented in Table 7-2. As with the full scale tests there is a small uncertainty associated with converting the analogue image signal to a digital format for processing, this uncertainty is represented in both Table 7-1 and Table 7-2

Table 7-1: Uncertainty in full scale experimental test data.

	Component Standard Uncertainty	Combined Standard Uncertainty	Total Expanded Uncertainty
CO concentration			
Calibration	±1%	±5%	±10%
Repeatability	±4%		
Random	±3%		
Temperatures			
Calibration	±1%	±1.5%	±3%
Repeatability	±1%		
Random	±1%		
Smoke Density			
Mass Scale	±2%	±5%	±10%
Flow Rate	±5%		
Contrast Transfer Function (CTF)*			
Path Length Uniformity	±2% to ±50%	±2.5% to ±50%	±5% to ±100%
Random	±2%		
* Variations in uncertainty are plotted as error bars in the respective figures.			

Table 7-2: Uncertainty in bench scale experimental data.

	Component Standard Uncertainty	Combined Standard Uncertainty	Total Expanded Uncertainty
Contrast			
Temperatures	±1%	±5%	±10%
Image Digitization	±2%		
Path Length	±5%		
Nonuniformity			
Temperature of Blackbody	±1%	±3.5%	±7%
Blackbody Uniformity	±0.5%		
Repeatability	±3%		
Image Digitization	±2%		
Spatial Frequency Response			
Path Length	±5%	±5%	±10%
Image Digitization	±2%		

8. SUMMARY

For thermal imaging cameras that will be used by the fire service, this study has identified the needs and issues involving the image performance of thermal imaging cameras. In this study, relevant information regarding the establishment of conditions under which to test the performance of TIC has been assembled with the objective of developing test conditions that are relevant and representative of fire service operations. Input from users, as well as existing standards, research reports, and test measurements were considered in the development of representative TIC performance testing conditions. The concept of Thermal Class as a means of categorizing the activities in which TIC are used by fire fighters is helpful in defining meaningful bounds on TIC test conditions. The four thermal classes link the various requirements of existing standards on related fire service equipment with experimental results from full-scale testing and the scientific literature.

This report presents the suite of imaging performance metrics and test methods that were developed to aid in the creation of a standard on thermal imagers used by the fire service. The performance metrics and test methods reflect the need of fire service TIC images to have sufficient contrast, temperature range, spatial resolution, and thermal sensitivity, along with reduced nonuniformity to facilitate effective TIC use.

Data collected during the development of these tests provides an indication of the wide range of imaging performance produced by TIC currently being used by the fire service. There was no particular TIC detector technology or model that excelled in every test. In fact, the test results show that each TIC technology tested was superior to the others in at least one test.

The standards development organizations will determine pass/fail criteria for each of the individual tests. In the future, data regarding the ability of users to perceive hazards with various types and quantities of image degradation will be provided to the standards development organizations. There may be interactions between the various image parameters. The standards development organization will determine, based on the the magnitude and degree of these interactions, whether they should be considered in the final pass/fail criteria.

9. REFERENCES

1. Woodworth, S.P., "Choosing a Thermal Imaging Unit," *Fire Engineering*, Vol. 153, (1): p. 83-84, 2000.
2. NFPA 1801, "Standard on Thermal Imagers for the Fire Service," *National Fire Protection Association*, Quincy, MA, 2009.
3. ASTM E. 1543-00, "Standard Test Method for Noise Equivalent Temperature Difference of Thermal Imaging Systems," *ASTM International*, West Conshohoken, PA, 2000.
4. Amon, F.K., Bryner, N.P., and Hamins, A., "Thermal Imaging Research Needs for First Responders: Workshop Proceedings," *National Institute of Standards and Technology*, Gaithersburg, MD, 2005.
5. ASTM E. 1213-97, "Standard Test Method for Minimum Resolvable Temperature Difference for Thermal Imaging Systems," *ASTM International*, West Conshohoken, PA, 2002.
6. ASTM E. 1311-89, "Standard Test Method for Minimum Detectable Temperature Difference for Thermal Imaging Systems," *ASTM International*, West Conshohoken, PA, 2004.
7. Donnelly, M.K., Davis, W.D., Lawson, J.R., and Selepak, M.S., "Thermal Environment for Electronic Equipment used by First Responders," Vol. (NIST Technical Note 1474), 2006.
8. Siegel, R. and Howell, J., "Thermal Radiation Heat Transfer," 4th ed., New York: *Taylor and Francis*, 2002.
9. Grosshandler, W.L., "RADCAL: A Narrow-Band Model for Radiation Calculations in a Combustion Environment," *National Institute of Standards and Technology*, Gaithersburg, MD, 1993.
10. Kruse, P.W. and Skatruc, D.D., "Uncooled Infrared Imaging Arrays and Systems." San Diego: *Academic Press*, 1997.
11. Dinaburg, J., "Thesis: Developing Performance Metrics for Thermal Imaging Cameras," in *Mechanical Engineering*. University of Maryland: College Park, Maryland, 2007.
12. Bryner, N.P., Johnson, E.L., and Pitts, W.M., "Carbon Monoxide Production in Compartment Fires - Reduced-Scale Enclosure Test Facility," NIST IR 5568, *National Institute of Standards and Technology*, 1994.
13. Pitts, W.M., Johnson, E.L., and Bryner, N.P., "Carbon Monoxide Formation in Fires by High-Temperature Anaerobic Wood Pyrolysis," *Proc. Combust. Institute*, Vol. 25: p. 69-70, 1994.
14. Crowson, F., Gagnon, B., and Cockerham, S., "Evaluation of Commercially Available Thermal Imaging Cameras for Navy Shipboard Firefighting," *Department of the Navy*, 1999.
15. Chrzanowski, K., "Evaluation of commercial thermal cameras in quality systems." p. 2556-2567, 2002.

16. Holst, G.C., "Testing and Evaluation of Infrared Imaging Systems." Winter Park, FL: *JCD Publishing*, 1998.
17. ANSI/ISA ANSI/ISA-12.12.01-2007, "Nonincendive Electrical Equipment for Use in Class I and II, Division 2 and Class III, Divisions 1 and 2 Hazardous (Classified) Locations," Research Triangle Park, NC, 2007.
18. ASTM B-. 07a, "Standard Practice for Operating Salt Spray (Fog) Apparatus," *ASTM International*, West Conshohocken, PA, 2007.
19. ASTM D. 1003-00, "Standard Test Method for Haze and Luminous Transmittance of Transparent Plastics. ASTM International," *ASTM International*, West Conshohocken, PA, 2000.
20. ASTM D. 6413, "Standard Test Method for Flame Resistance of Textiles (Vertical Test)," *ASTM International*, West Conshohocken, PA, 1999.
21. ASTM F. 1359-99a, "Standard Test Method for Liquid Penetration Resistance of Protective Clothing or Protective Ensembles Under a Shower Spray While on a Mannequin," *ASTM International*, West Conshohocken, PA, 2004.
22. ASTM E1862-97, "Standard Test Methods for Measuring and Compensating for Reflected Temperature Using Infrared Imaging Radiometers," *ASTM International*, West Conshohocken, PA, 2002.
23. ASTM E1897-97, "Standard Test Methods for Measuring and Compensating for Transmittance of an Attenuating Medium Using Infrared Imaging Radiometers," *ASTM International*, West Conshohocken, PA,
24. ASTM E1256-95(2001), "Standard Test Methods for Radiation Thermometers (Single Waveband Type) - used for measuring the temperature of a blackbody," *ASTM International*, West Conshohocken, PA, 2001.
25. IEC 60529Consol.Ed.2.1, "Degrees of Protection Provided by Enclosures (IP Code)," *International Organization for Standardization*
Geneva, Switzerland, 2001.
26. IEC 61000, "Electromagnetic Compatibility (EMC)," *International Organization of Standardization*, Geneva, Switzerland, 2005.
27. IEC 61508-SER.Ed.1.0, "Functional Safety of Electrical/Programmable Electronic Safety-Related Systems," *International Organization of Standardization*, Geneva, Switzerland, 2005.
28. ISO 12233, "Photography - Electronic Still-Picture Cameras - Resolution Measurements," *International Organization for Standardization*, Geneva, Switzerland, 2000.
29. MIL -STD.810E.Method.513.4, "Environmental Test Methods and Engineering Guidelines," *MIL-STD*, Wright-Patterson Airforce Base, OH, 1989.
30. VESA VESA-2005-5, "Flat Panel Display Measurements (FPDM2)," *Video Electronics Standards Association*, Milpitas, CA, 2005.

31. NFPA 1221, "Standard for the Installation, Maintenance, and Use of Emergency Services Communications Systems " *National Fire Protection Association*, Quincy, MA, 2007.
32. NFPA 1971, "Standard on Protective Ensembles for Structural Fire Fighting and Proximity Fire Fighting," *National Fire Protection Association*, Quincy, MA, 2007.
33. NFPA 1977, "Standard on Protective Clothing and Equipment for Wildland Fire Fighting," *National Fire Protection Association*, Quincy, MA, 1998.
34. NFPA 1981, "Standard on Open-Circuit Self-Contained Breathing Apparatus (SCBA) for Emergency Services," *National Fire Protection Association*, Quincy, MA, 2007.
35. NFPA 1982, "Standard on Personal Alert Safety Systems (PASS)," *National Fire Protection Association*, Quincy, MA, 2007.
36. NFPA 1852, "Standard on Selection, Care, and Maintenance of Open-Circuit Self-Contained Breathing Apparatus (SCBA)," *National Fire Protection Association*, Quincy, MA, 2008.
37. McGrattan, K., "Verification and Validation of Selected Fire Models for Nuclear Power Plant Applications," *Nuclear Regulatory Commission*, Washington, DC, January, 2006.
38. Tewarson, A., "Generation of Heat and Chemical Compounds in Fires", in *The SFPE Handbook of Fire Protection Engineering*, P.J. DiNenno, Editor. National Fire Protection Association and The Society of Fire Protection Engineers: Quincy, MA, 1988.
39. Rothman, L.S., Jacquemart, D., Barbe, A., Benner, D.C., Birk, M., Brown, L.R., Carleer, M.R., Chackerian, C., Chance, K., Coudert, L.H., Dana, V., Devi, V.M., Flaud, J.M., Gamache, R.R., Goldman, A., Hartmann, J.M., Jucks, K.W., Maki, A.G., Mandin, J.Y., Massie, S.T., Orphal, J., Perrin, A., Rinsland, C.P., Smith, M.A.H., Tennyson, J., Tolchenov, R.N., Toth, R.A., Vander Auwera, J., Varanasi, P., and Wagner, G., "The HITRAN 2004 molecular spectroscopic database." p. 139-204, 2005.
40. Silverstein, R.M., Bassler, G.C., and Morrill, T.C., "Spectrometric Identification of Organic Compounds," 3rd ed., New York: *John Wiley & Sons*, 1974.
41. Fang, J.B. and Breese, J.N., "Fire Development in Residential Basement Rooms," *National Institute of Standards and Technology*, Gaithersburg, MD, October, 1980.
42. Gann, R.G., Averill, J.D., Johnsson, E.L., Nyden, M.R., and Peacock, R.D., "Smoke Component Yields From Room-Scale Fire Tests," *National Institute of Standards and Technology*, Gaithersburg, MD, April, 2003.
43. Hamins, A., Maranghides, A., Johnsson, E.L., Donnelly, M.K., Mulholland, G.W., and Anleitner, R., "Report of Experimental Results for the International Fire Model Benchmarking and Validation Exercise #3," *National Institute of Standards and Technology*, Gaithersburg, MD, 2005.
44. Hamins, A., Maranghides, A., McGrattan, K., Johnsson, E.L., Ohlemiller, T.J., Donnelly, M.K., Yang, J., Mulholland, G.W., Prasad, K., Kukuck, S., Anleitner, R., and McAllister, T., "Experiments and Modeling of Multiple Workstations Burning in a Compartment. Federal Building and Fire Safety Investigation of the World Trade Center Disaster," *National Institute of Standards and Technology*, Gaithersburg, MD, 2005.

45. Peacock, R.D., Davis, S., and Lee, B.T., "Experimental Data Set for the Accuracy Assessment of Room Fire Models," *National Bureau of Standards*, Gaithersburg, MD, April, 1994.
46. Bryant, R.A., Ohlemiller, T.J., Johnsson, E.L., Hamins, A., Grove, B.S., Maranghides, A., Mulholland, G.W., and Guthrie, W.F., "The NIST 3 Megawatt Quantitative Heat Release Rate Facility - Description and Procedure," NIST IR 7052, 2004.
47. McGrattan, K.B., Baum, H., Rehm, R., Hostikka, S., and Floyd, J., "Fire Dynamics Simulator (Version 5): Technical Reference Guide," NIST SP 1018-5, *National Institute of Standards and Technology*, 2007.
48. Amon, F., Lock, A., and Bryner, N.P., "Measurement of Effective Temperature Range of Fire Service Thermal Imaging Cameras," in *SPIE Security+Defense*. SPIE: Orlando, FL, 2008.
49. Mooney, J.M. and Shepherd, F.D., "Characterizing IR FPA nonuniformity and IR camera spatial noise," *Infrared Physics & Technology*, Vol. 37, (5): p. 595-606, 1996.
50. Lock, A. and Amon, F., "Measurement of the Nonuniformity of First Responder Thermal Imaging Cameras," in *SPIE Security+Defense*. SPIE: Orlando, FL, 2008.
51. Lock, A. and Amon, F., "Application of Spatial Frequency Response as a Criterion for Evaluating Thermal Imaging Camera Performance," in *SPIE Security+Defense*. SPIE: Orlando, FL, 2008.
52. I3A, "Slant Edge Analysis Tool sfrmat 2.0." International Imaging Industry Association, 2000.
53. Taylor, B.N. and Kuyatt, C.E., "Guidelines for Evaluating and Expressing the Uncertainty of NIST Measurement Results," NIST TN 1297, *National Institute of Standards and Technology*, Gaithersburg, MD, 1994.

APPENDIX A

This appendix lists the performance metrics and test methods that may be incorporated into standards for thermal imaging cameras. The following performance metrics and test methods are presented in a generalized form designed to give the reader a sense of the scope of a standard. The Technical Committee responsible for a standard makes decisions regarding the content of the standard on a consensus basis. Before the final form of a standard document is published, draft versions of the document are offered to the public for proposed changes in scope and for revisions to text. At the discretion of the committee, all or part of the recommendations such as the ones provided in this report may or may not be included in the final standard document.

The performance metrics and test methods are divided into two groups, the first being listed in Table A-1. This group addresses the overall design robustness of the thermal imaging camera design. When appropriate, existing standard test methods are used. In other cases, when existing tests were not appropriate or were deemed inadequate, new test methods were developed specifically for first responder thermal imaging cameras.

Table A-1. Design Robustness Performance Metrics and Test Methods

Performance Metric	Test Method
Nonincendive Equipment	ANSI 12.12.01
Enclosure Protection	IP67
Electromagnetic Emission	IEC 61000-6-3
Electromagnetic Immunity	IEC 61000-6-2
Temperature Stress	Environmental Temperature Stress Test
Leakage Resistance	Immersion / Leakage Test
Vibration Resistance	Vibration Test
Impact Resistance	Impact-Acceleration Resistance Test
Corrosion Resistance	Corrosion Test
Heat Resistance	Heat Resistance Test
Flame Resistance	Heat and Flame Test
Tumble “Torture” Resistance	Tumble-Torture Test
Viewing Surface Abrasion Resistance	Viewing Surface Abrasion Test
Product Label Durability	Product Label Durability
Wire Pullout Resistance	Cable Pullout Test

The imaging performance of the thermal imaging camera is addressed by a second group of performance metrics and test methods, as listed in Table A-2. This group is the primary focus of the work conducted for this project and is discussed in greater detail in sections 6 and 7.

Table A-2. Imaging Performance Metrics and Test Methods

Performance Metric	Test Method
Contrast	Contrast Test- determines the maximum possible contrast that can be displayed by the thermal imaging camera.
Effective Temperature Range	Effective Temperature Range Test- determines the extreme range of temperatures (which control the camera’s automatic gain settings) that allow the user to see an intermediate-temperature target.
Image Uniformity	Uniformity Test- measures the thermal imaging camera’s ability to produce a perfectly uniform image. This test is performed at several different temperatures.
Spatial Resolution	Spatial Resolution Test- determines the level of detail that can be displayed by the thermal imaging camera.
Thermal Sensitivity	Thermal Sensitivity Test- determines the smallest measurable temperature difference indicated on the display screen. This test is performed at several different temperatures.

A draft standard may also include a “Image Recognition Test”, which is intended to act as a pass/fail criterion for some of the robustness test methods. For example, after a camera is tested for heat and flame resistance, the Image Recognition Test will be conducted to determine whether the camera’s image quality has been degraded.

APPENDIX B

Table B-1 lists existing standards that may have bearing on TIC operating conditions for functional and image quality tests.

Table B-1. Standards relating to TIC operating conditions and test methods

ASTM E 1213-97	<i>Standard Test Method for Minimum Resolvable Temperature Difference for Thermal Imaging Systems</i> – Test uses a trained observer, target near ambient temperatures.
ASTM E 1256-95	<i>Standard Test Methods for Radiation Thermometers (Single Waveband Type)</i> – used for measuring the temperature of a blackbody.
ASTM E 1311-89	<i>Standard Test Method for Minimum Detectable Temperature Difference for Thermal Imaging Systems</i> – Test uses a trained observer to determine thermal sensitivity near ambient temperatures.
ASTM E 1543-00	<i>Standard Test Method for Noise Equivalent Temperature Difference of Thermal Imaging Systems</i> – measures thermal sensitivity objectively, at ambient temperatures.
ASTM E 1862-97	<i>Standard Test Methods for Measuring and Compensating for Reflected Temperature Using Infrared Imaging Radiometers</i> – used for surface temperature measurements.
ASTM E 1897-97	<i>Standard Test Methods for Measuring and Compensating for Transmittance of an Attenuating Medium Using Infrared Imaging Radiometers</i> – used when measuring through obstructing media.
ASTM E 1933-99a	<i>Standard Test Methods for Measuring and Compensating for Emissivity Using Infrared Imaging Radiometers</i> - used for surface temperature measurements.
BS EN 60529	Enclosure protection rating system, IP 67 for water and dust ingress
BS EN 50081-2:1991	EMC emission
BS EN 50082-2:1992	EMC immunity
MIL-STD 810E	Method 513.4, Acceleration
NFPA 1221 <i>Standard for Installation, Maintenance and Use of Emergency Services Communications Systems</i>	
Section 8.3.5.4	“Mobile radios and associated equipment shall be manufactured for the environment in which they are to be used.” No mention of specific testing criteria.
Section 8.3.6.2	“Portable radios shall be manufactured for the environment in which they will be used and shall be of a size and construction to allow their operation with the use of one hand.” No mention of specific testing criteria.
NFPA 1971 <i>Standard on Protective Ensemble for Structural Firefighting</i>	
Section 6.6	No igniting, melting, dripping, or separating of garments tested at 260 °C for 5 min.
Section 6.9	Footwear must withstand 10 kW/m ² for 1 min
Section 6.10	Flashover conditions for gloves, hoods, wristlets, and multiplayer protective garment composites must withstand 83 kW/m ² for 30 s.

Table continued on next page.

Table B-1 continued...	
NFPA 1977 Standard on Protective Clothing and Equipment for Wildland Firefighting	
Section 6.2	Radiant protective test for garment and face/neck shroud, tested at 21 kW/m ² for 30 s.
Section 6.4	Heat and thermal shrinking resistance test, garment and face/neck shroud tested at 260 °C for 5 min. Helmets are tested at 177 °C for 5 min.
Section 6.14	Glove heat resistance tested at 204 °C for 5 min.
Section 6.22	Gloves materials are exposed to 83 kW/m ² for 30 s.
NFPA 1981 Standard on Open-Circuit Self-Contained Breathing Apparatus for Fire and Emergency Services	
Section 8.2	Cold soak- test for air flow performance, cycles cold/hot and hot/cold, -32 °C to 71°C
Section 8.5	Fabric components of SCBA are tested at 260 °C for 30 min.
NFPA 1982 Standard on Personal Alert Safety Systems	
Section 6.2	Electronic temperature stress test cycles PASS device through temperature fluctuations of 49 °C to 71 °C at 360 min/ 240 min cycles. (Test procedure 1)
	PASS device is cycled through temperature fluctuations of -20 °C to 71 °C at 240 min. cycles. (Test procedure 3)
Section 6.11	Heat resistance test, device exposed to 260 °C for 5 min.
NFPA 1800 Standard on Electronic Safety Equipment for Emergency Services	
UL 913	Standard on Intrinsic Safety
VESA	Flat Panel Display Measurements Standards, Version 2.0

INDEX

AC-Coupling.....	17	Mode Shift	53, 54
Aliasing.....	59	Modulation Transfer Function (MTF)	59
ANSI.....	23	Navy Testing.....	19
ASTM.....	23	NFPA.....	23
Barium Strontium Titanate (BST)15, 17, 18, 37, 57		Noise Floor.....	60
Bitdepth.....	53	Nonuniformity.....	56, 66
Black Body.....	13	Definition.....	57
Charge Coupled Device (CCD).....	17	Performance Metrics.....	20, 50
Chopper.....	17	RADCAL.....	14
Compartment Fires.....	24, 25	Robustness Test	51
Contrast.....	52, 63	SAFE-IR.....	22
Contrast Transfer Function (CTF) 30, 37, 73		Sight Distance.....	37, 40, 42
Hose Stream.....	47	Smoke/Soot.....	24, 27, 30, 31, 41
DC-Coupling.....	17	Spatial Resolution.....	59, 68
Effective Temperature Range (ETR)50, 54, 63		Temperature Dependence of Spatial Resolution.....	68
Emissive Paint.....	28, 31, 53	Thermal Classes.....	23, 50
Field of View (FOV).....	19, 27, 47	Thermal Imaging Cameras (TIC)	
Fire Dynamics Simulator (FDS).....	34	Design Componenets	17
Fire Environment.....	19, 24, 25	Image Performance.....	19, 20
Focal Plane Array (FPA).....	15	Image Quality.....	15
Fourier Transform.....	59	Imaging Performance.....	40
Fourier Transform Infrared Spectrometer (FTIR).....	30, 33, 43	Physical Robustness.....	19
Gas Analyzers, O ₂ , CO, CO ₂	31	Positioning.....	32
Heat Release Rate.....	27	Settings.....	15
Heat Release Rates.....	30	Target.....	28, 29, 31, 32
Hose Stream.....	34, 35, 44	Training.....	22
Image Quality.....	36	Uses.....	19, 20, 26, 27, 49
Image Recognition Procedure (IRP).....	50	Thermal Radiation.....	13
International Organization for Standardization (ISO).....	23	Thermal Sensitivity.....	61
ISO 12233.....	50, 59	Thermocouples.....	28, 31
Intervening Media.....	36	Thermoelectric Cooler (TEC).....	17
Large Fire Laboratory.....	28	UL.....	23
Microbolometers.....	17, 18, 37, 39, 57	Uncertainty.....	73
ASi.....	15, 17, 39	Emissive Paint.....	53
VOx.....	15, 17, 38	Hose Stream CTF.....	47
		VESA.....	23
		Victm, Simulated.....	31
		Visible Camera.....	52